UNCLASSIFIED

AD NUMBER
AD915482

| LIMITATION CHANGES |

TO:

Approved for public release; distribution is unlimited.

FROM:

Distribution authorized to U.S. Gov't. agencies only; Test and Evaluation; DEC 1973. Other requests shall be referred to Chairman, Department of Defense Explosives Safety Board, Washington, DC 20314.

| AUTHORITY |

DDESB ltr dtd 22 May 1974

THIS PAGE IS UNCLASSIFIED

EFFECT OF EARTH COVER ON FAR-FIELD FRAGMENT DISTRIBUTION

by

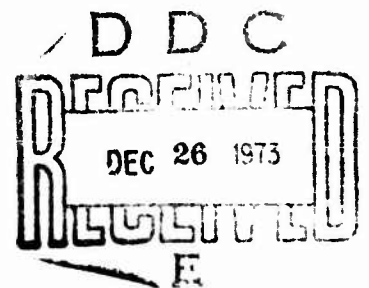L. E. FUGELSO

C. E. RATHMANN

GENERAL AMERICAN RESEARCH DIVISION

GENERAL AMERICAN TRANSPORTATION CORPORATION

NILES, ILLINOIS

DDC

DEC 26 1973

DECEMBER 1973

FINAL REPORT

GARD PROJECT NO. 1577

EFFECT OF EARTH COVER ON FAR-FIELD
FRAGMENT DISTRIBUTION

BY

L. E. FUGELSO

C. E. RATHMANN

PREPARED FOR

DEPARTMENT OF DEFENSE EXPLOSIVES SAFETY BOARD

WASHINGTON, D. C.

UNDER CONTRACT DABB09-73-0010 .

BY

GENERAL AMERICAN RESEARCH DIVISION

GENERAL AMERICAN TRANSPORTATION CORPORATION

NILES, ILLINOIS

DECEMBER 1973

GENERAL AMERICAN RESEARCH DIVISION

ABSTRACT

The effect of earth cover on the far-field fragment density expected from the accidental detonation of stored munitions was estimated by preparing three models of fragment-cover interaction. Comparisons of the theoretical calculations with limited experimental data show that the model wherein the crown of the earth cover does not retard any fragments gives the best agreement. Models for fragment-fragment interaction which effectively account for stack configuration lead to a simplified model for the effective number of munitions contributing to the far-field fragment density. An approximation technique for the rapid calculation of the far-field fragment density was prepared to assist in the ready evaluation of any model. Tentative quantity-distance relationships for four munitions were prepared. Parametric studies of the effect of altered mass distributions and fragment shape were conducted to assess possible differences between accidental detonation source parameters and arena data source parameters.

FOREWORD

This report was prepared for the Department of Defense Explosives Safety Board under Contract DAAB09-73-0010. The period of performance was January 9, 1973 through July 9, 1973.

Dr. T. A. Zaker of the DDESB was the technical monitor.

TABLE OF CONTENTS

LIST OF ILLUSTRATIONS

LIST OF ILLUSTRATIONS
(Continued)

LIST OF ILLUSTRATIONS
(Continued)

Chapter I

INTRODUCTION

1.1 Objectives of This Study

A theoretical and analytical examination of the far-field fragment distributions from the accidental detonation of stored munitions was undertaken to define and illustrate the dependence of the fragment hazard on the many parameters that describe the munition store. High explosive bombs and projectiles may be stored in rectangular block stacks containing a wide range of explosive quantity, between earth mound barricades in the open, in above ground magazine structures, or in earth-covered igloos. Explosive quantities up to 250,000 lbs are permitted in above ground stores, and up to 500,000 lb in earth-covered magazines. The present design of the revetment or igloo, as far as fragment retardation, prevents the fragments from striking an adjacent munition store and detonating it by impact. This study is concerned with the fragment hazards beyond, say, one thousand feet from the munition store and concentrates on those fragments which are dangerous to personnel, vehicles and structures there.

The retardation effect of the igloo is the primary interest of this study; however, in the systematic development of fragment density calculation, it became necessary to include stack models.

1.2 Method of Approach

A review of the existing experimental data on far-field fragment densities summarized the body of data in existence. The existing techniques for calculating the far field fragments were reviewed. Using these techniques as a springboard, an approximate technique for evaluation of the far-field fragment densities, assuming a known source on a unit hemisphere at ground zero, was devised to rapidly estimate the effects of the models that were

derived. Comparisons with the more sophisticated calculations for a single munition using measured arena data as the initial data were favorable.

Models for the effect of an igloo on the initial data were prepared. The models were (1) that the fragment from the munition must perforate the earth cover, (2) that the fragments pass through an earth cover that is in the process of breaking up and that a certain fraction are stopped while the remainder pass through, and (3) that the crown section of the earth cover is blown off and does not effectively stop any of the upper register fragments.

A model for the dependence of initial hemisphere data for a stack of munitions was prepared by considering that the fragments from each munition must perforate the expanding metal shell from any adjacent munition and further must penetrate the dense detonation products from the explosive filler of each adjacent munition.

Comparisons of each theory were made with experimental data and the models that best fit the data were selected.

In addition, it is known that initial fragment velocities and mean distributions of fragments from accidental detonations differ from the arena data. A parameter study was conducted to evaluate these effects. To better fit the far field data, consideration of another parameter, namely, the effective ballistic density, was included in this parameter study.

A tentative model for quantity-distance was developed from the results of this study and typical quantity-distance curves were calculated for four munitions.

1.3 Main Results

The model which most adequately describes the effect of the igloo is that the crown of the igloo is blown off. Only fragments with initial elevation angles less than 10° are retarded (these are completely stopped).

About a 10% reduction in fragment densities in the far-field is effected by the presence of an igloo. The model for the stack shows that only the munitions in the surface layers contribute significantly to the far-field fragment density.

The initial velocity for the fragments should be taken as the highest value from the arena data. The fragments that are thrown to the far-field must have a higher effective ballistic density than the mean value given in the arena data; i.e., the fragments that reach far distances tend to be elongated with the long axis aligned with the trajectory. Since these projectiles have a high mass/presented-area ratio, a more conservative injury criterion in terms of impact than any of those commonly applied thus far may be appropriate.

Because there is very little data on far-field fragment measurements and because the experiments were not systematically planned to measure the dependence of the far-field fragments on the several parameters of the typical munition storage configuration, and extensive experimental program to determine this is highly recommended. Until experimental verification of the predicted parameter dependence is experimentally verified, the analytical predictions given in this report must remain hypothetical.

Chapter II

EXPERIMENTAL AND THEORETICAL BACKGROUND

Several studies on far-field fragment distributions from the detonation of munitions, both theoretical and experimental, have been conducted. A summary of these studies is given in the following paragraphs.

2.1 Experimental Studies

Experimental determination of fragment distribution in the far-field has been accomplished for a limited number of munition stores. Because of the costs and time for detailed experimental determination of the far-field fragment hazard, these experiments are few in number and, since in most instances the primary purpose of the experiment was blast effects, evaluation of structural damage,or detonation communication, the fragment study was a secondary goal.

In 1945, the ANESB undertook a series of detonations of various munitions contained within standard Army and Navy storage igloos (ANESB 1947). A series of eight detonations of large stacks was conducted; blast wave propagation and structural damage to barracks by blast were the primary objective. Detailed fragment measurements were made on only one shot containing 425 MK33,1100-lb bombs in a Navy igloo. There were 250,000 lbs. of 50/50 Amatol in the stack. Figure 2-1 shows the fragment density (in number of fragments per square foot) vs. range along the line where the maximum fragment densities occurred. Qualitative descriptions of fragments from the remaining experiments and from the subsequent model igloo tests indicated that this fragment pattern was replicated.
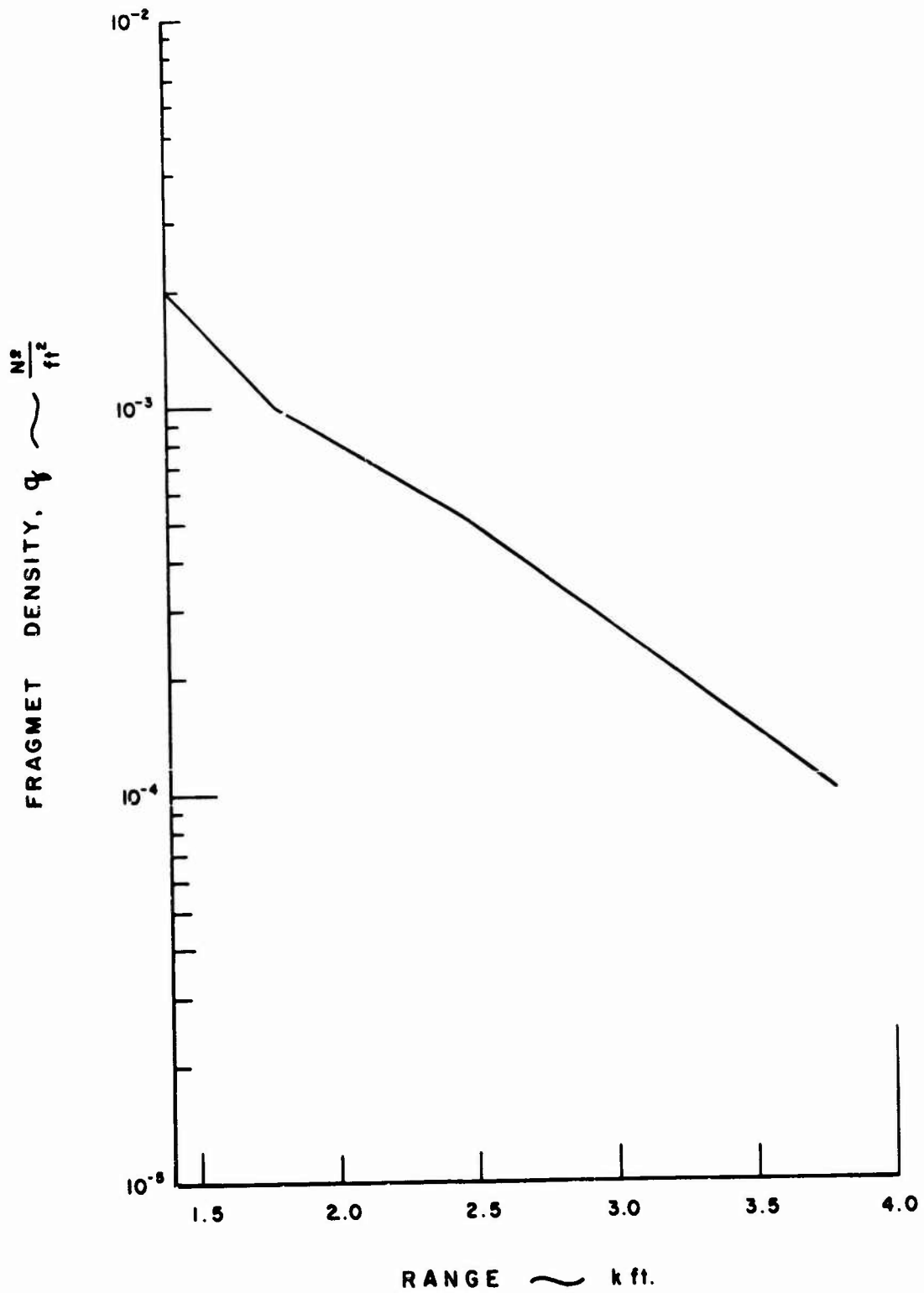
Figure 2-1. FRAGMENT DENSITY VERSUS RANGE FOR ARCO TEST I.
(W = 250,000 lb , 50/50 AMATOL , 425 1100-lb. MK 33 BOMBS)

5

A series of four stack detonations in revetments was carried out in the Big Papa tests (Peterson et. al. 1968). The first two detonations were rectangular stacks of M117, 750-pound bombs and M66A2 2,000-pound bombs, each bomb being primed. The third shot was a similar mixed stack, but in a hexagonal stack arrangement. Fragment densities were measured on those shots; in the first two the collection areas were 90,000 ft^2 areas, with only three collection areas within 3500 feet from the stack. On the third shot the collections were smaller and many more were placed from 1000 feet to 2500 feet. The fourth shot was a stack of M117 750-pound bombs in a rectangular array with one bomb primed. The rest detonated by blast or fragment effects. No far-field fragment distributions were measured in this shot. Figure 2-2 shows the fragment density for the first two shots along a line normal to the axes of the bombs.

The remaining experimental data on fragments comes from close-in measurements of fragments. Several military engineering installations have measured fragment properties in arena tests in which one horizontal munition, primed, is detonated with the fragments intercepted a short distance away. As a function of azimuth angles (measured from the nose), an average initial fragment velocity and fragment distributions with mass are measured. The arena results are summarized in the JMEM manuals (JMEM 1970).

Draper and Watson (1970) report some modified arena data for stacks of munitions, in particular a sequence of experiments on stacks of 155mm TNT-filled projectiles. Their interim report on raw fragment collection data gives a qualitative indication of how fragment mass distributions and initial fragment velocities change as the stack size changes. They tested stacks 3x3x1, 5x4x1, 6x6x1, 12x6x1, and 40x6x1.
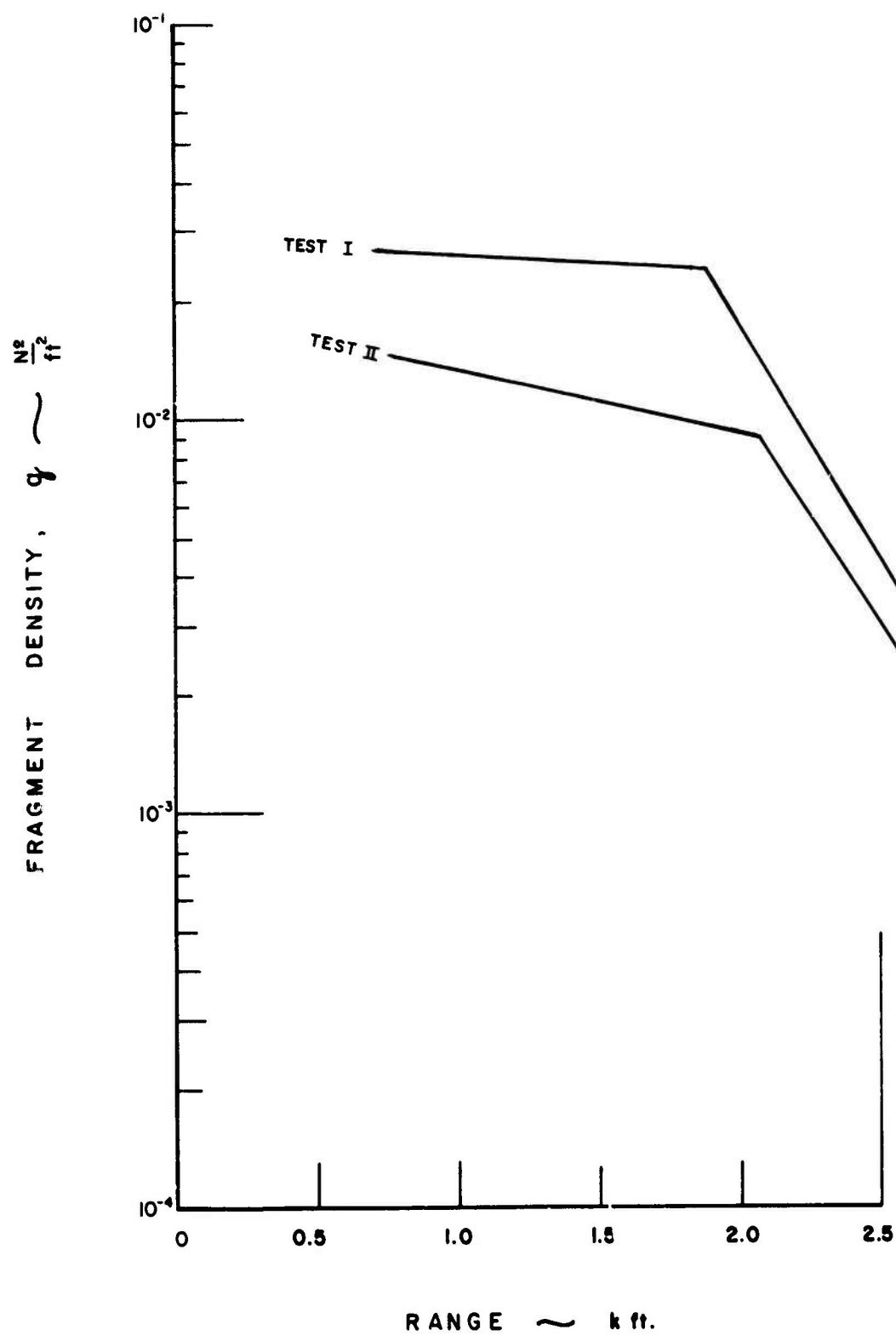
Figure 2-2, FRAGMENT DENSITY VERSUS RANGE - BIG PAPA TESTS.
(PERPENDICULAR TO BOMB AXES)

7

Far-field fragment distributions were measured from small stacks of M117, 750-pound tritonal-filled bombs in a test conducted at NWC (Feinstein and Nagaoka 1970). The stacks were 2x3x1 and 5x3x1 (length x height x depth). All bombs were primed. Fragment and mass densities were measured from 500 feet to 1500 feet from the stacks on the nose, side and base directions. Figure 2-3 shows the fragment density in the side direction from these two shots.

A 10x100x1 stack of 155 mm, TNT loaded, projectiles was detonated at Yuma (Feinstein and Nagaoka 1970) with fragment and mass densities measured in the nose, base and side directions. One projectile was primed.

A large stack (13,696) of 155 mm projectiles contained inside a standard Army igloo was detonated in Eskimo I (Weals 1973). The projectiles had TNT as a filler. Their axes were vertical and approximately 20 of these projectiles were primed. Figure 2.4 shows the measured fragment densities along several lines from this experiment. Figure 2-5 shows the plan view of the experiment and defines the rays relative to the igloo structure.

2.2 Theoretical Studies

Very few theoretical predictions of far-field fragment patterns from munitions have been made. Zaker, et al., (1970) generated a method for calculating far-field fragment densities from the arena data for a single munition. For a given interval of fragment mass and an initial velocity, (given as a function of azimuth angle measured from the bomb nose), they compute the ranges wherein the fragments will fall (for all possible elevation angles). In each increment of range, the number of fragments over all mass intervals is summed and the fragment densities are then calculated. They present predictions for far-field fragment densities for stored single munitions. Feinstein (1972) extended this calculation with an interpolated mass distribution for the larger mass intervals. Schreyer and Romesberg

Figure 2-3. FRAGMENT DENSITY VERSUS RANGE - SMALL STACKS
OF M117 750-lb. BOMBS (SIDE SPRAY DIRECTION).
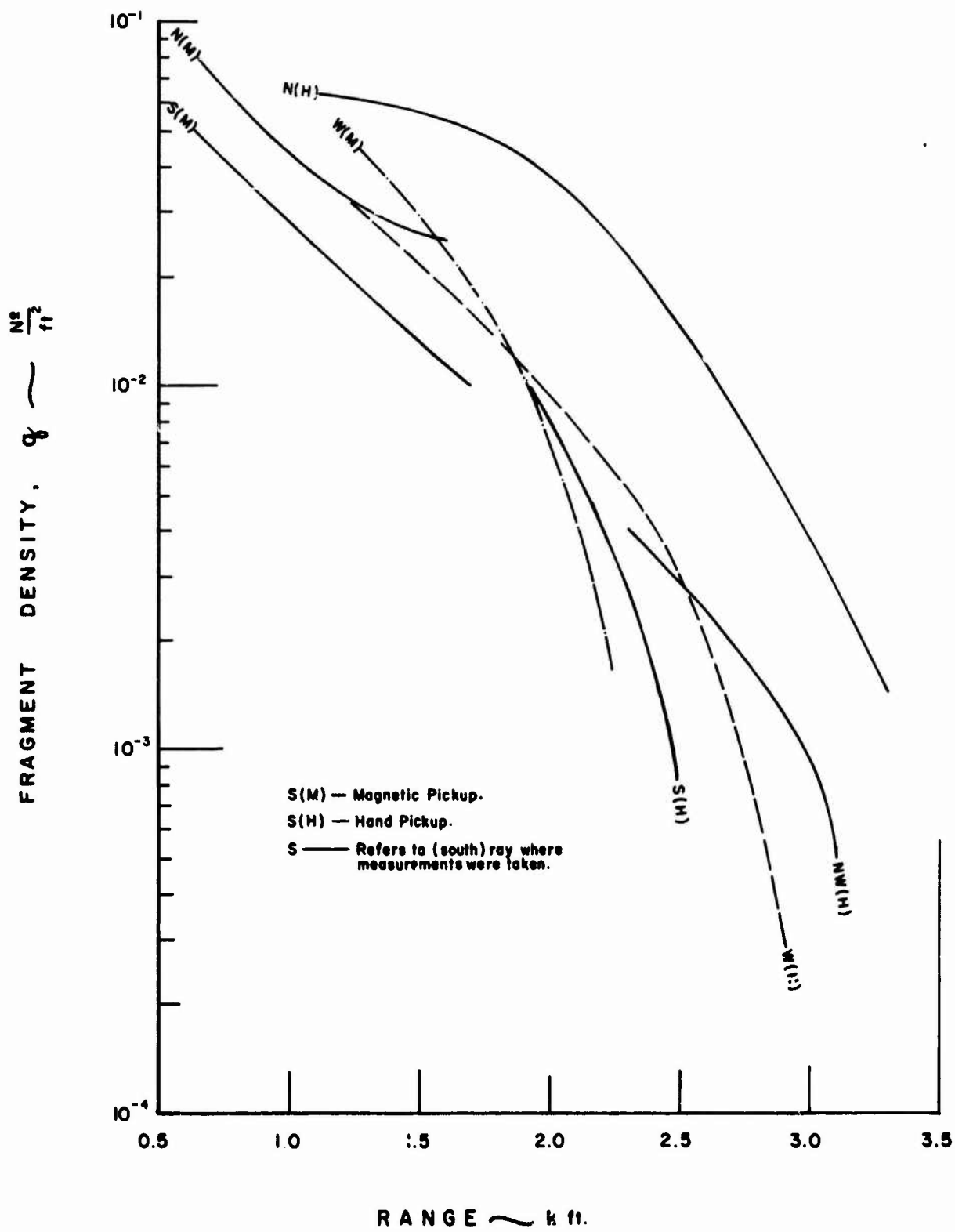
Figure 2-4, FRAGMENT DENSITY VERSUS RANGE - ESKIMO I
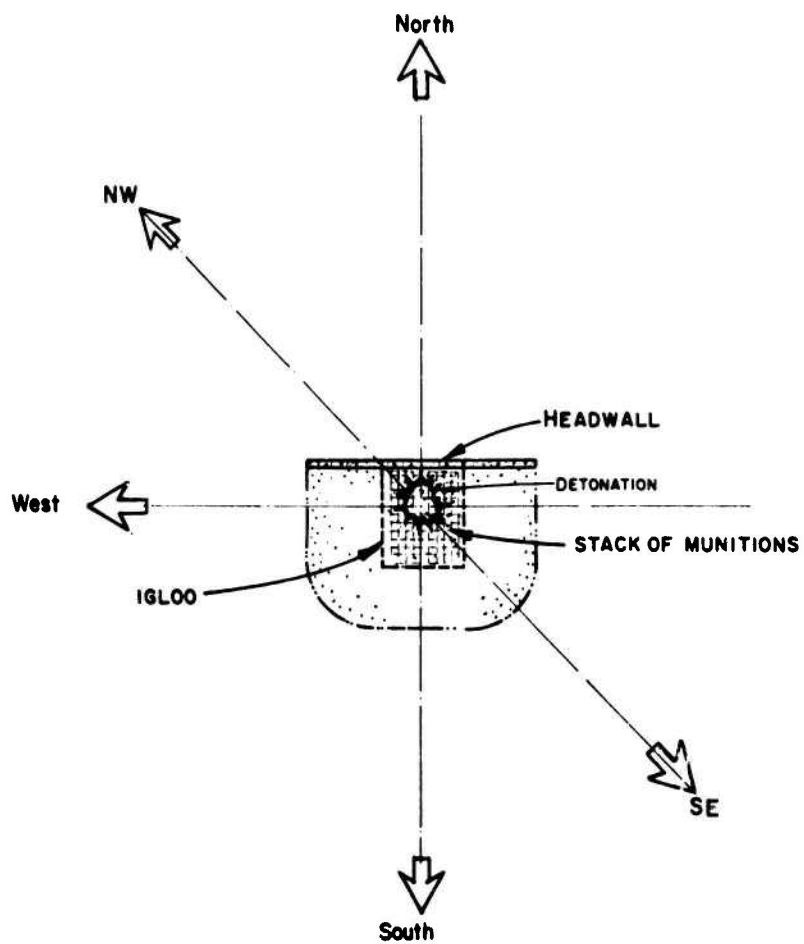
Figure 2-5. PLAN SHOWING RAYS WHERE FRAGMENT DENSITIES WERE MEASURED. (ESKIMO I)

11

(1970) (also Romesberg 1971) prepared a similar program to calculate
fragment distributions that would be expected in the Big Papa experiment.

In all these programs, the initial data on the fragments was taken
from the arena data. In Zaker's and Feinstein's work, the distribution over
mass was based in tabular form from the arena data, while Romesberg and
Schreyer used the mean fragment mass.

Feinstein attempted to extend the single munition calculation procedure
using an angle dependent factor for his initial data obtained from experimental
arena data on model stack munitions (Feinstein and Nagaoka 1970). Schreyer
and Romesberg determined an effective number of single munitions by comparing
the single munition prediction with an experiment from the Big Papa series.

2.3 Some Comments

To summarize, currently available information consists of:

1) theoretical calculations for far-field fragment densities from
    single, unbarricaded munitions, and

2) several experimentally-measured far-field fragment densities from
    stacked munitions in a variety of configurations.

Parametric representations of far-field densities from stacked munitions,
with or without an earth cover, are virtually non existent.

Very little work has been done in quantitatively evaluating the far-
field fragment hazards from accidental detonations of stored munitions. The
experimental studies are far too sparse to allow any interpolation or
extrapolation for ranges at which specific fragment densities will occur.
The various experiments vary from one type of munition to another; the
orientation, mode of ignition and protective covering vary without any
systematic pattern. Only in the fragmentary (no pun intended) results of
Draper and Watson (1970) is there any systematic investigation of the effect

of varying a single parameter (in this case, the number of munitions in a stack n x m x 1). Any predictive technique requires some knowledge of how the basic physical parameters of interest (e.g.,initial fragment velocity) vary with the parameters that describe the storage configuration (e.g.,number). Any theoretical calculation of far-field fragment densities must incorporate the dependence on munition storage parameters and the check on any theory is its comparison with experimental results. With the current data available, these comparisons are extremely restricted.

Chapter III

BASIC MATHEMATICAL ANALYSES

3.1 Approximation to Solutions of the Ballistic Equations

The solution of the ballistic equations to obtain the range of a fragment, given its initial velocity, elevation angle, mass, presented area and drag, is necessary to the evaluation of the fragment densities that may be expected. The differential equations that describe the motion and trajectory are nonlinear and the solutions to these equations are either numerical or approximate. The equations of motion are solved numerically and then approximations to these solutions which facilitate the evaluation of the far-field fragment densities are devised. Consider the motion of a fragment, initially propelled with velocity, V_0, at an angle, α_0, with the horizontal plane. This motion is confined to two dimensions, i.e., no yaw effects and no cross wind effects are considered. The forces acting on the fragment are drag and gravity. Figure 3-1 depicts the trajectory and defines the coordinates. The equations of motion are

$$m \frac{dV_x}{dt} = - \frac{\rho C_D A}{2} V_x V$$

$$m \frac{dV_y}{dt} = - \frac{\rho C_D A}{2} V_y V - mg$$

$$\frac{dX}{dt} = V_x \tag{3-1}$$

$$\frac{dY}{dt} = V_y$$

$$V^2 = V_x^2 + V_y^2$$

where   m is the mass of the fragment

C_D is the drag coefficient
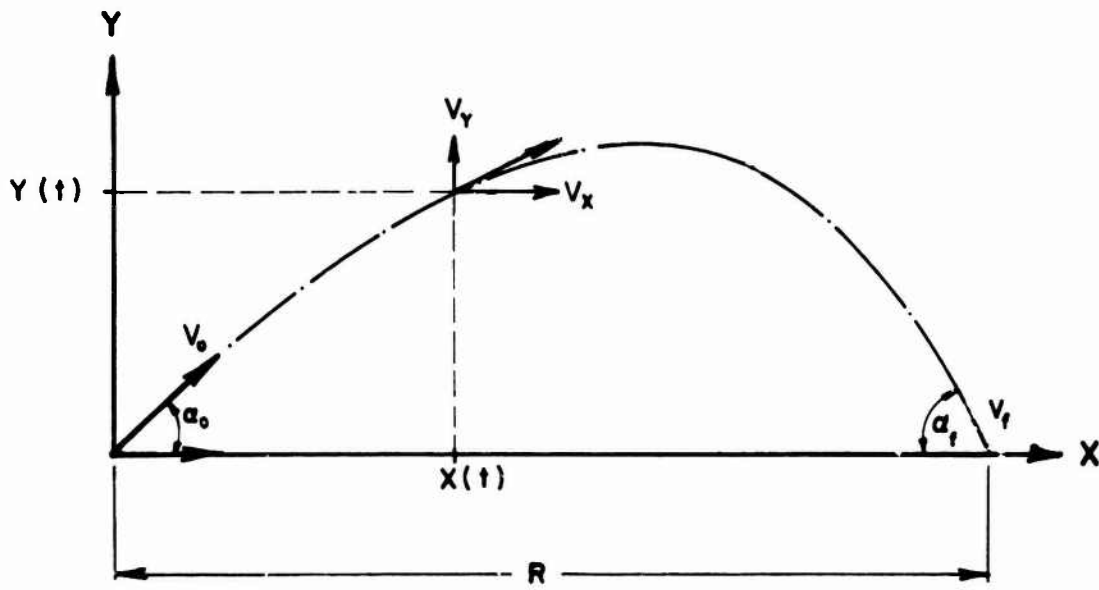
Figure 3-1, TRAJECTORY OF A FRAGMENT

15

ρ is the air density

A is the cross section area of the fragment normal to the trajectory

g is the gravitational acceleration

V_x, V_y are the horizontal and vertical components of the fragment velocity

t is the time

The initial conditions are, at $t = 0$

$$X = Y = 0$$

$$V_x = V_0 \cos \alpha_0$$

$$V_y = V_0 \sin \alpha_0$$

where V_0 is the initial fragment velocity and α_0 is the initial elevation angle.

The presented area, A, can be represented approximately as a function of the fragment mass through

$$A = \left(\frac{m}{\kappa}\right)^{2/3} \tag{3-2}$$

where κ is the ballistic density. For a tumbling fragment, this area A is taken as the mean presented area.

where κ is the ballistic density.

Define a parameter, β, through

$$\beta = \frac{\rho C_D}{2\kappa^{2/3}} \tag{3-3}$$

Then the first two equations of (3-1) can be written.

$$m \frac{dV_x}{dt} = -\beta m^{2/3} V_x V$$

$$m \frac{dV_y}{dt} = -\beta m^{2/3} V_y V - mg \tag{3-1'}$$

The drag coefficient is a function of the velocity as is shown in Figure 3-2. For fragment velocities exceeding the sound velocity in air, the drag coefficient is essentially constant ($C_D \sim 1.28$), while for velocities below the sound velocity in air, it has another constant value, ($C_D \sim 1.08$). Only when the fragment velocity is close to the sound velocity does the drag coefficient vary significantly. The fragments under consideration have an initial velocity several times the sound speed in air; most of the trajectories of these fragments are accomplished while the fragment velocities are supersonic. Thus, for simplicity of analysis and scaling, assume the drag coefficient to be constant with its supersonic value, $C_D = 1.28$.

The equations of motion are to be solved from t = 0, up to a time when y returns to zero, i.e., when the fragment trajectory intersects a horizontal plane through the source. The value of x at that time is the range, R, of the fragment. The velocity, V_f, is the impact or terminal velocity and the trajectory makes an angle, α_f, with the horizontal.

What is desired are the solutions

$$R = f_1(V_0, \alpha_0, m)$$
$$V_f = f_2(V_0, \alpha_0, m)$$
$$\alpha_f = f_3(V_0, \alpha_0, m)$$

Introduce the new independent variable, S, the arc length along the trajectory. Now

$$\frac{dS}{dt} = V. \tag{3-4}$$

The equations of motion become

$$mV \frac{dV_x}{dS} = - \beta m^{2/3} V_x V$$

$$mV \frac{dV_y}{dS} = - \beta m^{2/3} V_y V - mg \tag{3-5}$$
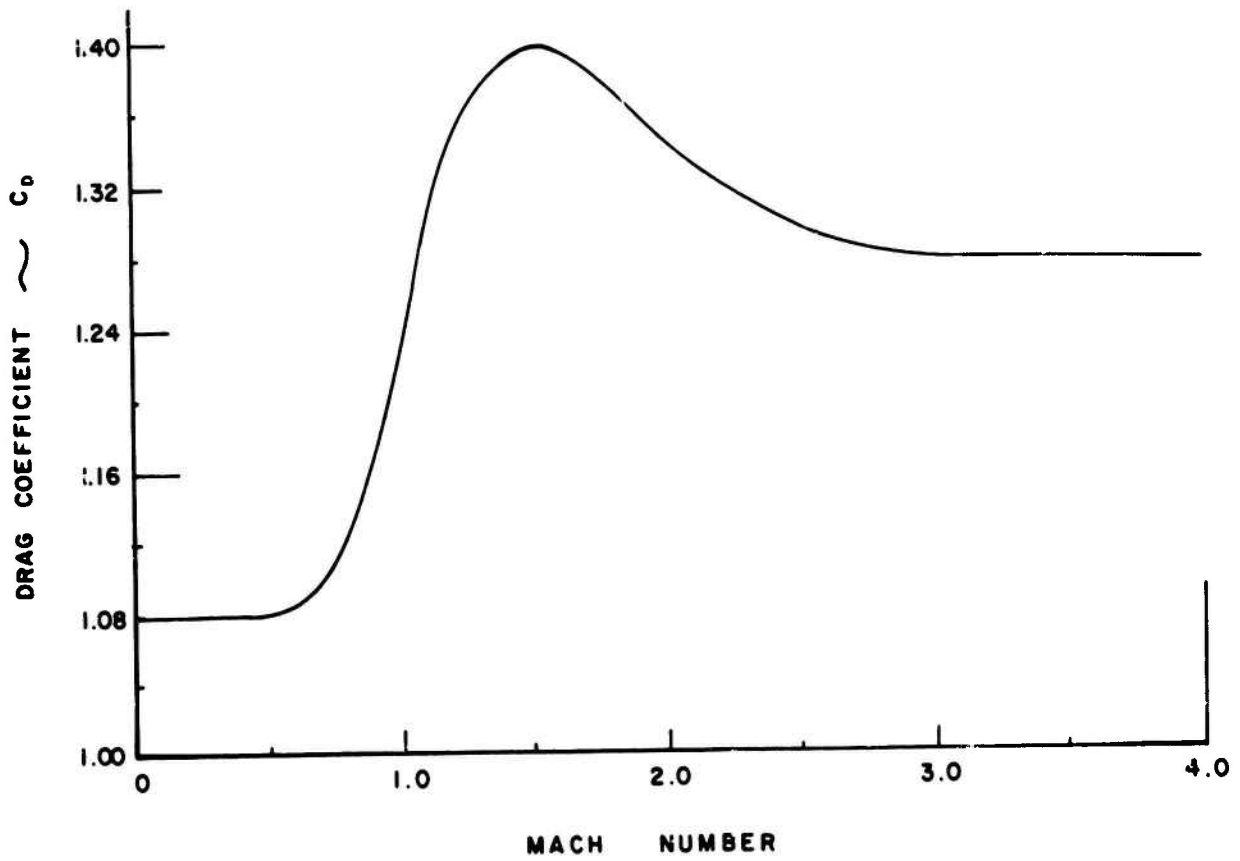
Figure 3-2. DRAG COEFFICIENT FOR A FRAGMENT AS A FUNCTION OF FRAGMENT VELOCITY.

$$\frac{dX}{dS} = \frac{V_x}{V}$$

$$\frac{dY}{dS} = \frac{V_y}{V}$$

The initial conditions are: at $S = 0$

$$V_x = V_0 \cos \alpha_0$$

$$V_y = V_0 \sin \alpha_0$$

$$X = Y = 0$$

The equations are put into a dimensionless form through the introduction of a length scale, L, and velocity scale, V_0.

$$L = \frac{m}{\beta}^{1/3} \tag{3-6}$$

The equations of motion can be written

$$\frac{dv_x}{ds} = - v_x$$

$$\frac{dv_y}{ds} = - v_y - \frac{\varepsilon^2}{v}$$

$$\frac{dx}{ds} = \frac{v_x}{v}$$

$$\frac{dy}{ds} = \frac{v_y}{v} \tag{3-7}$$

$$v^2 = v_x^2 + v_y^2$$

$$\varepsilon^2 = \frac{m^{1/3}g}{\beta V_0^2}$$

with $x = \frac{X}{L}$, $y = \frac{Y}{L}$, $v_x = \frac{V_x}{V_0}$, $v_y = \frac{V_y}{V_0}$, and $s = \frac{S}{L}$

The parameter, ε, is the ratio of the terminal free fall velocity of the fragment to its initial velocity.

The initial conditions are, at $s = 0$

$$v_x = \cos \alpha_0$$

$$v_y = \sin \alpha_0$$

$$x = y = 0$$

In this form, the equations are to be solved as a function of s until $s=s_1$ where $y(s_1) = 0$. The values of x and v at this value of s define the range r, and terminal velocity.

$$r = x(s_1) = f_1(\alpha_0, \varepsilon)$$

$$v_f = \sqrt{v_x^2(s_1) + v_y^2(s_1)} = f_2(\alpha_0, \varepsilon)$$

$$\alpha_f = \tan^{-1} \left[\frac{v_y(s_1)}{v_x(s_1)} \right] = f_3(\alpha_0, \varepsilon)$$

The three functional forms f_1, f_2, and f_3, are determined by numerical integration, using a Runge-Kutta technique.

The parameter, ε, is a function of the initial fragment velocity, its mass and its ballistic density. From the arena data for these fragment parameters.the range of ε which is applicable to this problem is determined. The fragment masses range from .02 lb to .3 lb and the initial velocities from 2000 ft/sec to 10,000 ft/sec. The ballistic density data is given by a single value, determined from the mean value of the average presented area. This mean value is typically 600 grains/inch^3.

Using this value of κ, and letting $\rho = 525$ grains/ft^3.

$$\varepsilon = 137.04 \, \frac{m^{1/6}}{V_0}$$

$$\beta = 1.7146 \times 10^{-3}$$

Figure 3-3 shows curves of constant ε as a function of V_0 and m.

The parameter ε varies between .01 and .04 for the dominant portion of the arena data. The curve with $\varepsilon = 0.02$ goes through the middle of the

$$\epsilon = 137.04 \frac{m^{\frac{1}{3}}}{V_o}$$
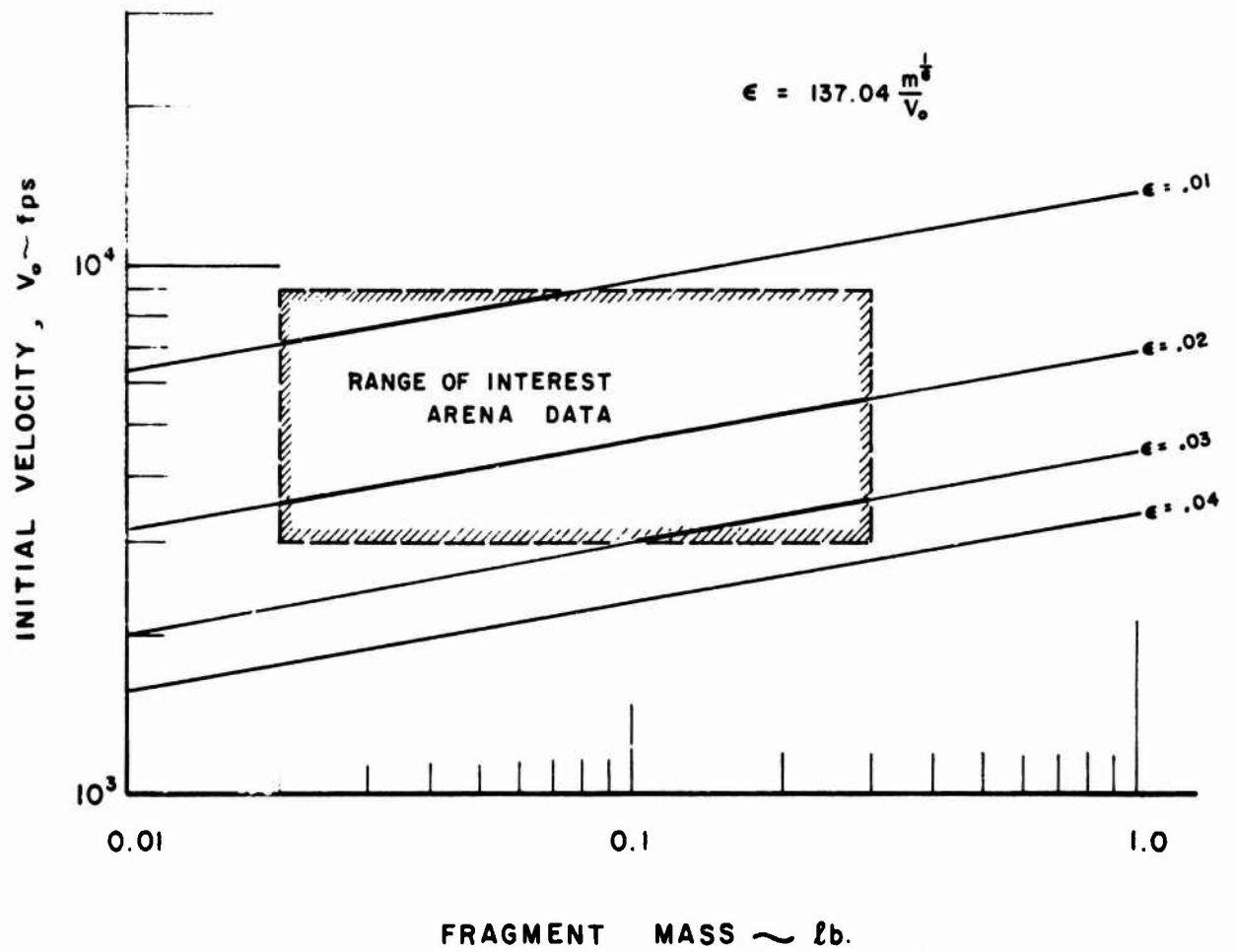
Figure 3-3, BALLISTIC PARAMETER ϵ AS A FUNCTION OF FRAGMENT MASS AND INITIAL VELOCITY.

range of the arena data. We will be concerned with slightly larger fragments, (e.g., 1.0 lb at initial velocities near 5000 ft/sec), for which $\epsilon = 0.02$ is representative of these larger fragments also.

If we take κ twice its mean value, then

$$\epsilon \approx 137.04 \; 2^{1/3} \frac{m^{1/6}}{V_o}$$

and the range of ϵ shifts to from .01 to .06.

The non-dimensional range and terminal velocities were calculated for values of ϵ from .005 to 0.10. The results are shown in the next three figures. Figure 3-4 shows r as a function of α_o for various values of ϵ. Figure 3-5 shows α_f versus α_o and Figure 3-6 shows V_f versus α_o.

The range versus elevation angle curves show very little variation in shape in the range $0.01 \leq \epsilon \leq 0.06$. The maximum of the curve shifts slightly from 18° at $\epsilon = 0.01$ to 22.5° at $\epsilon = 0.6$. Thus, if these curves are normalized such that their maxima are unity, we find the curves almost identical. From Figure 3-3, note that the curve for $\epsilon = .02$ goes through the middle of the arena data. Deviations in shape of the range curves from this are minimal. Thus, the ballistic curves for $\epsilon = .02$ are selected to describe all ballistic parameters.

Note the changes in shape of the V_f and α_f curves are quite small in the range $0.1 \leq \epsilon \leq .06$.

Figure 3-7 shows the maximum of the range versus elevation angle curve as a function of ϵ. This curve can be approximated to a high degree of accuracy by

$$r_{max} = 0.5140 - 1.0358 \ln \epsilon \qquad (3-9)$$

We use then an approximation of the form

$$r(\alpha_o, \epsilon) = r_{max} (\epsilon) f(\alpha_o) \qquad (3-10)$$
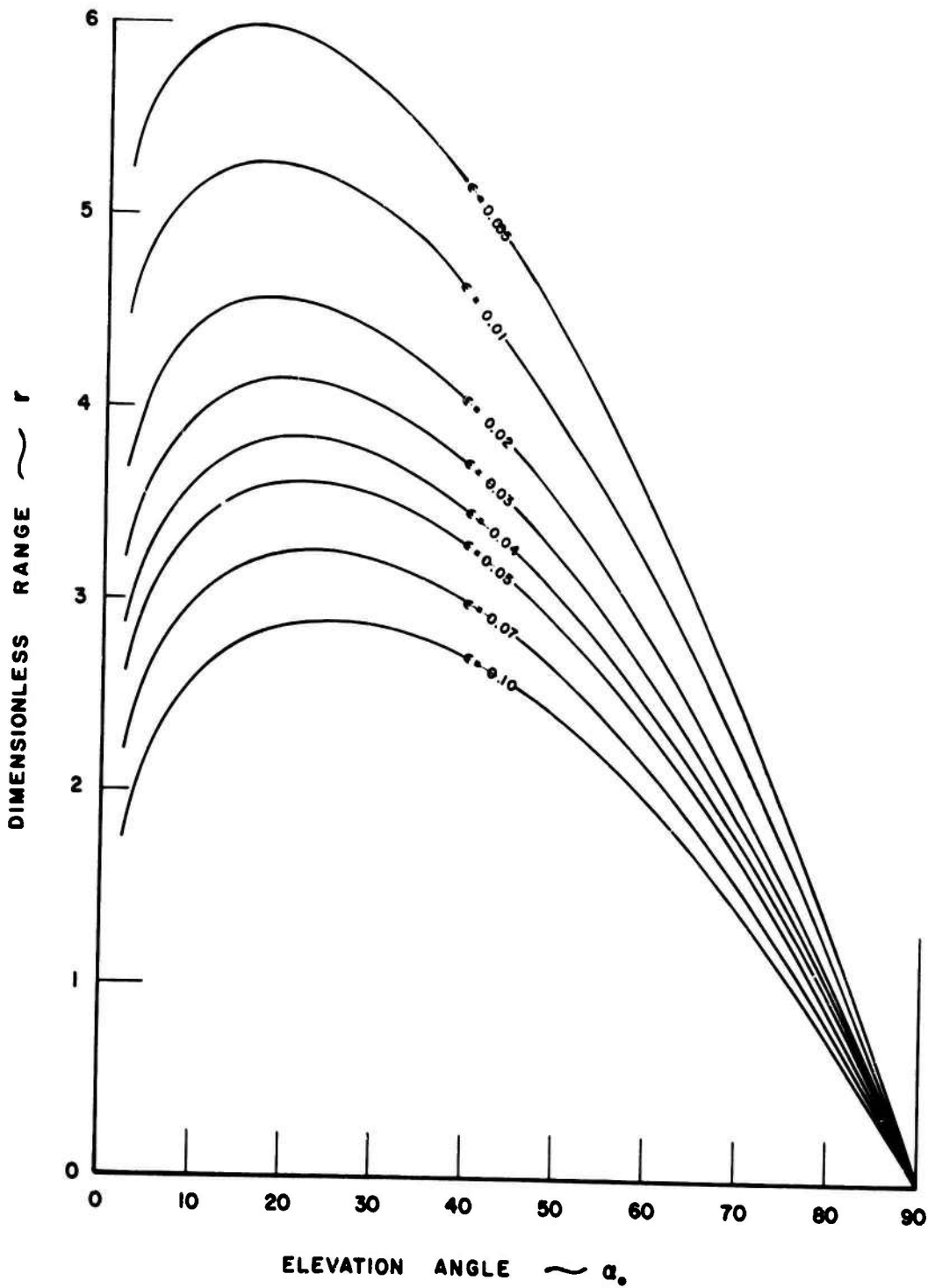
Figure 3-4. BALLISTIC TRAJECTORY,
DIMENSIONLESS RANGE VS ELEVATION ANGLE

23
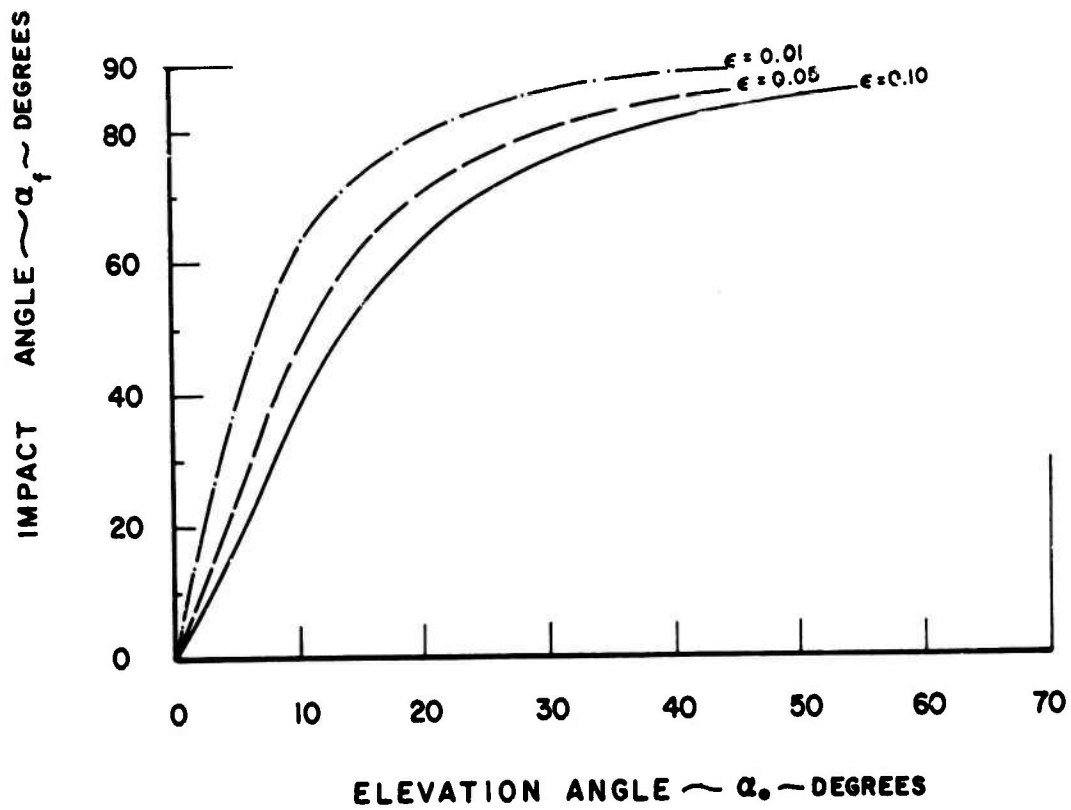
Figure 3-5, IMPACT ANGLE VS ELEVATION ANGLE.
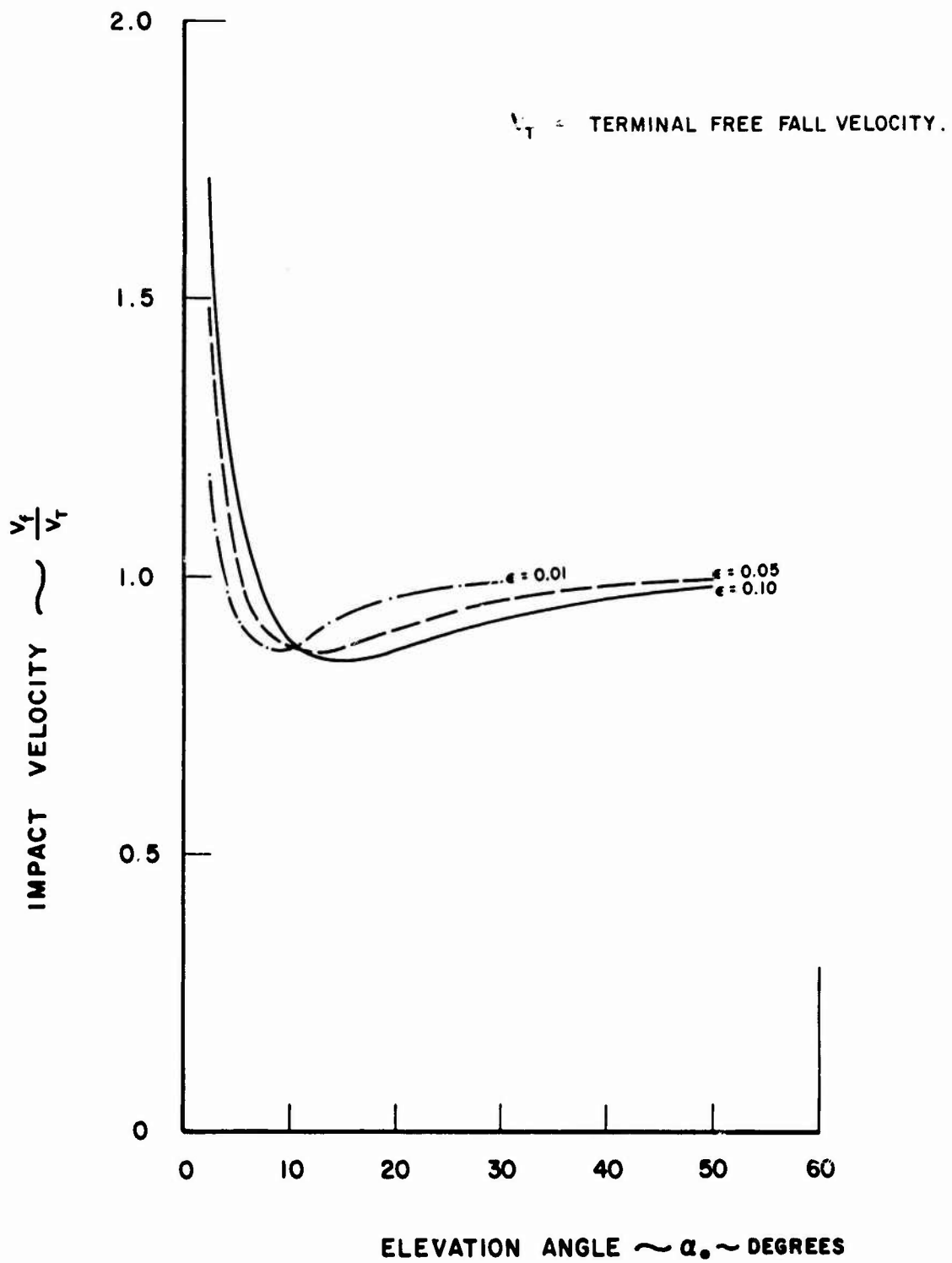
Figure 3-6, IMPACT VELOCITY VS ELEVATION ANGLE.

25
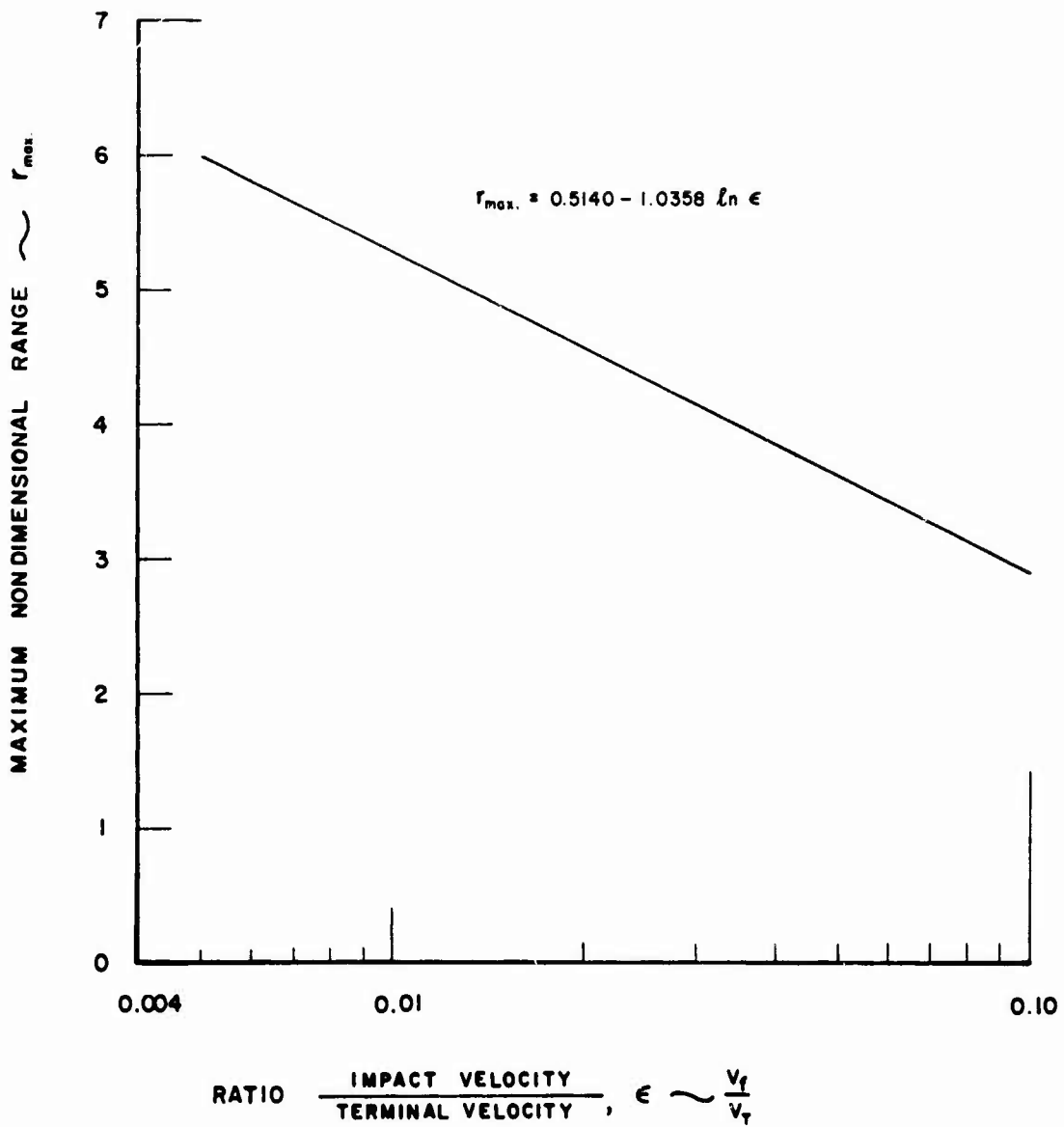
Figure 3-7, MAXIMUM NON DIMENSIONAL RANGE VERSUS ϵ – RATIO IMPACT VELOCITY / TERMINAL VELOCITY.

where $f(\alpha_0)$ is determined from the curve for $\epsilon = 0.02$. After some trial and error, an approximate fit for $f(\alpha_0)$ was obtained.

$$f(\alpha_0) = \frac{3\sqrt{3}}{2}\ \sqrt{\xi}\ (1-\xi)[1+\tilde{A}(\xi - \frac{1}{3})^2] = h(\xi) \qquad (3-11)$$

with

$$\tilde{A} = 3.25, \xi < \frac{1}{3}$$
$$\tilde{A} = 2.00, \xi > \frac{1}{3}$$
$$\xi = \sin \alpha_0$$

Figure 3-8 shows the approximation to $f(\alpha_0)$ versus elevation angle. The fit is within .1% for $7.5° < \alpha_0 \le 40°$.

Other approximations are

$$\alpha_f \approx 90\ [1 - \exp\ (-\frac{\xi}{.175}] \qquad (3-12)$$

$$\frac{V_f}{\epsilon} = (\frac{1}{\epsilon} - 1.9)\ \exp\ (-\frac{\xi}{.01}) + 1.6\ \exp\ (-\frac{\xi}{.06})$$
$$- 0.7\ \exp\ (-\frac{\xi}{.14}) + 1$$

3.2 Calculation of the Fragment Density

An approximate technique for the rapid estimation of fragment densities in the far-field as a result of a detonation of a munition store is derived in this section. This approximate procedure utilizes the approximate forms for the ballistic parameters developed in the previous section.

Consider ranges which are sufficiently large so that the munition store can be treated as a point. Figure 3-9 shows the coordinate system that we use. The point where we will compute the fragment density is defined by a range, R, measured from the center of the munition store and an azimuth angle, ϕ, measured from some reference axis on the ground surface. When the munitions detonate, the fragments at the source are described as follows. On a unit hemisphere surrounding the origin, the number of fragments per unit
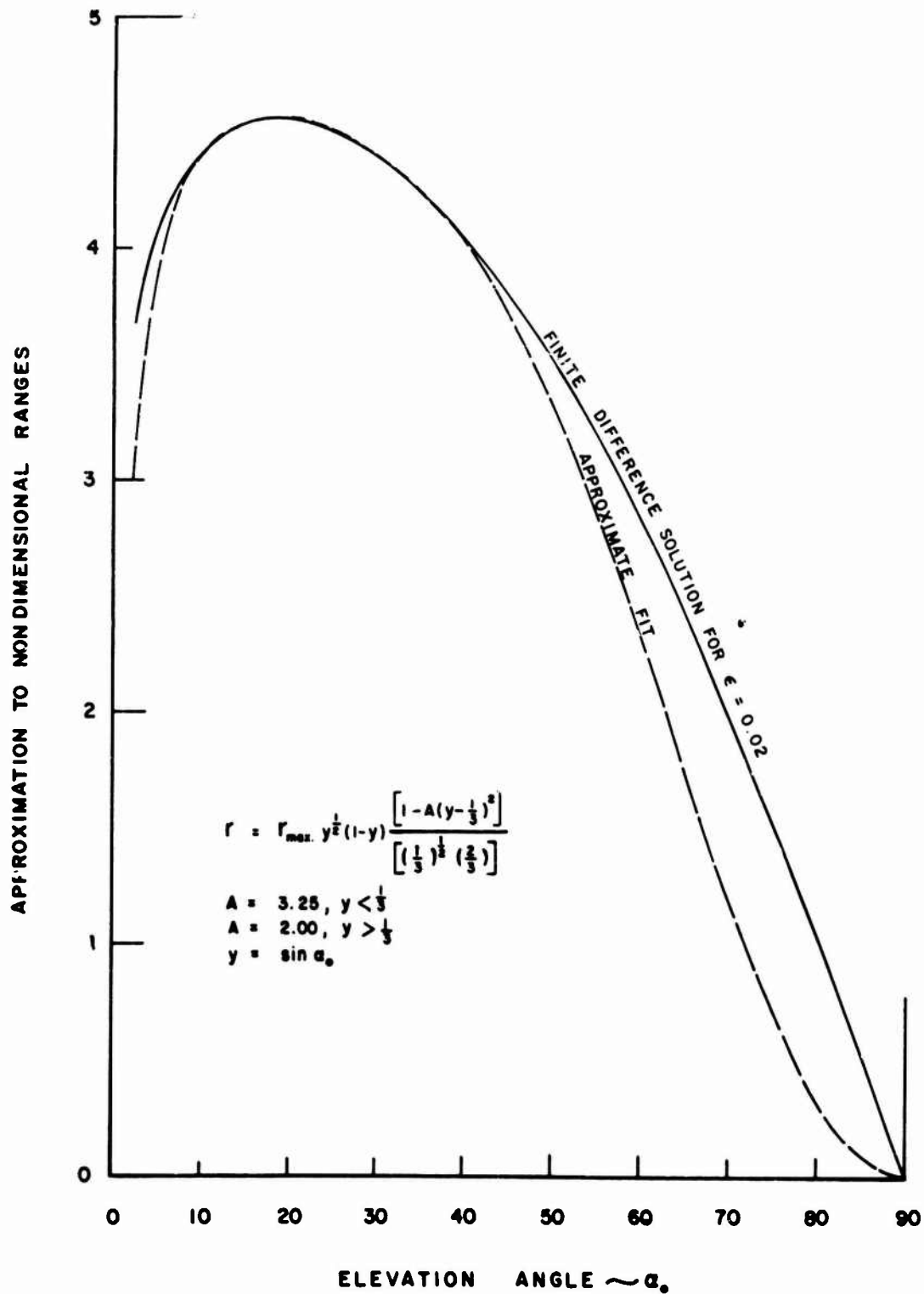
Figure 3-8. APPROXIMATION TO NONDIMENSIONAL RANGES VS
ELEVATION ANGLE, FIT TO $\epsilon = 0.02$.

28
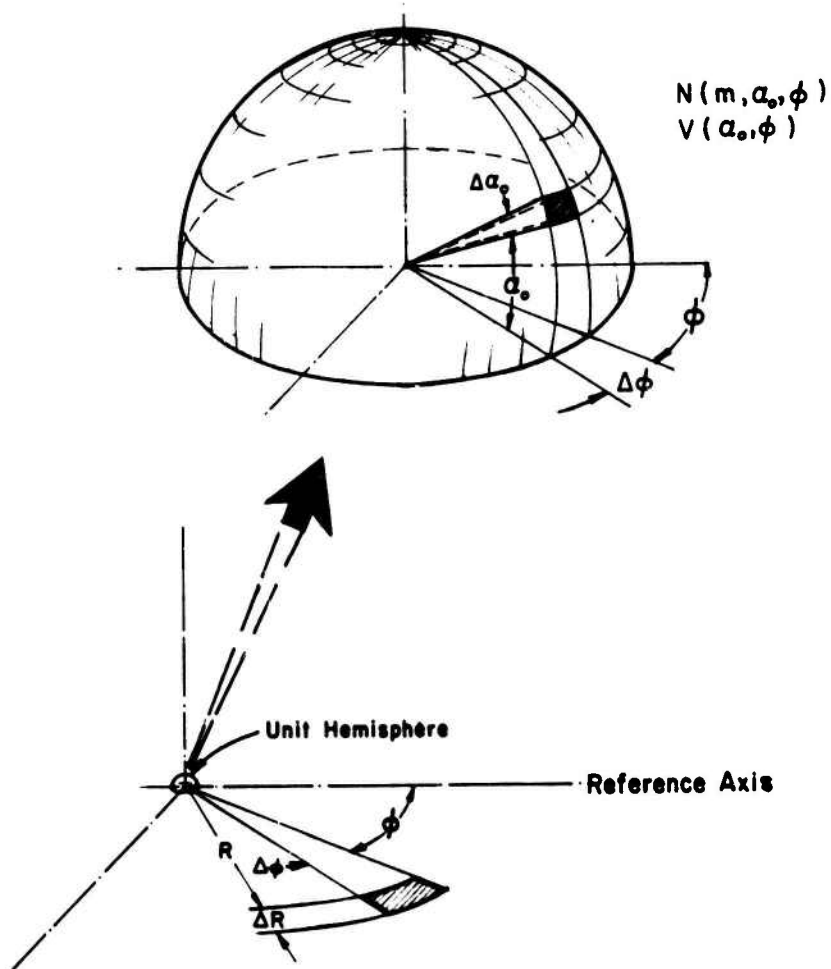
Figure 3-9, ILLUSTRATION OF COORDINATE SYSTEM AND UNIT
HEMISPHERE USED FOR CALCULATION OF FAR-FIELD FRAGMENT DENSITIES.

solid angle in a given mass increment are known as a function of azimuth angle and elevation angle. Also the initial velocity of the fragments is known as a function of these angles. Thus at fixed α_0 and ϕ, there is a probability density function $f(m, \alpha_0, \phi)$ such that

$$f(m, \alpha_0, \phi) \, dm$$

represents the number of fragments per unit solid angle with mass between m and m+dm. Further define a cumulative distribution function

$$F(m, \alpha_0, \phi) = \int_m^\infty f(\bar{m}, \alpha_0, \phi) \, d\bar{m} \qquad (3\text{-}14)$$

This defines the number of fragments per unit solid angle with mass greater than m.

In an infinitesimal element of azimuth, $\Delta\phi$, the number of fragments that fall beyond R is calculated by integrating over a slice of the unit hemisphere. Denote this number by $N(R,\phi)$.

$$N(R,\phi) = \left[\int_0^{\pi/2} \cos\alpha_0 \, d\alpha_0 \int_{m_1(R, \alpha_0, \phi)}^\infty f(\bar{m}) \, d\bar{m} \right] \Delta\phi \qquad (3\text{-}15)$$

The lower limit, $m_1(R, \alpha_0, \phi)$ is the mass of the fragment that just reaches R given the elevation angle α_0 and the initial fragment velocity at α_0 and ϕ. All fragments (with the same ϕ and α_0) which have masses larger than m_1 (R, α_0, ϕ) will fall at larger ranges than R. (Figure 3-10 illustrates the domain of integration in the α_0, $\bar{m}$ plane.) By considering $N(R, \phi)$ and $N(R + \Delta R, \phi)$ for an infinitesimal ΔR, the number of fragments in the small area $R\Delta R\Delta\phi$ is

$$n(R, \Delta R, \phi) = \Delta R \Delta\phi \left(\frac{\partial N}{\partial R}\right)_\phi \qquad (3\text{-}16)$$

The fragment density at R is then

$$q(R,\phi) = \frac{1}{R} \left(\frac{\partial N}{\partial R}\right)_\phi \qquad (3\text{-}17)$$

Using the expression for N from Equation (3-15),
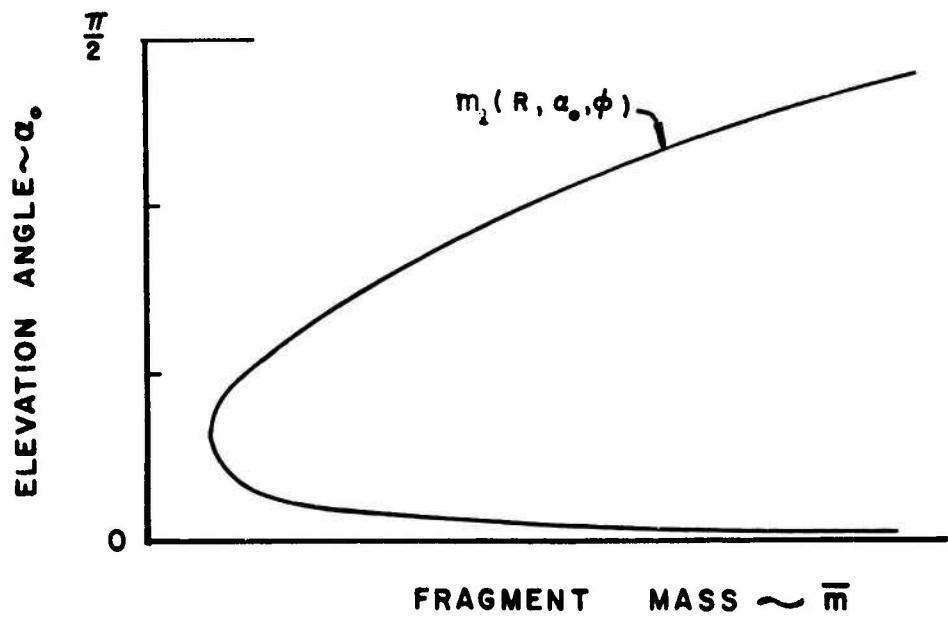
Figure 3-10. DOMAIN OF INTEGRATION IN $\overline{m} - \alpha_o$ PLANE

$$q(R,\phi) = \frac{1}{R} \int_0^{\pi/2} \cos\alpha_0 \, d\alpha_0 \; f(m_1(R,\alpha_0,\phi)) \left(\frac{\partial m}{\partial R}\right)_{\alpha_0,\phi}$$

The partial derivative $\left(\frac{\partial m}{\partial R}\right)_{\alpha_0,\phi}$ can be evaluated from the expression for the range

$$R = \frac{m^{1/3}}{\beta} h(\xi) \left\{.5140 - 1.0358 \ln \frac{m^{1/6}}{V_0} \left(\frac{g}{\beta}\right)^{1/2}\right\} \qquad (3\text{-}18)$$

Thus

$$\left(\frac{\partial m}{\partial R}\right)_{\alpha_0,\phi,m_1} = \frac{\beta}{h(\xi)} \frac{3\,m_1^{2/3}}{\left\{-.0039 - 1.0358 \ln\left[\frac{m^{1/6}}{V_0}\left(\frac{g}{\beta}\right)^{1/2}\right]\right\}} \qquad (3\text{-}19)$$

To evaluate this integral, an approximation for $F(m,\alpha_0,\phi)$ is required. A reasonable approximation to the arena data is the Thomas (1944) approximation

$$F(m,\alpha_0,\phi) = N_0(\alpha_0,\phi) \exp\left\{- (m/\mu(\alpha_0,\phi))^{1/3}\right\}$$

where $N_0(\alpha_0,\phi)$ and $\mu(\alpha_0,\phi)$ are parameters indicating, respectively, the total number of fragments per unit solid angle of α_0 and ϕ_0 and one-sixth the mean fragment mass in the direction given by α_0 and ϕ.

From tnis expression for $F(m,\alpha_0,\phi)$, it follows that

$$f(m,\alpha_0,\phi) = \frac{N_0(\alpha_0,\phi)}{3\mu^{1/3}(\alpha_0,\phi)m^{2/3}} \exp\left\{-(m/\mu(\alpha_0,\phi))^{1/3}\right\} \qquad (3\text{-}20)$$

Then, with $\xi = \sin\alpha_0$ as the integration variable,

$$q(R,\phi) = \frac{\beta}{R} \int_0^1 \frac{d\xi N_0(\alpha_0,\phi)}{\{\mu(\alpha_0,\phi)\}^{1/3} h(\xi)} \frac{\exp\left\{-[m_1(R,\alpha_0,\phi)/\mu(\alpha_0,\phi)]^{1/3}\right\}}{\left\{-.0039 - 1.0358 \ln\left(\frac{m^{1/6}}{V_0}\left(\frac{g}{\beta}\right)^{1/2}\right)\right\}} \qquad (3\text{-}21)$$

If the source is isotropic, the expression simplifies somewhat.

$$q_I(R) = \frac{\beta N_0}{R\mu^{1/3}} \int_0^1 \frac{d\xi \; \exp\left\{-(m_1(R,\alpha_0)/\mu)^{1/3}\right\}}{h(\xi)\left[-.0039 - 1.0358 \ln\left(\frac{m^{1/6}}{V_0}\left(\frac{g}{\beta}\right)^{1/2}\right)\right]} \qquad (3\text{-}22)$$

This approximate calculation is checked by calculating the far-field fragment density in the side spray direction for a single munition with its axis horizontal. The values for μ and V_0 were obtained from the arena data by averaging these numbers in the range $60° < \psi < 120°$, where ψ is measured from the axis of the munition extended, $\psi = 0°$ denoting the nose end of the munition. Table 3-1 shows the values used in this calculation.

Table 3-1

INITIAL FRAGMENT PARAMETERS - SIDE SPRAY
DIRECTION - AVERAGED FROM ARENA DATA

Munition	Explosive	$N_0\left(\dfrac{\text{Fragments}}{\text{Steradian}}\right)$	$V_0\left(\dfrac{\text{ft}}{\text{sec}}\right)$	μ(lbs)	$\kappa\left(\dfrac{\text{gr}}{\text{in}^3}\right)$
155 mm shell	TNT	500	4000	.010	660
175 mm shell	Comp B	3000	5000	.00429	660
500 lb bomb	H-6	4500	7000	.00286	590
750 lb bomb	Tritonal	6000	8000	.00429	590

In the side spray direction, there is no dependence of any parameters on either α_0 or ϕ, and the integral takes on the isotropic form (Eq. 3-22). The values of q for these four munitions were calculated by numerically evaluating this integral. The results are shown in Figures 3-11 through 3-14. Feinstein's (1972) calculated values of q in the direction $\psi = 90°$, obtained by numerical integral of the arena data over the unit hemisphere is shown for each case. The two models have the same general trend and agree throughout the range 500 ft-2000 ft to within a factor of 2.

An estimate of the error induced in the calculation of q when the ballistic range approximations of the above are used was obtained by comparing the solution for the 500 lb bomb with a calculation using the tabular values of range from the numerical solution to the equations of motion. The error in q was from 0.15% to 0.50%. The error was primarily at
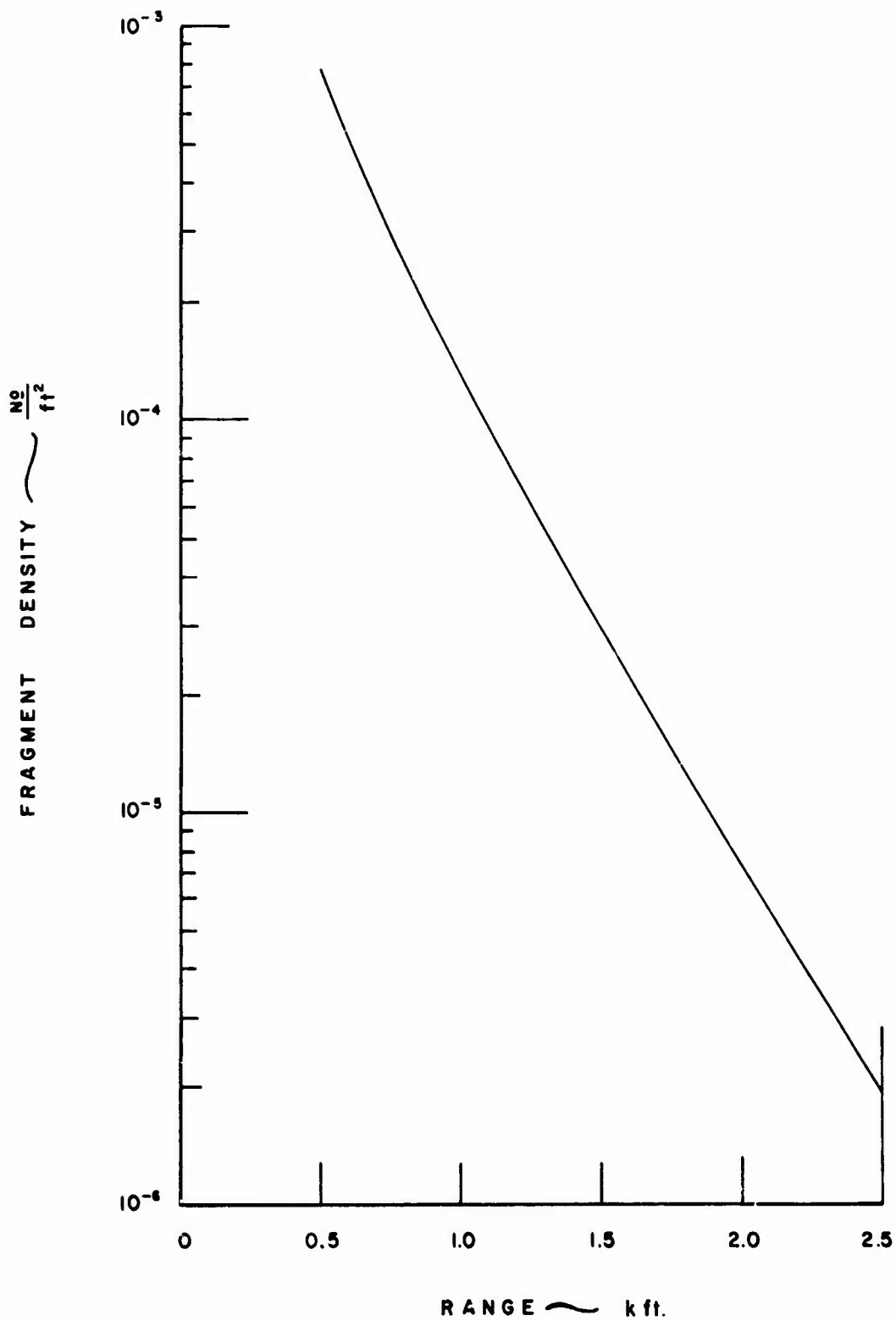
Figure 3-11, SINGLE MUNITION FRAGMENT DENSITY VERSUS RANGE M107
155mm PROJECTILE (TNT LOADED SIDE DIRECTION)

34
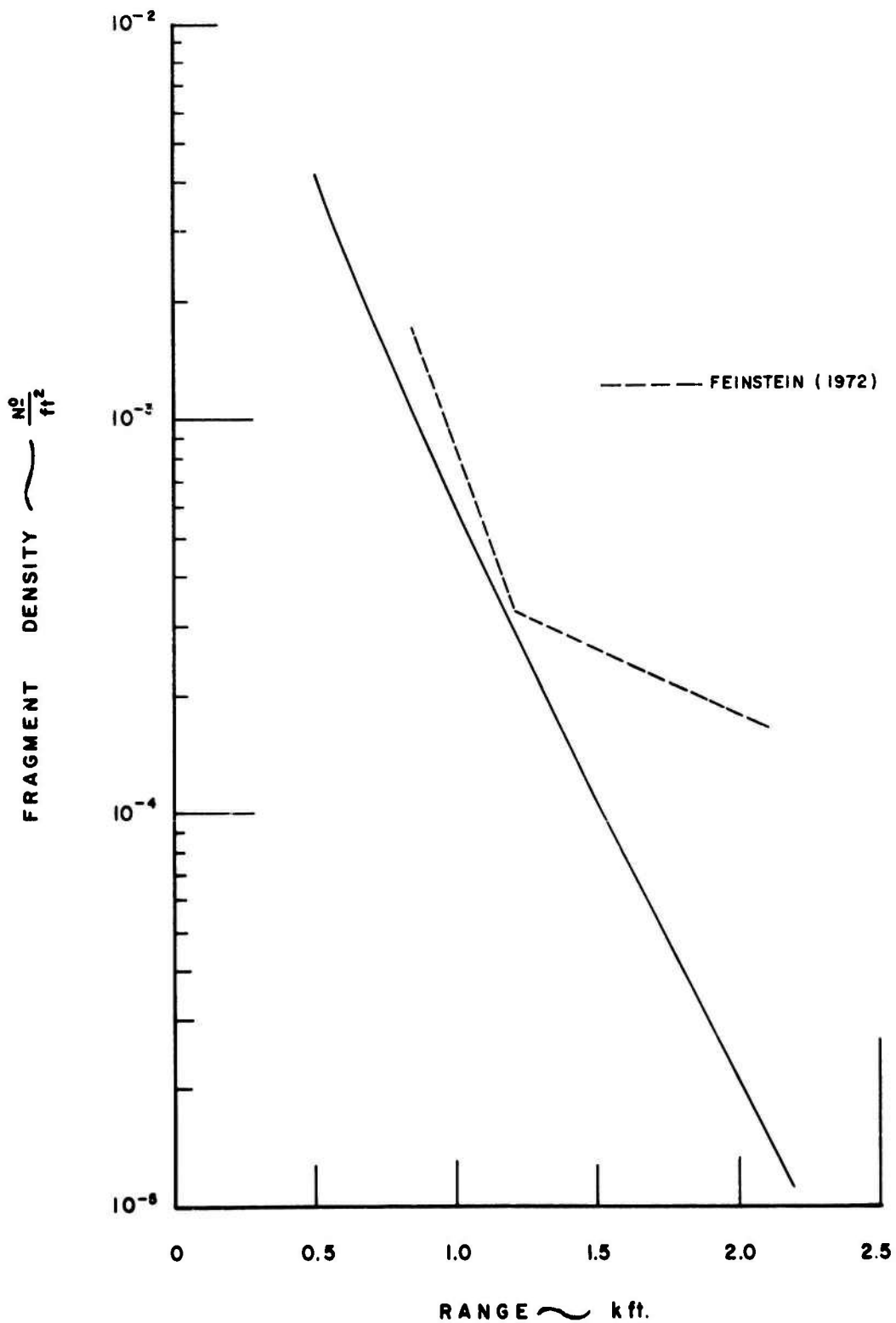
Figure 3-12. SINGLE MUNITION FRAGMENT DENSITY VERSUS RANGE
M 437 A2 175 mm PROJECTILE (SIDE DIRECTION)
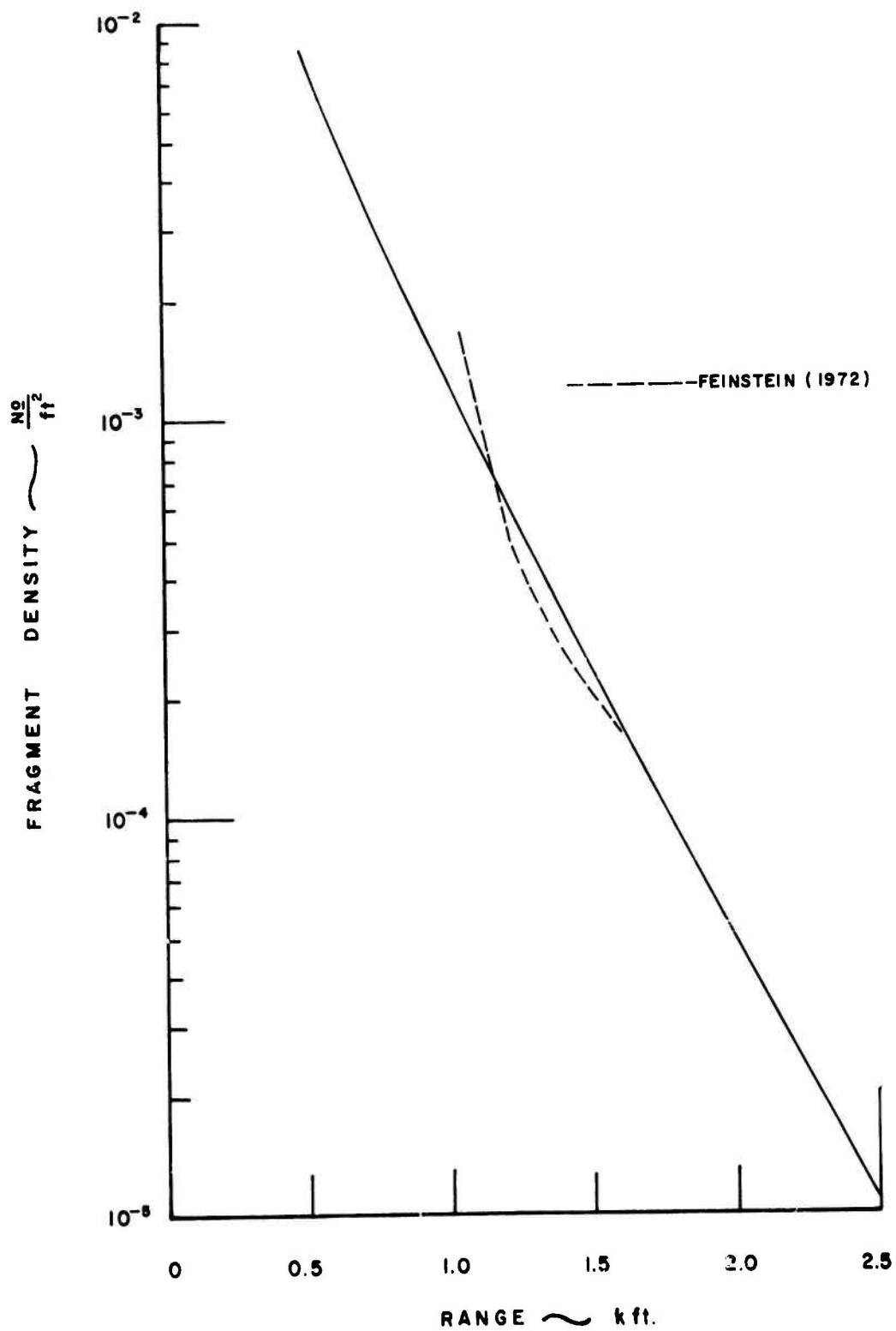
Figure 3-13, SINGLE MUNITION FRAGMENT DENSITY VERSUS RANGE
M117 750-lb. BOMB (SIDE DIRECTION).
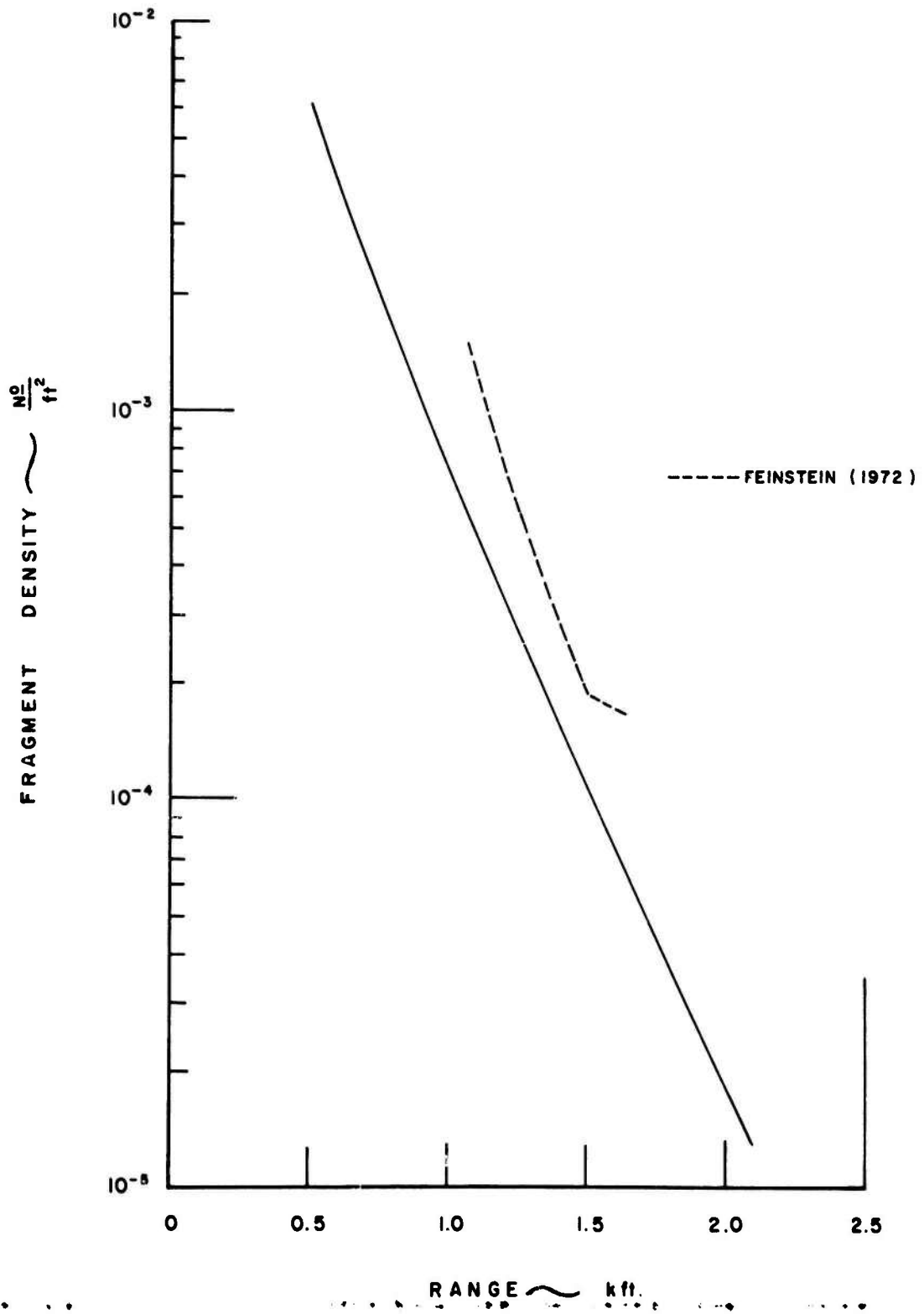
Figure 3-14, SINGLE MUNITION FRAGMENT DENSITY VERSUS RANGE
MK 82 500-lb. BOMB (SIDE DIRECTION)

very small $\alpha_0 (0. < \alpha_0 < 5°)$ or large $\alpha_0 (\alpha > 50°)$, where the integrand is small.

From an examination of the integrand for the approximate integration over α_0, a very simple and crude approximation to q may be obtained.

$$q \approx \frac{\hat{A}}{R} \exp (-\hat{B}R) \qquad (3-23)$$

where $\hat{A}$, and $\hat{B}$ are constants for each weapon (Table 3-2).

Table 3-2

CONSTANTS $\hat{A}$, $\hat{B}$ FOR APPROXIMATION TO q

Munition	$\hat{A}$ (No/ft)	$\hat{B}$ ($\times 10^3$ ft^{-1})
155 mm projectile	.8177	1.898
175 mm projectile	6.103	2.380
500 lb bomb	10.32	2.711
750 lb bomb	11.68	2.309

This crude approximation agrees with the integral to within 10% for $500 \leq R \leq 2000$ ft.

This chapter has described a rapid technique for estimating fragment densities and mass densities in the far-field. Further, the results of this approximate procedure compare favorably with Feinstein's (1972) computer code predictions. The basic parameters that describe the single munition are the initial fragment velocity, the ballistic density of the fragments and the form of the probability density function giving the number of fragments in any mass interval. When the more complicated problem of munition stacks and stacks within igloos is attached, the obvious place to start is to assess the changes in the source parameters induced by the more complicated configuration.

Chapter IV

ANALYTICAL MODELS FOR STACK AND COVER EFFECTS
ON FAR-FIELD FRAGMENT DENSITIES

4.1 Introduction

In this chapter, several models are described which attempt to explain the effects of the cover and the stack configuration on the far-field fragment density. There are several common features in these models which will be qualitatively summarized here; more detailed exposition of the features will be found in the appropriate sections.

The initial fragment distribution and other initial parameters when a single munition is initiated under the influence of a proper fuze are well defined through physical measurements. When a stack of the munitions is initiated at a single munition and the remaining munitions detonate by sympathetic detonation, induced by either blast or fragment impact, the initial fragment distributions and initial velocities from any single munition in the stack may be drastically altered. For example, Feinstein and Nagaoka (1970), Feinstein (1972a, 1972b) found in the detonation of 1000 (10 x 100 x 1) 155 mm TNT-loaded projectiles, many large fragments none of which ever appeared in the data from any arena tests. Similar observations were made at the Eskimo I test (Weals 1973). Draper and Watson (1970) report altered fragment distribution patterns and increased initial fragment velocities in the nose and base directions from their stack experiments.

The second feature is that fragments from one munition may interact with fragments from other munitions, the blast waves from other munition or a piece of the cover structure. Its velocity will change and its trajectory may be altered.

Consider the simultaneous detonation of adjacent stacked munitions. Fragments emanating from any one weapon will collide and interact with fragments from all the other weapons in the stack. Each collision will result in a change in the speed and direction of each fragment involved in the collision. Hence, the overall effect of the collision processes will be to alter the speed and direction of all fragments involved in the collisions; i.e., the collision process will alter the mass and velocity distributions of the fragments emanating from any one weapon. Furthermore, the altered distributions of weapon fragments will depend on the location of the weapon within the stack and the geometry of the stack.

Now consider another related problem, that of a weapon detonated within an earth-covered igloo. The blast wave from the detonation causes the earth cover to move outwards. Shortly thereafter, fragments from the weapon interact with the earth cover. The situation is similar to that above in that the overall effect of the interaction is also to change the mass and velocity distributions of the fragments from the weapon.

It should be noted that the most complex problem to be considered, that of a stack of munitions detonating within an igloo, can be reduced to the two problems discussed above by adopting the following approach. Essentially all of the fragment-fragment interactions occur within a region limited to the immediate neighborhood of the weapons. Furthermore, it is reasonable to assume that fragments from any one weapon can significantly interact only with fragments from weapons in proximity to each other. The altered fragment mass and velocity distributions for this group of munitions can be transposed to an origin. In effect, a group of stacked weapons can be replaced by a single equivalent weapon that interacts with the earth cover as mentioned earlier.

4.2 Fragment-Fragment Interactions

Since the largest number of fragments from a single munition are ejected to the side, consider only this side-spray and idealize the munition to infinite cylinders. When a single weapon detonates, the cylindrical shell breaks up such that all fragments leave at the same initial velocity. This initial velocity and the mass distribution of the fragments are considered independent of angle and are known. Because the region of concern is the immediate neighborhood of the weapon, the effects of gravity may be neglected, so that the trajectories are straight lines given by:

$$S = \frac{m}{\beta} \ln (1 + \beta m^{1/3} V_o t) \tag{4-1}$$

It is seen that, for a given time, there is a maximum distance beyond which no fragments will be found, and that more massive fragments travel longer distances.

The mass distribution of fragments ejected at any angle is assumed given as

$$f(m) = \frac{1}{3} \left(\frac{1}{m^2 \mu}\right)^{1/3} \exp \{- (m/\mu)^{1/3}\} \tag{4-2}$$

where μ = (average mass)/6 = known constant

Choose a distance, $S = d$, and a time t. Let $\bar{m}$ be the zero of eq. (4-1). The fraction of total fragments of mass greater than $\bar{m}$:

$$\frac{N (\bar{m})}{N_o} = \int_{\bar{m}}^{\infty} f(m) \, dm = \exp \{- (\bar{m}/\mu)^{1/3}\} \tag{4-3}$$

where $N(\bar{m})$ = number of fragments of mass greater than $\bar{m}$.

N_o = total number of fragments

The number of fragments located at a distance greater than d at a given time, t:

$$N(d; t) = N(\bar{m}) = N_0 \exp \{- (\bar{m}/\mu)^{1/3}\} \tag{4-4}$$

Another expression for N(d; t) is simply

$$N(d; t) = \int_V \rho^* \, dV \tag{4-5}$$

where ρ^* = number of fragments of mass $\bar{m}$ per unit volume

In polar coordinates

$$N(d; t) = 2\pi \int_d^{S_{max}} \rho^* \, S \, dS \tag{4-6}$$

Equating eqs. (4-4) and (4-6) leads to ρ^* (d; t, $\bar{m}$), the density of fragments of mass $\bar{m}$, at time t, at distance d:

$$\rho^*(d;t,\bar{m}) = -\frac{N_0}{6\pi d} \left(\frac{1}{\bar{m}^2 \mu}\right)^{1/3} \left(\frac{\partial \bar{m}}{\partial S}\right)_{S = d} \exp \{-(\bar{m}/\mu)^{1/3}\} \tag{4-7}$$

The derivative is found from eq. (4-1). Eq.(4-7) yields fragment densities only in the immediate neighborhood of the weapon.

Now consider two munitions with their axes parallel which are detonated at the same time. If no collisions between fragments are considered, fragment densities from two weapons would be simply the superposition of the fragment densities from each weapon individually. However, if fragments from both weapons occupy the same region of space at the same time, there will be a finite probability of collision. We calculate the fraction of a differential volume element (at a given distance and time) occupied by fragments from each munition and set the probability of collision proportional to their product.

Refer to the collision geometry of Figure 4-1. Then the probability of collision, $P(d_1, d_2; t)$, is given by

$$P(d_1, d_2; t) = \frac{\Delta V_1 \Delta V_2}{(\Delta V)^2} \qquad (4\text{-}8)$$

ΔV_1 = volume occupied by fragments of mass,

m, from weapon 1

ΔV_2 = volume occupied by fragments of mass,

m, from weapon 2

Now $\dfrac{\Delta V_i}{\Delta V} = \left[\dfrac{\text{No. of fragments of mass } m_i}{\text{unit volume}}\right] \times \left[\text{volume of fragment of mass } m_i\right]$

or $\dfrac{\Delta V_i}{\Delta V} = \rho_i{}^*(d_i; t, m_i) \dfrac{m_i}{\rho_f}$

where ρ_f = fragment mass density

Hence, in this case,

$$P(d_1, d_2; t) = \frac{1}{\rho_f^2} \left[\rho_1{}^*(d_1; t, m_1)\right]\left[\rho_2{}^*(d_2; t, m_2)\right] m_1 m_2 \qquad (4\text{-}10)$$

Equation (4-10) yields the probability of collision between a fragment of mass m_1 and a fragment of mass m_2 occurring at the point (d_1, d_2) at time t.

Obviously, the fragments which collide are the only ones which undergo velocity transformations; the fragments which do not collide proceed on their original trajectories. Hence, the number of collisions occurring at a given point in space must be known, and can be calculated as:

$$N_{coll}(d_1, d_2; t, m_1, m_2) = \left[N_1(d_1, d_2; t, m_1)\right]\left[N_2(d_1, d_2; t, m_2)\right]\left[P(d_1, d_2; t)\right]$$
$$(4\text{-}11)$$

where N_{coll} = number of collisions occurring at (d_1, d_2) at time t

between fragments of mass m_1 and m_2
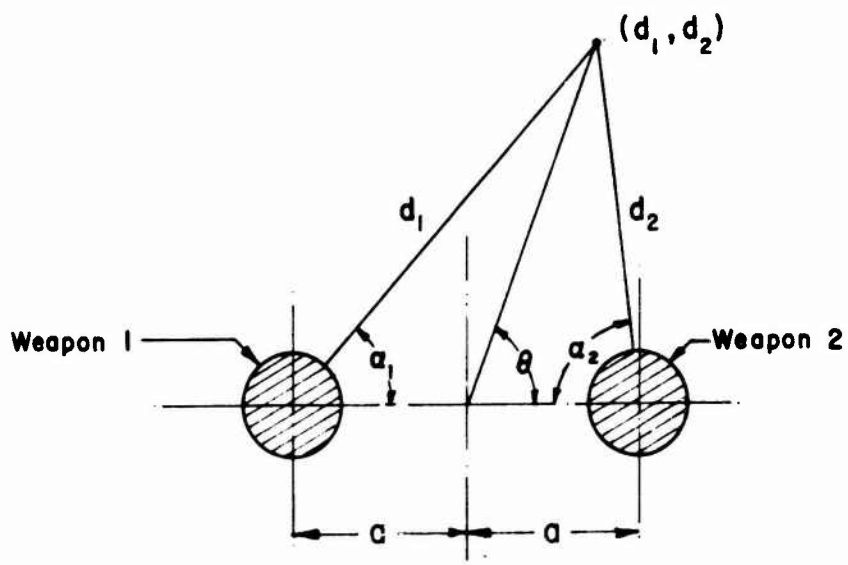
Figure 4-1, INTERACTION GEOMETRY

$N_i(d_1,d_2;t,m_i) =$ number of fragments of mass m_1 from weapon i

at (d_1, d_2) at time t

$$\text{Now assume } N_i(d_1, d_2; t, m_i) = \begin{Bmatrix} \text{Number of fragments of mass } m_i \text{ from} \\ \text{weapon i present at } (d_1, d_2) \text{ at time} \\ \text{t in the absence of weapon j} \end{Bmatrix}$$

$$- \begin{Bmatrix} \text{Number of fragments of mass } m_i \text{ from} \\ \text{weapon i which have collided prior to} \\ \text{reaching } (d_1, d_2) \end{Bmatrix} \tag{4-12}$$

Inherent in this assumption is the limitation that each fragment can undergo only one collision. $N_i(d_1, d_2; t, m_i)$ can be expressed in terms of $\rho_i^*(d_i; t, m_i)$ and $P(d_1, d_2; t)$, and is therefore a known function.

Then, the number of collisions for all space and time are known for all values of m.

The number of fragments from each weapon undergoing collisions at any point in space at any time is equal to the number of collisions occurring at that point at that time, and is known. The collision process is illustrated in Figure 4-2. It should be noted that the case illustrated is for the situation in which each fragment maintains its identity; i.e., fragments do not split due to the collision. The equations describing the collision of two fragments are

$$m_1 V_{1_k} + m_2 V_{2_t} = m_1 V_{1_t}' + m_2 V_{2_t}'$$

$$m_1 V_{1_n} - m_2 V_{2_n} = m_1 V_{1_n}' + m_2 V_{2_n}'$$

$$e(V_{1_n} + V_{2_n}) = V_{1_n}' + m_2 V_{2_n}'$$

$$V_{1_t}' = V_{1_t}$$

$$V_{2_t}' = V_{2_t}$$

The subscripts 1 and 2 refer to fragments 1 and 2; the unprimed values refer to conditions before impact and the primed, after impact. The first two equations describe the conservation of momentum, while the third describe the energy loss; e is the coefficient of restitution; e = 1 for perfectly elastic impact and e = 0 for perfectly inelastic impact; in general, $0 \le e \le 1$.

For the number of fragments which collide, N_i, the results of the collision can be determined. Note that the coefficient of restitution, e, is a parameter which must be supplied; this allows the results of a collision to be determined assuming perfect elasticity, perfect plasticity, or cases in between. At the high velocities expected in this problem, $e \sim 0$. From the manner in which the results of the collision process vary in space, the number of collisions occurring in space, and the number of fragments which do not collide, the new mass and velocity distributions as angular functions can be determined.

An approximation is now devised for the estimation of the interaction effects of two munitions. The motion of a typical fragment mass, m_1, ejected from munition 1 at the angle α_1 is calculated under the following assumptions. We ignore the changes in trajectory direction and approximate the additional resistance to the test fragment as drag effected by a continuous cloud of fragments emanating from munition 2. First the number density at (d_2, α_2) at time t from the second munition is calculated. This is given by Eq. (4-7). With the mass distribution function described as

$$\rho^*(d_2;t,m) = \frac{N_0}{6\pi d_2 \mu^{1/3}} \frac{m^{1/3}}{d_2 - V_0 t \exp(-\beta m^{1/3} d_2)} \exp\left[-(m/\mu)^{1/3}\right]$$

$$\text{with} \quad d_2 < V_0 t \tag{4-13}$$
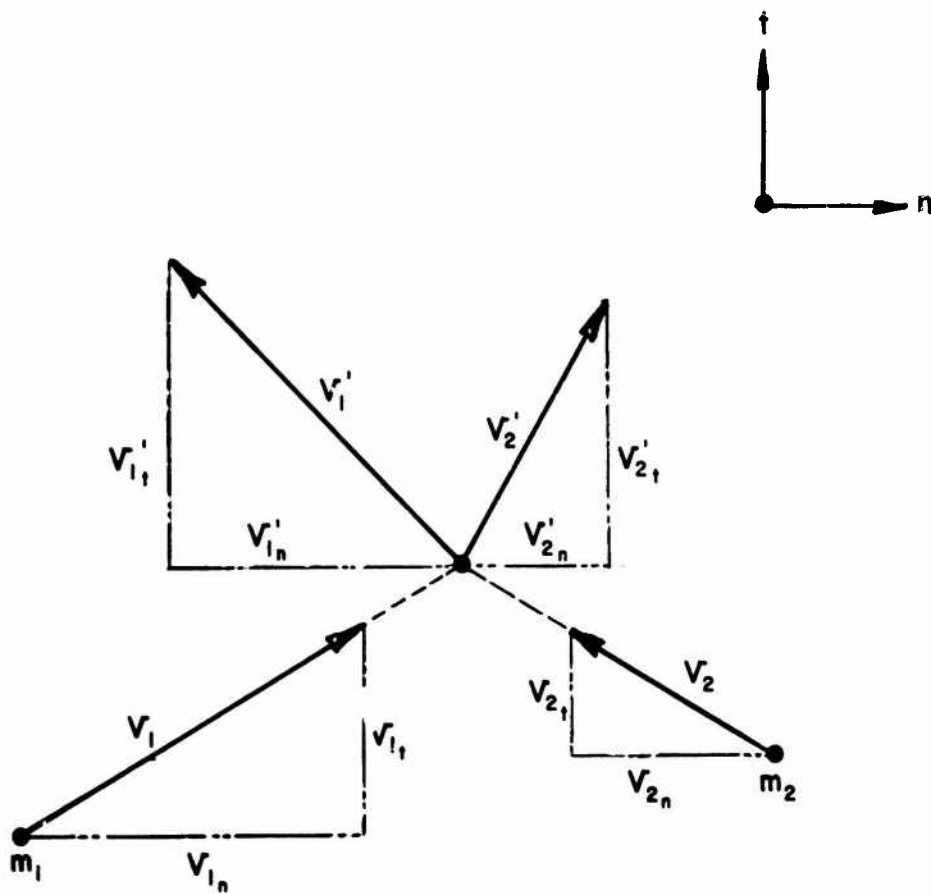
Figure 4-2, FRAGMENT COLLISION PROCESS

This density is calculated for the four munitions of interest in this report. Figure 4-3 shows ρ^*, the number density of fragments versus d, for the second munition (in this example, the M117 750-lb bomb).

The density curves show a slow rise from the arrival of the first (and largest fragments) followed by a rapid rise near the propagation of the fragments with mean mass, 6μ. Effectively the fragments propagate outwards as a shell. The propagation characteristics of this shell are those associated with the mean fragment mass. At this shell radius, the mass density rises rapidly to a relatively large value. Hot, condensed combustion products from the detonation of the explosive filler are contained within this shell. At these early times, the hot gases have not had time to expand and their density is very nearly that of the solid explosive.

Now if the test fra $\sim\sim^+$ is ejected at such an angle that it misses the shell of fragments from the second munition, the probability of it colliding with any fragments from the shell is very small. If, on the other hand, the fragment intersects this shell, the probability of interaction is almost unity. As a matter of fact, many such collisions may occur. The best model for the motion of the fragment is that the fragment must perforate a continuous steel shell of approximately the same thickness as the original munition. The drag force for this is

$$F_D = \beta m^{1/3} V^2 \frac{\rho_{cloud}}{\rho_{air}} \qquad (4-14)$$

. We calculate the relative reduction in the fragment velocity as it perforates the shell

$$\frac{V}{V_{air}} = \exp\{-(\rho - \rho_{air})h\} \qquad (4-15)$$

Calculations of this reduction in velocity for fragment mass up to 0.01 lb, and original munition wall thickness up to .01 ft shows that the
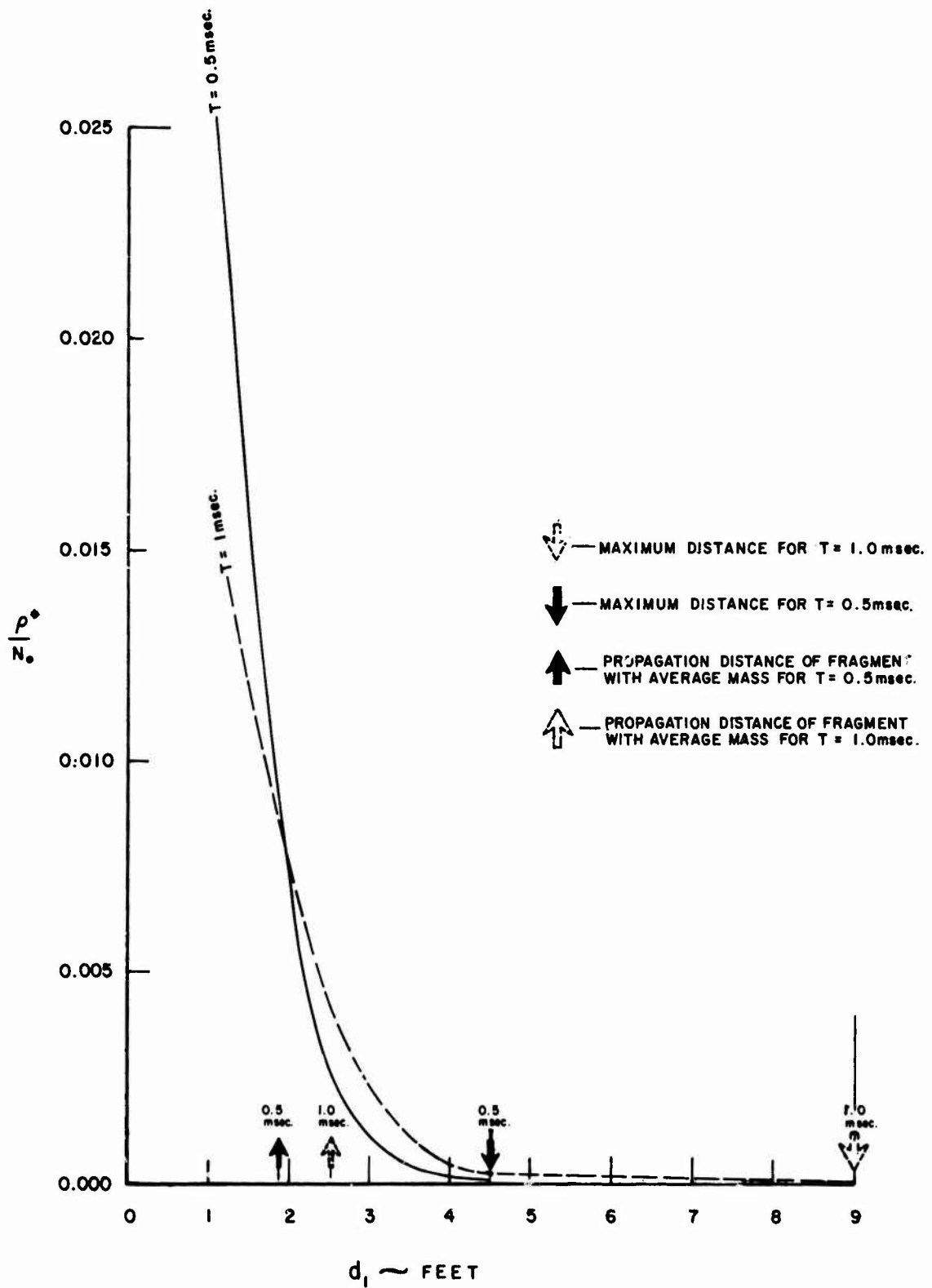
Figure 4-3, NUMBER DENSITY OF FRAGMENTS FROM A M117 750-lb BOMB ALONG A RAY.

49

velocity reductions are greater than 50%. For 1 lb fragments, the velocity reduction is about 10%.

After penetration of the shell, the test fragment must move through the hot, condensed combustion products. This material is about one fourth as dense as steel and the length of traverse of a fragment within the hot, dense gas is at least an order of magnitude larger than the traverse through the steel shell. Thus a 1-lb fragment's velocity will be reduced by roughly 40% and any fragment smaller than .25 lb will be effectively stopped.

Thus, the test fragment from one munition is effectively stopped if it intersects the shell with mass μ expanding from the second munition. The limiting value of α_1, for which fragments of mass m_2 just intercept this shell from the second munition can be readily expressed.

$$\tan \alpha_1 = \frac{d_2}{d_1} \tag{4-16}$$

where (referring to Figure 4-1)

$$d_1 = r + \beta m^{1/3} \ln(1 + \beta m^{1/3} V_o t)$$
$$d_2 = r + \beta \mu^{1/3} \ln(1 + \beta \mu^{1/3} V_o t)$$

with r the radius of the munition.

Bounds on α_1 are

$$\sin^{-1} \left(\frac{r}{2a}\right) \leq \alpha_1 \leq \frac{\pi}{4} \text{ when } m \geq \mu$$

where a = intermunition spacing

For test fragments with $m \sim \mu$ expand the logarithms in a power series

$$\tan \alpha_1 = \frac{r + V_o t - \beta \mu^{1/3} V_o^2 t^2}{r + V_o t - \beta m^{1/3} V_o^2 t^2} \tag{4-17}$$

If $m \geq \mu$, but nearly equal, $\alpha_1 \sim \frac{\pi}{4}$

When fragments that are to be hurled to large distances are considered, only fragments with $m > \mu$ need to be considered, but the majority

of those are not too much larger than μ. Thus the value of $\alpha_1 = \frac{\pi}{4}$ as the limiting value for interception of the fragments of interest is a good approximation. It should be noted that the assumption $a \sim d_1$ is required for this approximation to be valid. If the intermunition spacing is significantly larger, the limiting value of d_1 will be correspondingly smaller.

The conclusion is reached that a fragment from one munition will be completely stopped by the fragments and the gases from an adjacent munition if the (test) fragment intersects any fragment with mass less than or equal to 6μ, and the only fragments that effectively escape from the adjacent munition have their original trajectories outside a 45° angle from the line joining the centers.

The case of three or more adjacent stacked munitions, while more complex in terms of mathematics, can easily be detailed on a conceptual basis by extending the approach discussed here. Only three, or perhaps four, adjacent weapons need to be considered, since fragments from a weapon will interact significantly only with fragments from weapons adjacent to each other. Stack geometries to be considered for 3 and 4 weapons are shown in Figure 4-4. These geometries allow determination of the interactions among fragments from the weapons shown in Figure 4-5.

The determination of the mass and velocity distributions of fragments from a multiple-weapon stack is achieved by considering portions of the stack as shown in Figure 4-5, for example, replacing them by equivalent single weapons, and repeating the process until the entire stack is replaced by an equivalent single weapon.

Consider, for example, three collinear munitions. The fragments that emanate from the center munition will be stopped by the adjacent munition on either side in an angular range up to 45° from the line joining

2 WEAPONS

3 WEAPONS

4 WEAPONS

Figure 4-4, STACK GEOMETRIES CONSIDERED FOR ANALYSIS

52
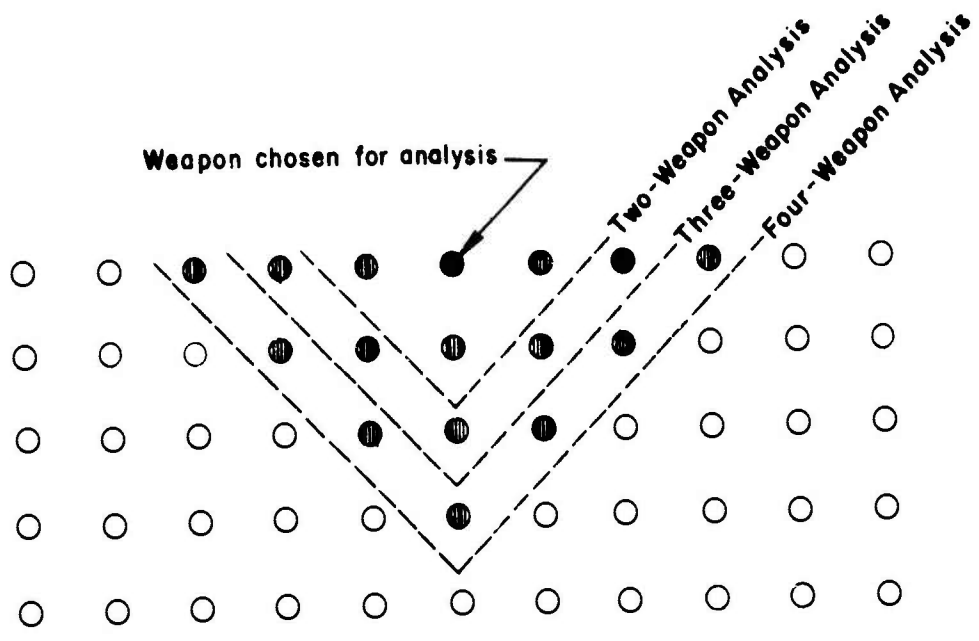
Figure 4-5. FRAGMENT-FRAGMENT INTERACTIONS DETERMINED BY ANALYZING THE CONFIGURATIONS OF FIGURE 4-4 (EQUAL SPACING BETWEEN WEAPONS).

their centers. Each end munition will be affected as in the case of just
two munitions. It is a very simple and straightforward process to build up
more complicated stack models based on this approximate model. It suffices
to note that no fragments will escape if a munition is completely surrounded.

All fragments from munitions within the stack are sufficiently retarded
by their neighbors such that they will not reach the far-field. The frag-
ments from one munition in the surface layer from 45° to 135° will be thrown
to the far-field. Thus the following model for the effective number of
munitions in a stack is generated. Let N_S be the number of munitions in this
side layer and N_T the number of munitions in the top layer. Then the far-
field fragment density is approximately

$$q(R) = N_S \int_0^{\pi/4} F_S(\alpha_0, R) d\alpha_0 + N_T \int_{\pi/4}^{\pi/2} F_T(\alpha_0, R) d\alpha_0 \qquad (4\text{-}18)$$

where $F(\alpha_0, R)$ is defined by the approximation defined in Chapter III. If
both layers have the same munition orientation relative to the normals
to the respective surfaces, we can approximate the integrals as

$$q(R) = (0.9\ N_S + 0.1\ N_T) q_1 \qquad (4\text{-}19)$$

where q_1 is the far-field fragment density from a single munition.

In this model we have neglected the changes in direction of the frag-
ments due to collision. For the larger fragments that would interact only
with the larger fragments from the adjacent munition, the probability of
collision is very small. One other feature that has been neglected is
that the blast waves from two adjacent munitions will interact and the
resulting pressure field will alter the trajectories of fragments. The

blast interaction effects are minimal in the direction normal to the line joining the munitions.

4.3 Fragment-Cover Interactions

Look next at the effect of the igloo structure on the fragments. We assume that the fragment distribution from the stacks are known and that they can be represented on a unit hemisphere located within the confining structure. At each direction on this unit hemisphere, the initial fragment velocity, the mass distribution and the shape of the fragments are known. Now if there were no earth covers, it would be simple matter to compute the far-field fragment density. The cover, however, will retard or stop some or all of the fragments. In the next few paragraphs, we will construct three models that represent possible interactions of the cover with the fragments.

The typical earth-covered igloo structure is a cylindrical steel arch, with a rectangular floor plan; the front and rear wall are vertical. The rear wall and the cylindrical portions are covered with earth, (Figure 4-6 shows the cross section through the cylindrical arch); the earth cover has a minimum of two feet at the crown. The front wall is of reinforced concrete and has doors of structural steel plate.

When the stack detonates, a fraction of the energy goes into breaking up the munition cases, a fraction into kinetic energy and the fragments to be thrown out, and a fraction remains in the blast wave. This last fraction, which remains in the air blast, can be estimated by the Fano formula. The blast will interact with cover and cause it to deflect and break up. A certain fraction of this blast energy will be absorbed in the breakup of the cover and in the kinetic energy of the cover fragments, (which will consist of steel arch fragments, earth clods, concrete fragments and pieces
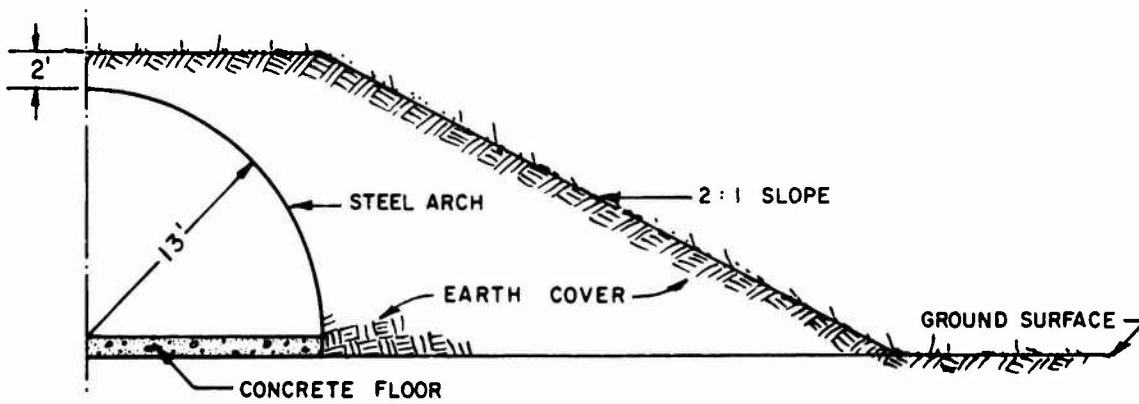
Figure 4-6, CROSS SECTION THROUGH ARMY STANDARD IGLOO MAGAZINE

56

of the door). From the studies of the blast that is propagated to large distances from explosions within igloos this fraction of energy absorbed by the cover is quite small, being of the order of 10% of the blast energy released from the open stack. If all of this absorbed energy shows up as kinetic energy of the earth cover, the typical earth cover fragment velocity will be of the order of 1000-2000 ft/sec.

The assumption is made that in the case of a stack of weapons contained within an earth cover all interactions between fragments from adjacent weapons occur substantially before any fragments interact with the earth cover. With this assumption, the stack can be replaced by a single equivalent weapon with known mass and velocity distributions.

Consider a cylindrical shell contained within a semi-cylindrical earth cover. When the munition is detonated, the resulting blast wave creates an overpressure on the inside of the earth cover, causing it to move radially outwards in a known manner*, see Figure 4-7. The earth cover is considered to have no strength in the tangential direction. As the earth cover moves out, it breaks up into small fragments which are contained between an inner and an outer radius. The cover fragments' mean motion can be determined from Newtons' Law. If gravity is again neglected, all interactions between fragments and the earth cover occur along radii; i.e., the only result of a fragment-cover interaction is to alter the magnitude of a fragment's velocity, but not its direction.

---

* Depending on the relative sizes of the stack and the igloo, either the blast wave or the fragments will arrive at the earth cover first. The effect of the blast wave in either case is considered independent of the effect of the fragments; the blast wave merely specifies initial conditions for the fragment-cover interactions. The following analysis applies in either case.
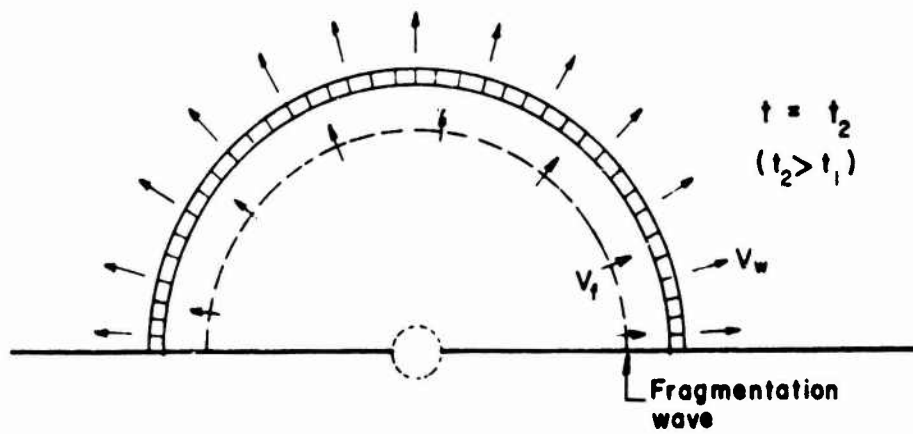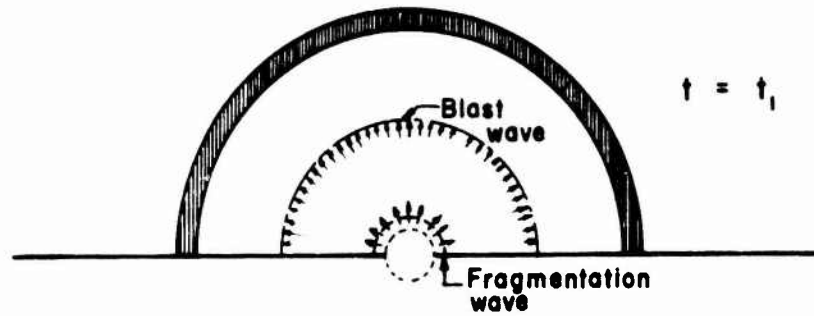
Figure 4-7, MODEL FOR FRAGMENT - COVER INTERACTIONS (ASSUMING BLAST WAVE ARRIVES AT COVER BEFORE FRAGMENTATION WAVE).

Define three regimes: pre-interaction, interaction, and post-inter-
action. Only air drag affects the fragments during the pre- and post-
interaction regimes. If the cover is considered as a continuum of infinitesi-
mally small particles, the retardation force between the fragment and the
earth cover during the interaction regimes can be expressed in the form of
a drag force:

$$F_R = (1/2)\rho_e C_D A_f (V_f - V_w)^2 \qquad (4-20)$$

where

ρ_e = mass density of the earth cover

C_D = drag coefficient

A_f = effective cross-sectional area of the fragment

V_f = speed of fragment

V_w = mean speed of cover

There are at least two convenient ways to approximate the motion of the
earth cover after detonation. One method is to assume that the thickness
of the earth cover remains constant as the cover moves; this specifies
that the density of the cover decreases as $(1/R^2)$ in order to conserve mass.
The other view is to assume that the density of the cover is a constant,
so that the thickness of the cover decreases as $(1/R^2)$ as the cover moves out.

Solutions of the equations of the pre-interaction regime specifies at
what radius and time the interaction between a fragment of mass m and the
earth cover will commence; the solution yields the initial values required
for the solution of the equations of the interaction regime. The inter-
action equation determines the velocity with which the fragment leaves
the wedge after passing through it. It should be obvious that some fragments
will not penetrate through the cover. By considering the masses and velo-
cities of fragments as specified by these distributions for the weapon, it
is possible to estimate the fragments which will and will not penetrate the

cover. It can be seen that the effect of the cover is to alter the mass and velocity distributions of the fragments. These new distributions are assumed again to be the initial ones for a single equivalent weapon, and estimations of far-field fragment densities and damage levels proceed according to GARD's current technique.

Based on these comments, the first model to approximate the effect of the earth cover is presented. The earth cover moves out very slowly compared with the fragments from the stack and the fragments from the stack must perforate an earth layer which is essentially intact. The earth cover, is however broken up and behaves essentially as a fluid. The main effect of the cover is increased drag on the fragments. Experiments by Allen et al. (1957a, 1957b) on the retardation of steel spheres by sand show that, for high fragment velocities, the main retardation is essentially of this form; i.e., the resisting force on a fragment is

$$F = (\frac{1}{2}) \rho \ C_D \ V^2 A = \beta^* m^{1/3} V^2$$

where ρ_s is the sand density

C_D is 1.6 for spheres perforating sand

V is the fragment velocity

A is the presented are of the fragment

$\beta^* = \beta \rho_s / \rho_{air}$

We assume that the soil cover resists the fragment in the same way as sand. In this model, the effect of the cover is to reduce the fragment's velocity as it passes through the cover. Since the cover does not move appreciably during the perforation process, we assume it is stationary and that the fragment must penetrate the original thickness. Further we can neglect the cover velocity in calculating the resisting force on a

fragment. Denoting the distance from the munition stack to the inner wall of the igloo by d, and the thickness of the igloo by h (where d and h are functions of the initial angle and azimuth angle) the fragment velocity at the time the fragment strikes the inner wall, is

$$V_1 = V_0 \exp(-\beta m^{-1/3} d) \qquad (4\text{-}22)$$

The fragment velocity when it emerges from the earth layer is

$$V_2 = V_1 \exp(-\beta^* m^{-1/3} h) \qquad (4\text{-}23)$$

By comparing the fragment velocity, V_2, with the fragment velocity at a distance, r + h, in air alone, we define an effective initial velocity $V_{0_{eff}}$

$$V_{0_{eff}} = V_0 \exp(-\beta^* m^{-1/3} h)$$

The effect of the earth cover, in this model is to retard the fragment; the magnitude of this effect can be represented as a fictitious lower initial velocity on the unit hemisphere. Using the value of $\rho_{earth} = 100$ lb/ft^3, $C_D = 1.60$ and the value of h as a function of elevation angle from the center of the igloo, we can readily calculate the far-field fragment density (we assume the hemisphere data for the side-spray direction). Figure 4-8 through 4-11 show the reduction in far-field fragment density for a single munition. This model is denoted as the penetration model on the figures.

There is yet another way to consider the action of the earth cover as it moves out; i.e., it breaks up into chunks rather than infinitesimal particles. The problem then becomes very similar to that of the two side-by-side munitions whose fragments interact. This approach involves calculation of the probability of collision, and the effects of the interaction process are calculated essentially identically to the method described in
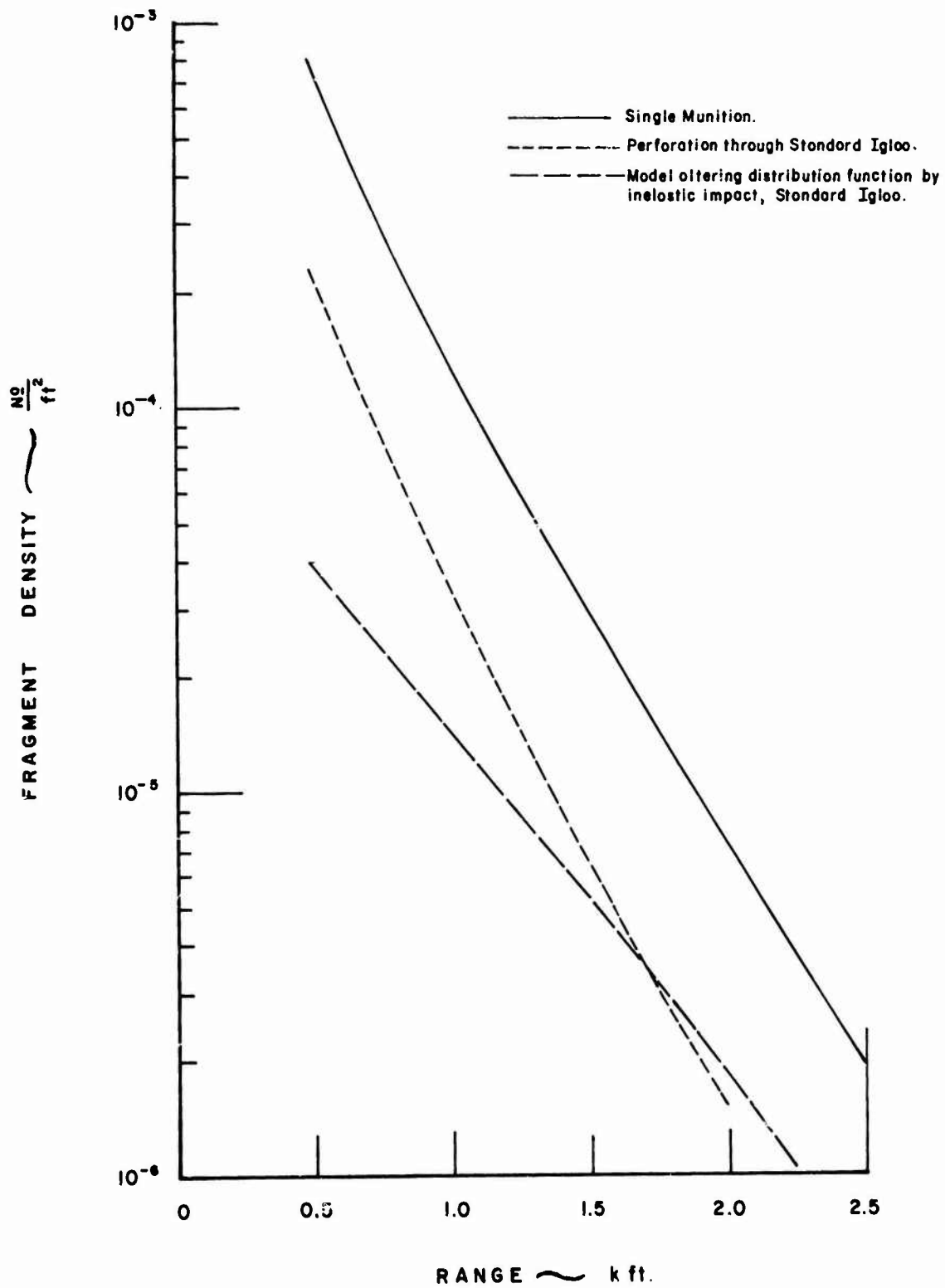
Figure 4-8. EFFECT OF EARTH COVER ON FRAGMENT DENSITY VERSUS RANGE
M107 155 mm PROJECTILE TNT LOADED (SIDE DIRECTION)

62
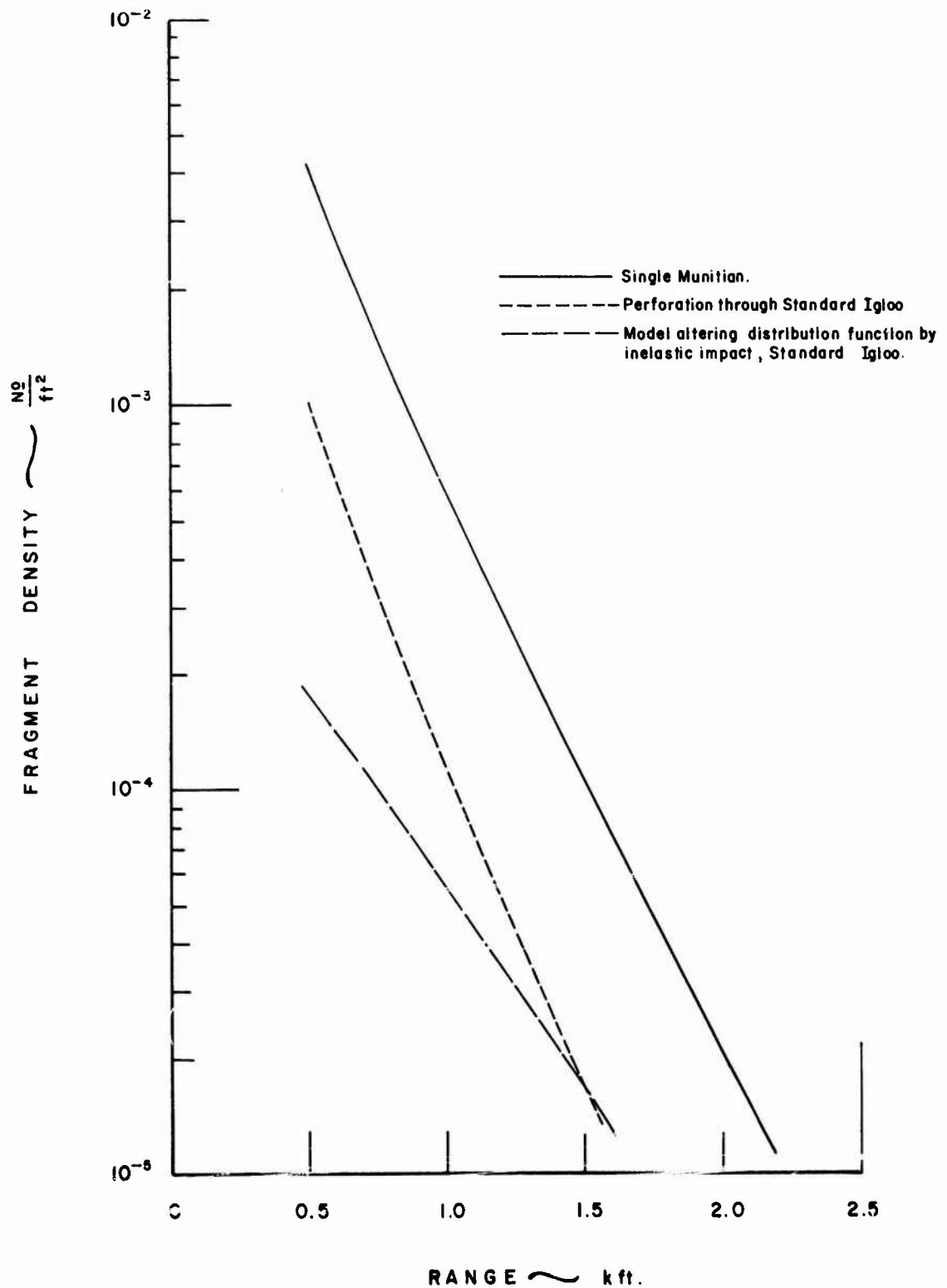
Figure 4-9, EFFECT OF EARTH COVER ON FRAGMENT DENSITY VERSUS RANGE
M437 A2 175 mm PROJECTILE (SIDE DIRECTION)
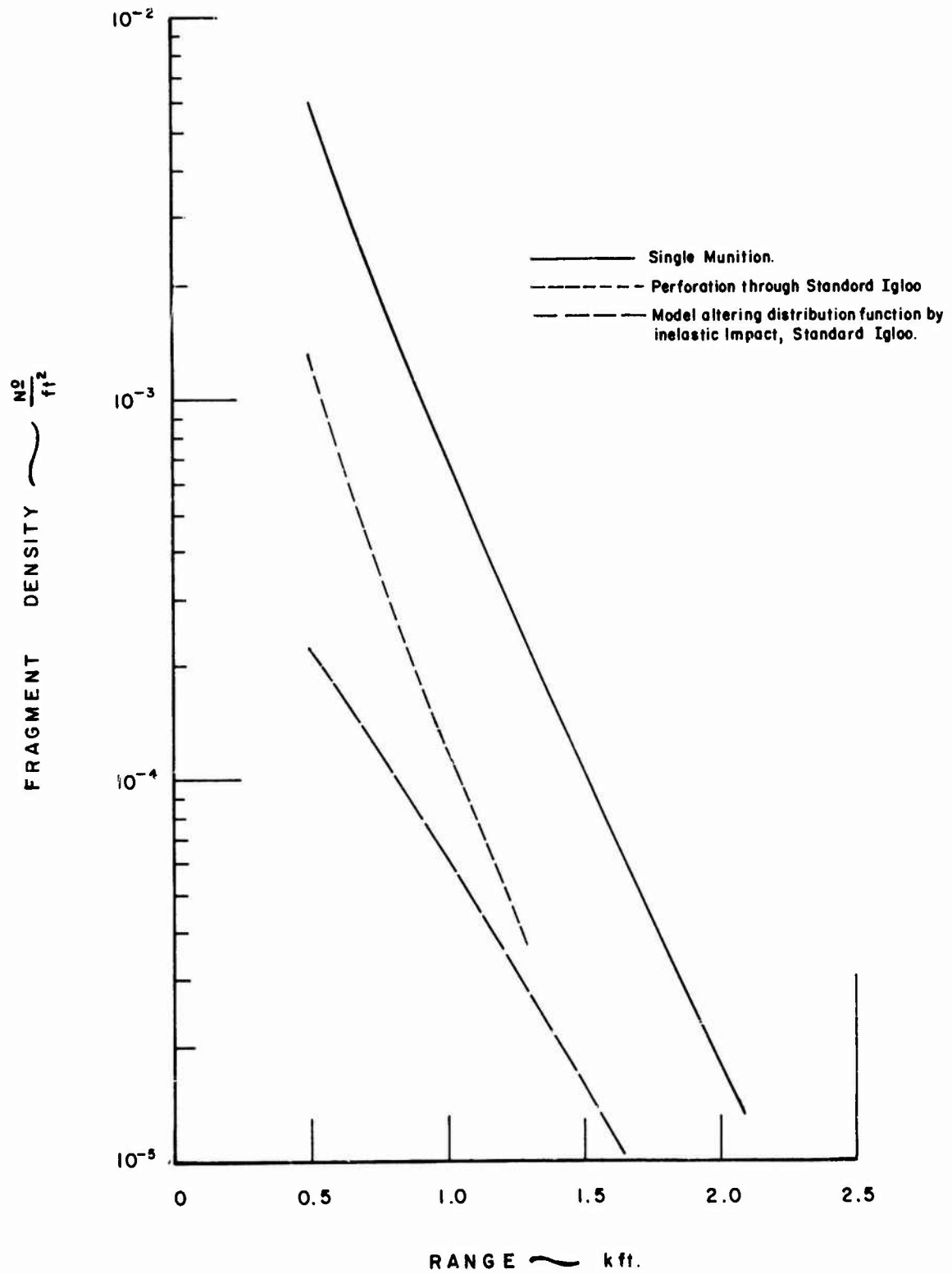
Figure 4-10, EFFECT OF EARTH COVER ON FRAGMENT DENSITY VERSUS RANGE
MK 82 500-lb BOMB (SIDE DIRECTION)

64
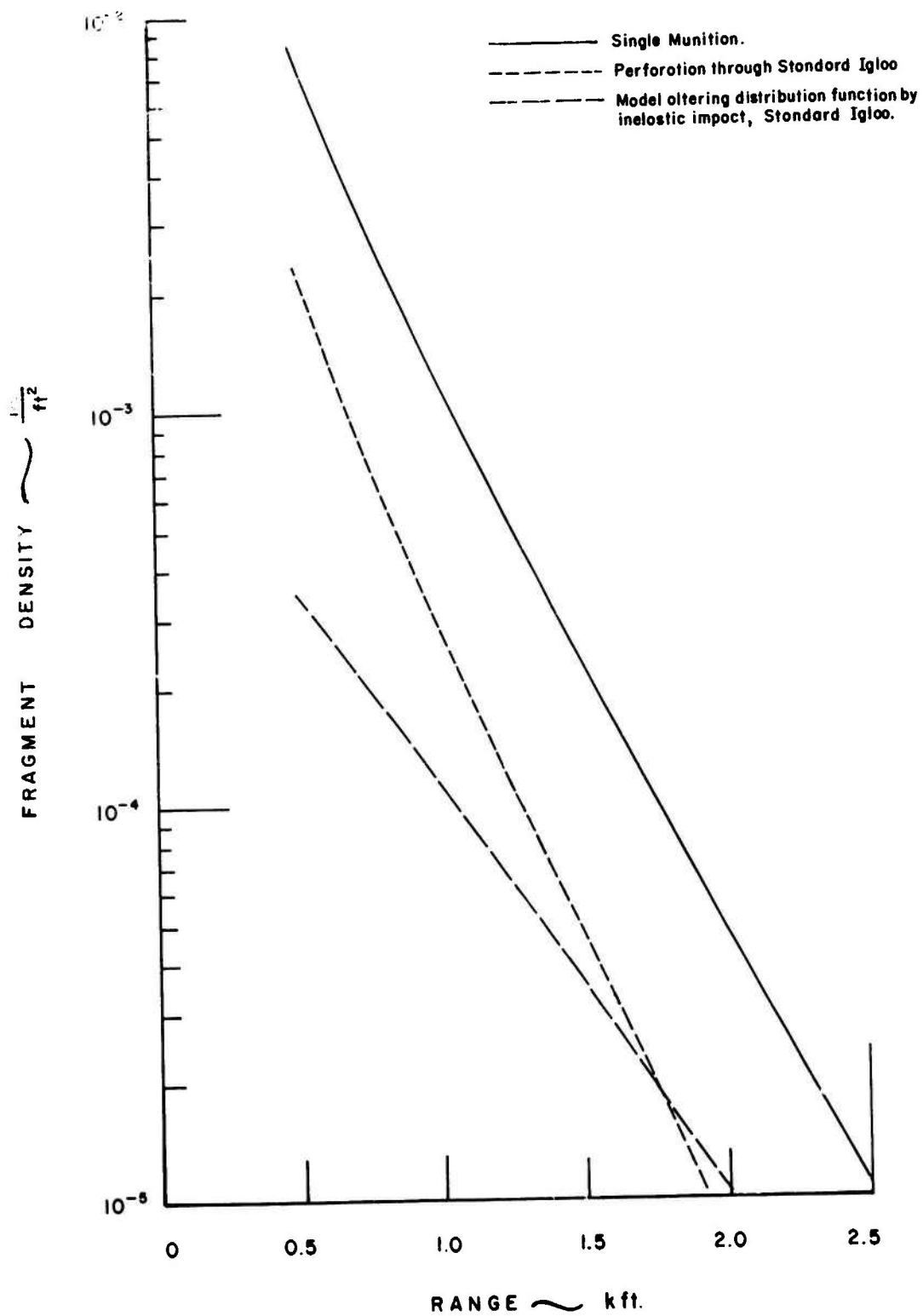
Figure 4-11, EFFECT OF EARTH COVER ON FRAGMENT DENSITY VERSUS RANGE
M117 750-lb. BOMB (SIDE DIRECTION)

65

the preceding section. Results using this method are senitive to the
mass distribution assumed for the chunks of the earth cover. The mathematical
models developed for fragment-fragment interaction can be used for the
fragment-cover interaction.

This second model again assumes the cover doesn't move very far when
the fragments overtake it, but the interaction of fragments with the cover
is described differently. The cover is assumed to break up into fragments
that have a mass distribution similar to the fragment-distribution. If
a bomb fragment strikes an earth clod which is larger, it is stopped
completely. If it strikes a cold which is smaller, it is not affected.
This model is a simplification of completely inelastic impact in which the
velocity of the fragment and clod, upon impact, have the same final
velocity,

$$V_f = \frac{V_F M_F + V_e M_e}{M_F + M_e}$$

where
V_f is the final velocity of both

V_F is the fragment velocity at impact

V_e is the earth clod velocity at impact

M_F is the mass of the fragment

M_e is the mass of the earth clod

The effect of this model is to reduce the number of fragments (on the
unit hemisphere)that are thrown out. Mathematically this is represented
by an altered mass distribution $f_i(m)$

$$f_i(m) = f(m)[1 - \exp(-(\frac{m}{\mu})^{1/3} \gamma h)]$$

where γ represents the probability of impact of a fragment by an earth clod
when the fragment traverses one foot of earth.

It is very hard to estimate accurately the value of γ to be used in this equation. We take it as the probability that a metal fragment will strike at least one earth fragment in $\frac{1}{3}$ foot penetration of the earth cover. Also we assume, for lack of better estimates, that the μ of the earth clod distribution is the same as that for the fragment distribution. With these crude estimates we show the far-field fragment densities for this type model in Figures 4-8 through 4-11 for a single munition and the standard igloo.

This model, with the very optimistic values for a fragment getting through without impact, gives very low values for the far-field fragment density.

Under the effect of the blast, the cover breaks up and moves out. Thus a third type of interaction must be considered wherein the cover fragments move essentially at the same velocity as the munition fragments and the number of collisions is minimal. The third model differs from the other two in that it is assumed that the earth cover breaks up and moves away fast enough so that no interaction between metal fragments and the cover will occur for any initial elevation angle greater than the final crater lip. For elevation angles lower than the final crater, the blast is trying to move a very large amount of earth and will not break it up. For the higher angles, the cover is assumed completely ineffective in stopping fragments and for the lower angles, all fragments are considered to be stopped. Figure 4-12 schematically illustrates this model. Estimates of α_m, the angle to the top of the residual cover are obtained from the profiles of the craters in the Arco detonations and Eskimo I. An estimate of $\alpha_m \sim 10°$ is consistent with this data. In this model then, the calculation of the fragment density in the far-field is effected by replacing the lower limit in the integration over α_0 in Equations 3-21 or 3-22 by α_m.
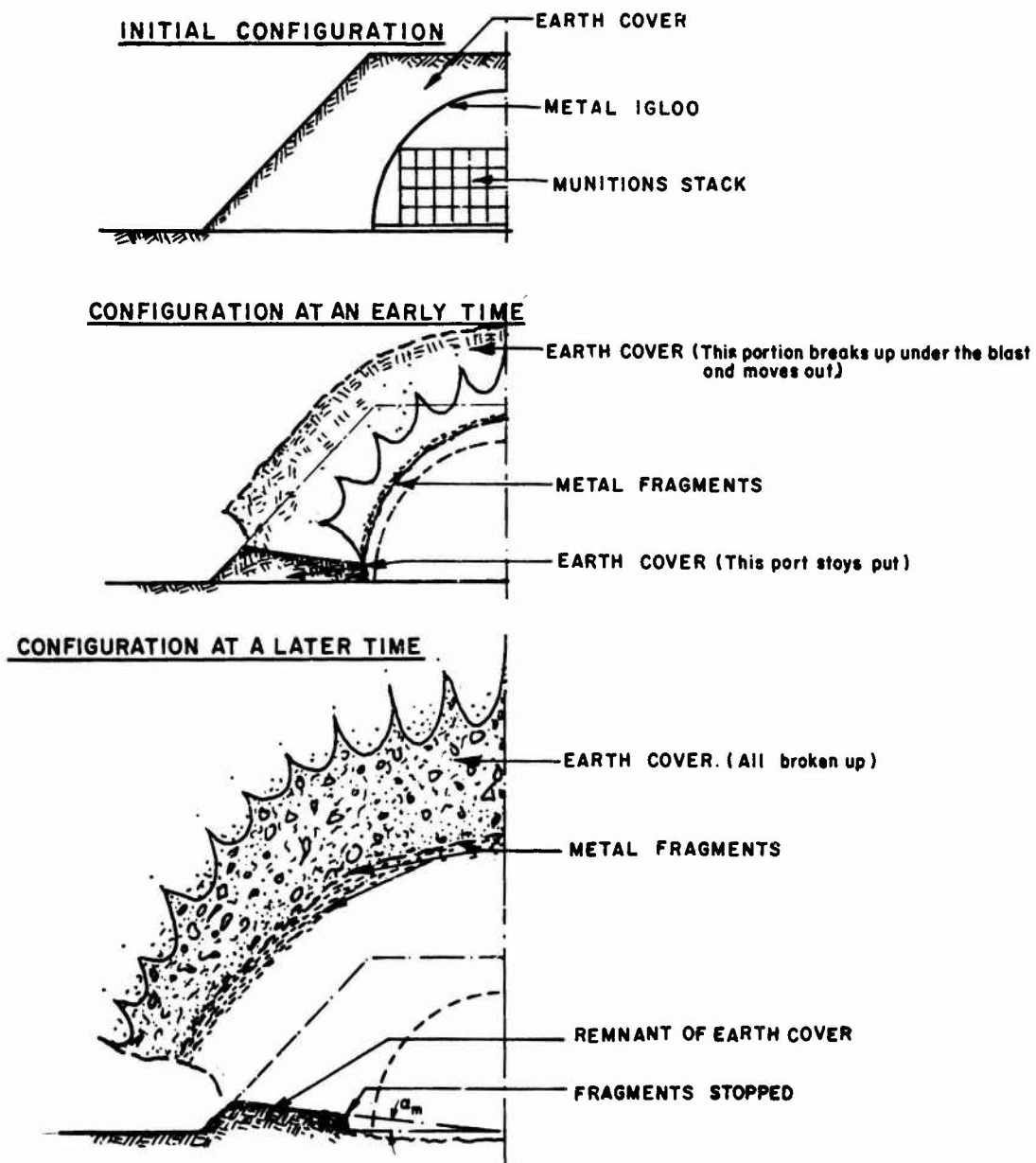
Figure 4-12, SCHEMATIC DIAGRAM ILLUSTRATING THE THIRD MODEL
OF EARTH COVER EFFECT ON FRAGMENTS.

68

4.4 Other Parameters

The effect on the far-field fragment density when two of the initial fragment parameters are altered is now examined. As noted, the fragment mass distribution seems to be changed when a stack of munitions is detonated with a single munition primed (Draper and Watson, 1970, Feinstein and Nagaoka, 1970, Feinstein, 1972b). The observations indicate that more large fragments are generated. There is no available data, however, on the mass distribution that is obtained; therefore, a simple model to examine this effect is used. Assume the altered mass distribution has the same functional form as the arena data but with fewer total fragments and a larger mean fragment mass. This is effected in the formula by changing the value of μ to $\gamma\mu$, where γ is a constant factor and by changing N_0 to $\frac{N_0}{\gamma}$, to conserve the total mass of fragments emitted. The effect of this change is illustrated for fragment densities in the side direction for the M117 750 lb bomb. Figure 4-13 shows the fragment density versus γ for $1 \leq \gamma \leq 10$ at selected ranges between 1000 ft and 2500 ft. For the smaller range, the fragment density decreases with increasing γ, decreasing about an order of magnitude as γ increase about an order of magnitude. At the other extreme (i.e., ranges of 2000 and 2500 feet), the change in fragment density with γ is very slight, being about 30% over the range of γ presented. Although there are fewer total fragments for larger γ, there is a larger fraction of large fragments and the larger fragments are hurled to larger distances than smaller fragments.

As far as the far-field fragment hazard is concerned, the effect of changing the mass distribution in a stack detonation is slight.

Now turn to a feature whose effect will not be slight in estimating the far-field fragment hazard. In solving the ballistic trajectory equations,
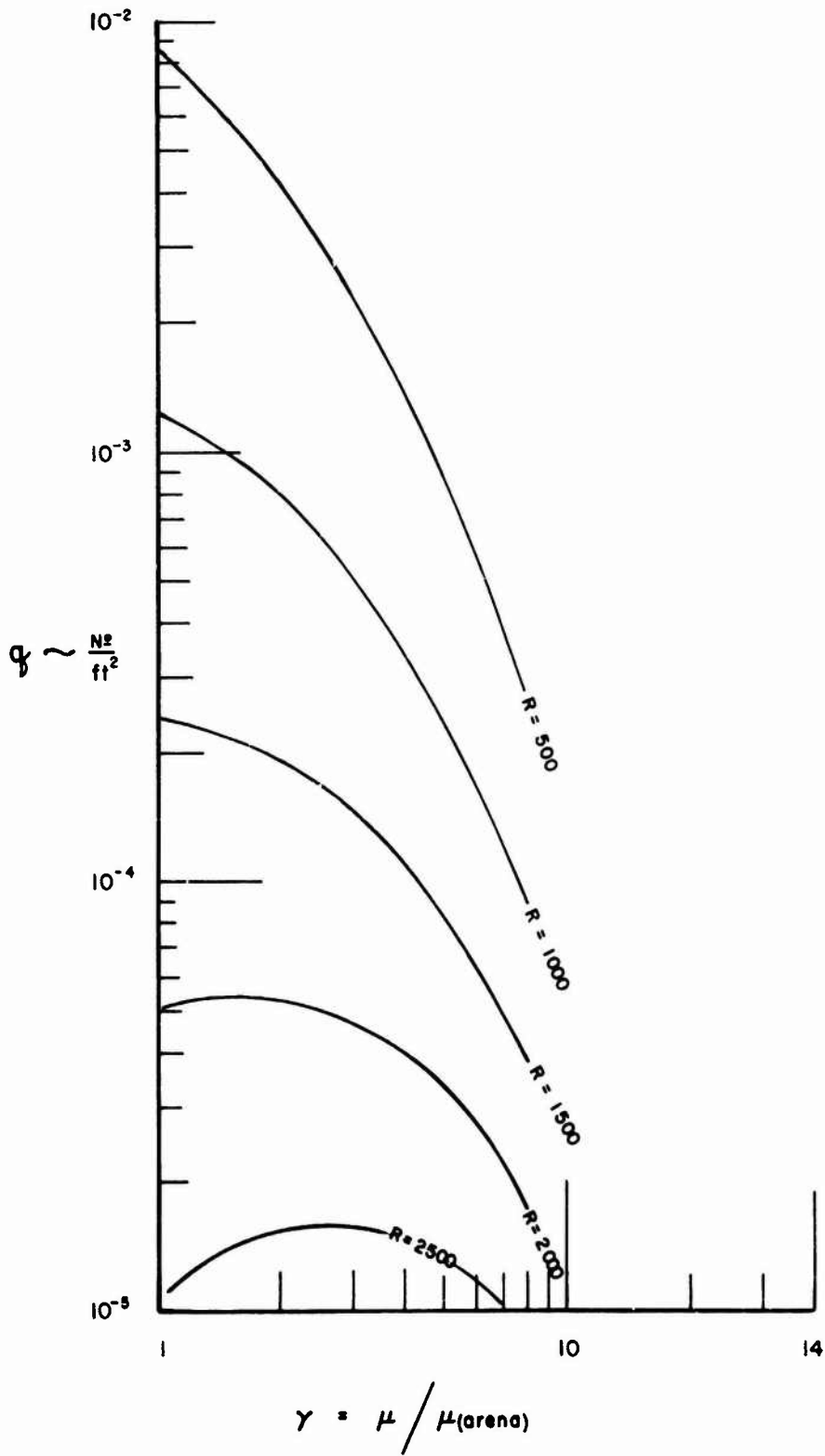
Figure 4-13. EFFECT ON q FROM CHANGES OF MASS DISTRIBUTION AT
VALUES OF R. M117 750-lb. BOMB (SIDE DIRECTION)

it is normally assumed (in all the theoretical works presented) that the fragments are spinning as they leave the detonation site and that the presented area can be represented (at least over the larger trajectories) as the mean presented area. It would be possible for some fragments to be ejected with no or little spin or, if spinning at the outset, to stabilize with their major axis roughly parallel to the trajectory. In this case the presented area would be minimized and the ballistic density maximized.

For example, look at a fragment with square cross-section and with an aspect ratio of 2:1, aligned with the trajectory. For steel fragments, the ballistic density is 3960 gr/in^3 or six times the mean value.

The far-field fragment density was calculated for various values of the ballistic density, ranging from the mean value given in the arena data to four times the arena data (i.e., from $\sim$ 600 gr/in^3 to 2500 gr/in^3). Figure 4-14 shows the fragment density versus ballistic density at selected ranges from 1000 feet to 2500 feet for the M117 750 lb bomb in the side spray direction. At the larger ranges (e.g. 2500 feet) a dramatic increase in the fragment density is noted, increasing by almost two orders of magnitude as the ballistic density changes by a factor of four. It is suggested that this factor is quite important for far-field fragment estimations. Now it is improbable that all fragments will be stabilized and oriented to the trajectory, but even if only 10% of them are, while the remaining 90% are spinning; the increase of the far-field fragment density will be dramatic. This increase in effective ballistic density could also be interpreted as a smaller effective drag coefficient on the fragment during its travel. Increases in the drag coefficient by 50%, equivalent to changes in the ballistic density by a factor of 3, are unlikely.
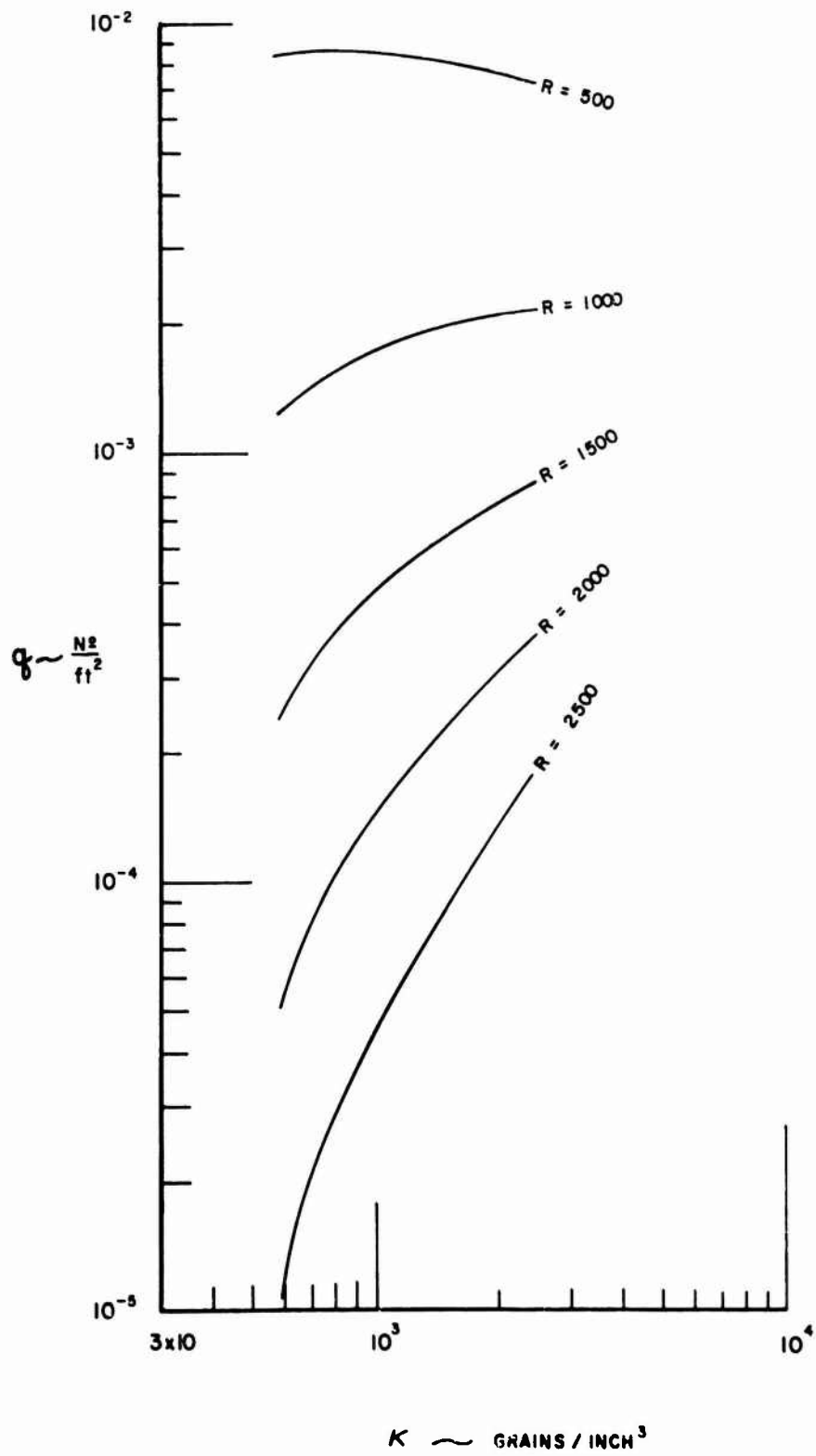
Figure 4-14. EFFECT ON q FROM CHANGES OF BALLISTIC DENSITY AT
VALUES OF R.   M 117 750-lb. BOMB (SIDE DIRECTION)

The effect of increased initial velocity observed by Draper and Watson (1970) is less dramatic in increasing the far-field fragment density. An examination of the maximum range of a fragment of mass explains this. The maximum range is

$$R = \beta \left(\frac{\kappa}{\kappa_A}\right)^{2/3} m^{1/3} \left[.5140 - 1.0368 \ln\left(137 \left(\frac{\kappa}{\kappa_A}\right)^{1/3} \frac{m^{1/6}}{V_o}\right)\right] \quad (4\text{-}24)$$

where κ is the actual ballistic density

κ_A is the arena data average ballistic density

V_o is the initial velocity

The dominant dependence on V_o is with $\ln V_o$ while the dominant dependence on κ is as $\kappa^{2/3}$.

Note changes in V_o by a factor of 2 or 3 may be expected, while the value of κ for selected projectiles could range easily up to 5-10 times the arena value.

Chapter V

COMPARISON OF THE THEORETICAL MODELS WITH EXPERIMENTAL DATA

5.1 Stack Models and Measurements

The elementary theory suggests that the effective number of munitions is related to the number of munitions in the surface layers on the top and the exposed side where

$$N_{eff} = 0.9N_S + 0.1\ N_T$$

First, the theoretical calculations are compared with the fragment density in the far-field (500 feet to 1500 feet) for the side spray direction from the 2x5 and 5x3 stacks of M117 750 lb bombs tested at NWC (Feinstein and Nagaoka, 1970). In the former $N_T = 2$, and $N_T = 5$ in the latter, while $N_S = 3$ for both. Thus

$$N_{eff} = \begin{cases} 2.9 \text{ for } 2 \times 3 \text{ stack} \\ 3.2 \text{ for } 5 \times 3 \text{ stack} \end{cases}$$

Figure 5-1 shows the comparison using the arena data approximation. The comparison is quite good.

The next comparison is with the first two events in the Big Papa test. These tests were the detonation in an open revetment of a mixed stack of M117 750 lb bombs and M66A2 2000 lb bombs. The 750 lb and 2000 lb bomb are both tritonal filled and have the same C/M ratio. The arena data for the 2000 lb bomb has the same fragment velocity (within 10%) and the same average fragment mass as the 750 lb bomb with approximately $\frac{8}{3}$ more fragments. Therefore, each 2000 lb bomb is replaced by 2-2/3 750 lbs for the purpose of comparison.
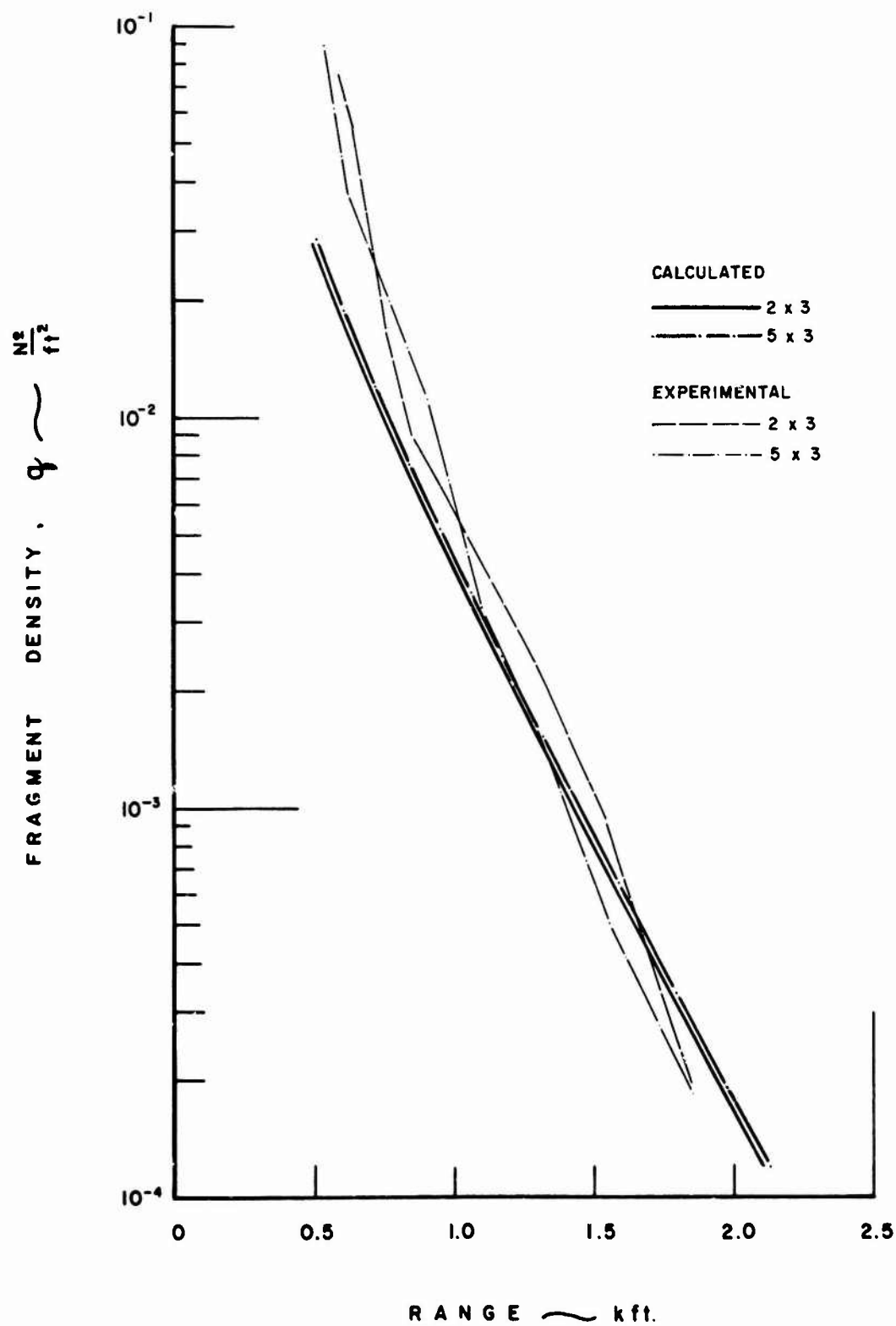
Figure 5-1. COMPARISON OF CALCULATED FRAGMENT DENSITY VERSUS
RANGE WITH EXPERIMENT-SMALL STACK OF M117 750-lb BOMBS
(SIDE SPRAY DIRECTION)

The stacks for these detonations were rectangular. Details of the stack composition are given in Peterson (1968). In the first test, there were 64 750-lb bombs in the top layer and 4 750-lb and 12 2000-lb bombs in the side. For the second test, there were 21 750-lb bombs in the top and 4 750-lb and 8 2000-lb bombs on the side.

Thus N_{eff} = 39 in the first case and 25 in the second. The comparison between theory (using arena data) and measured values is not very good; between 2000 ft and 3000 ft there is roughly a factor of 50 between the two. Schreyer and Romesberg (1970) noted that using arena data and a multiplier, an effective stack of 267 bombs was required to match the data between 2000 and 3000 ft.

Peterson (1968) measured the mass of the smallest fragments at 1800 and 3000 ft. These fragments are much smaller than that predicted from the ballistic equations. The initial velocity required for these fragments is well in excess of 25,000 ft/sec. However, if the effective ballistic density was twice the arena average these small fragments could reach these distances with no increase in initial velocity. Therefore, the fragment densities, were recalculated using N_{eff} and κ = 1200 grains/in^3. Figure 5-2 shows the comparison of the predicted and experimental. The comparison is not great (a factor of $\sim$ 2 at 2000 ft), but probably reasonable. There are very slight changes in q from 500 to 1500 ft. suggesting that the agreement with the NWC 2x3, 5x3 tests remains valid.

A more realistic source model would probably have the smaller fragments starting out with a higher velocity than the larger fragments and would also exhibit dependence of the shape factor on the size. Since there is no data available on this dependence, no attempt to fit any such variation was made.
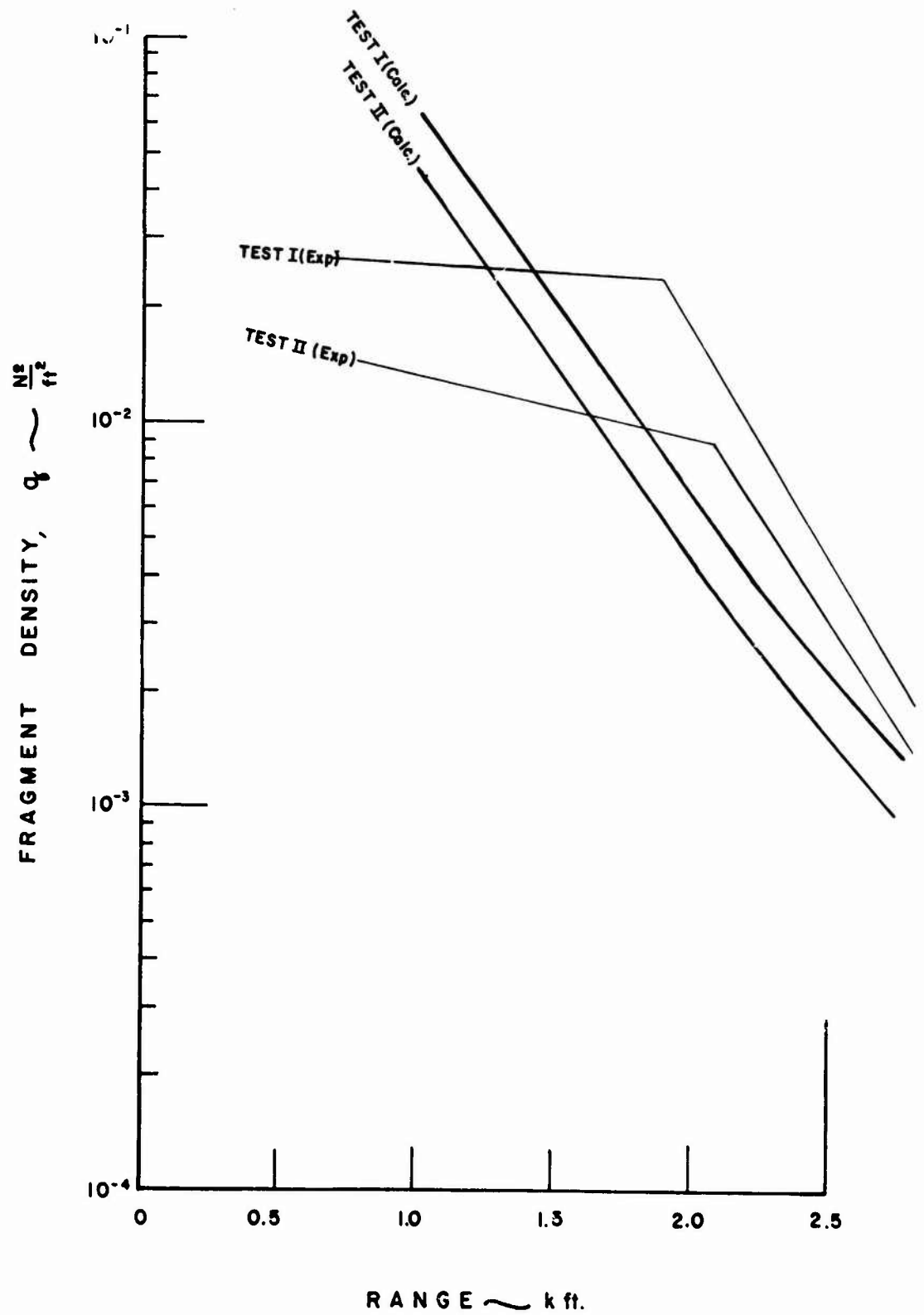
Figure 5-2. CALCULATED FRAGMENT DENSITY VERSUS RANGE-BIG PAPA

5.2 Igloo Models and Measurements

There is only one experiment for weapons contained within an igloo that can be compared with the theoretical far-field fragment densities. The Eskimo I test of 13696 155mm projectiles detonated in a standard Army Igloo were measured. The projectiles were placed in a stack shown in Figure 5-3. The munitions were oriented vertically. Figure 2-5 shows the plan view of the test, and indicates the lines along which fragment measurments were made.

The number of the projectiles on the top layer for considering fragments off the end is 3700; off the side almost half of these are screened by the odd shape of the stack; thus N_T = 2300 there. Off the end N_S = 240 and off the side N_S = 230. First the far-field fragment densities from this stack were calculated as if the stack were in the open, using the isotropically averaged arena data. These values are quite low beyond 1000 ft. This predicted density has a $\partial q/\partial R$ greater than that measured. The two models with strong cover-fragment interaction will have an even greater $\partial q/\partial R$ and would thus deviate further.

The mass distribution of the fragments were measured at each range. (Weals, 1973, Feinstein, 1972b). Figure 5-4 shows the minimum mass fragment recovered as a function of range for this experiment. Also plotted is the theoretical minimum mass versus range using κ = 660 grains/in^3, V_0 = 5000 fps; κ = 1200 grains/in^3, V_0 = 5000 fps; and κ = 660 grains/in^3, V_0 = 40,000 ft/sec. In line with the previous fit to the Big Papa experiment the velocity increase to account for the mass is rejected as the prime explanation and the ballistic density corresponding to the more slender projectile is accepted.

The calculations were repeated, but a value of κ = 1200 gr/in^3 was used. The calculated values agree to within a factor of two for most

METAL IGLOO

TYPICAL MUNITIONS
PALLET STACK
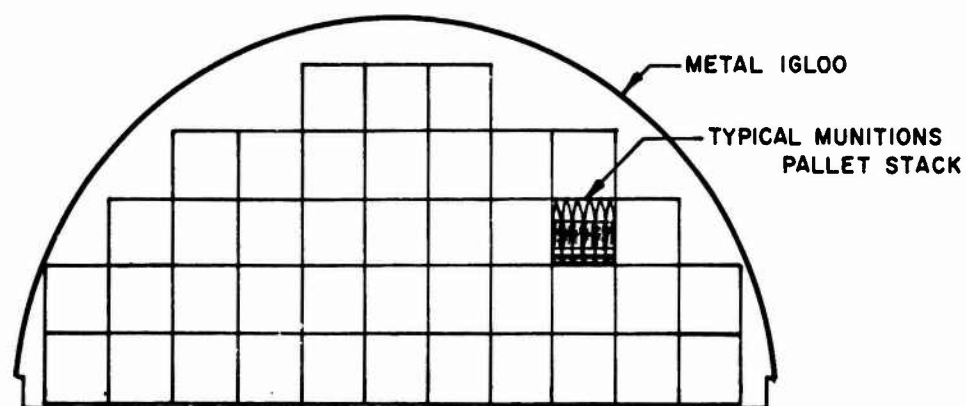
Figure 5-3,   CROSS SECTION OF PALLET STACK IN IGLOO MAGAZINE
ESKIMO I.

79
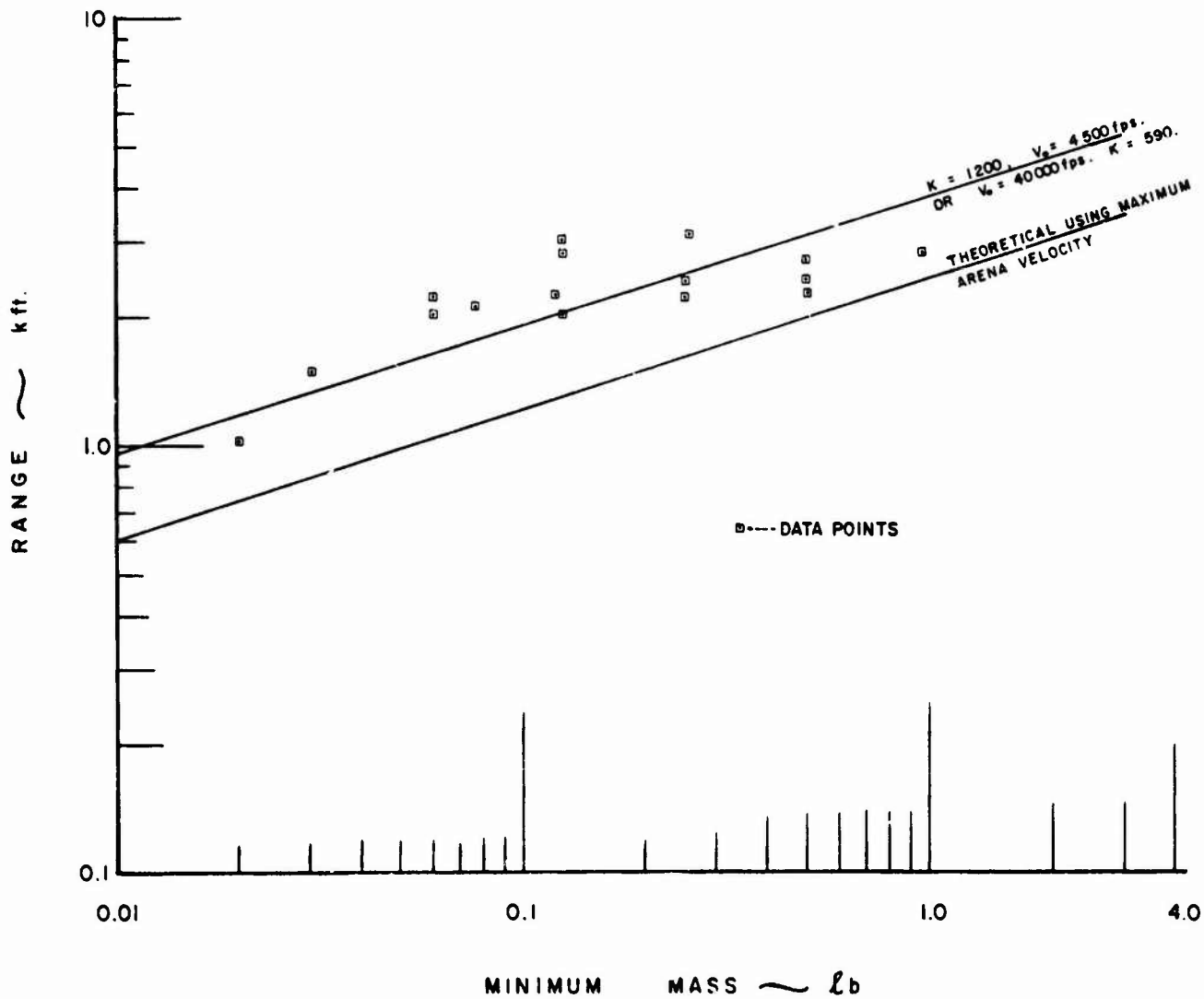
Figure 5-4, MEASURED MINIMUM MASS FRAGMENTS VERSUS RANGE-
ESKIMO I (EXP. WEALS 1973) COMPARED WITH THEORY-
FRAGMENTS EJECTED AT OPTIMUM LAUNCH ANGLE.

80

of the range and the slope is qualitatively in agreement. The perforation model for the igloo effect would yield values lower than these by better than an order of magnitude. The model wherein fragments are stopped for low elevation angles, but otherwise unimpeded, yields values which are in good agreement with the measurements. Figure 5-5 shows the measured data and the theoretical predictions for this model. (For fragments in the direction of the headwall, assume the headwall is destroyed by the blast and offers no resistance to low elevation angle fragments in that direction.) For this model the N_{eff} are as follows:

Headwall N_{eff} = 0.9 (240) + 0.1 (3700) = 586 $\sim$ 600

Side N_{eff} = 0.7 (280) + 0.1 (2300) = 426 $\sim$ 425

Back N_{eff} = 0.7 (240) + 0.1 (3700) = 538 $\sim$ 550

5.3 Comments

The theoretical predictions for far-field fragment densities for the accidental detonation of stacked munitions and of stacked munitions within igloo magazines compares quite well with the few adequate measurements of the far-field fragment densities.

A commentary of the assumptions that are used and of the models that were developed that best fit the data is useful.

i. The fragment densities in the far-field are calculated using an approximation to the exact solution to the ballistic trajectory equations. The approximation technique is very good for the fragment masses and initial velocities of interest. The ballistic equations that this approximation represents ignores any yaw effects and any wind conditions. The spin of the fragments is approximated by assuming an effective mean presented area only and no deviations from the spinless trajectory by Magnus and cross forces
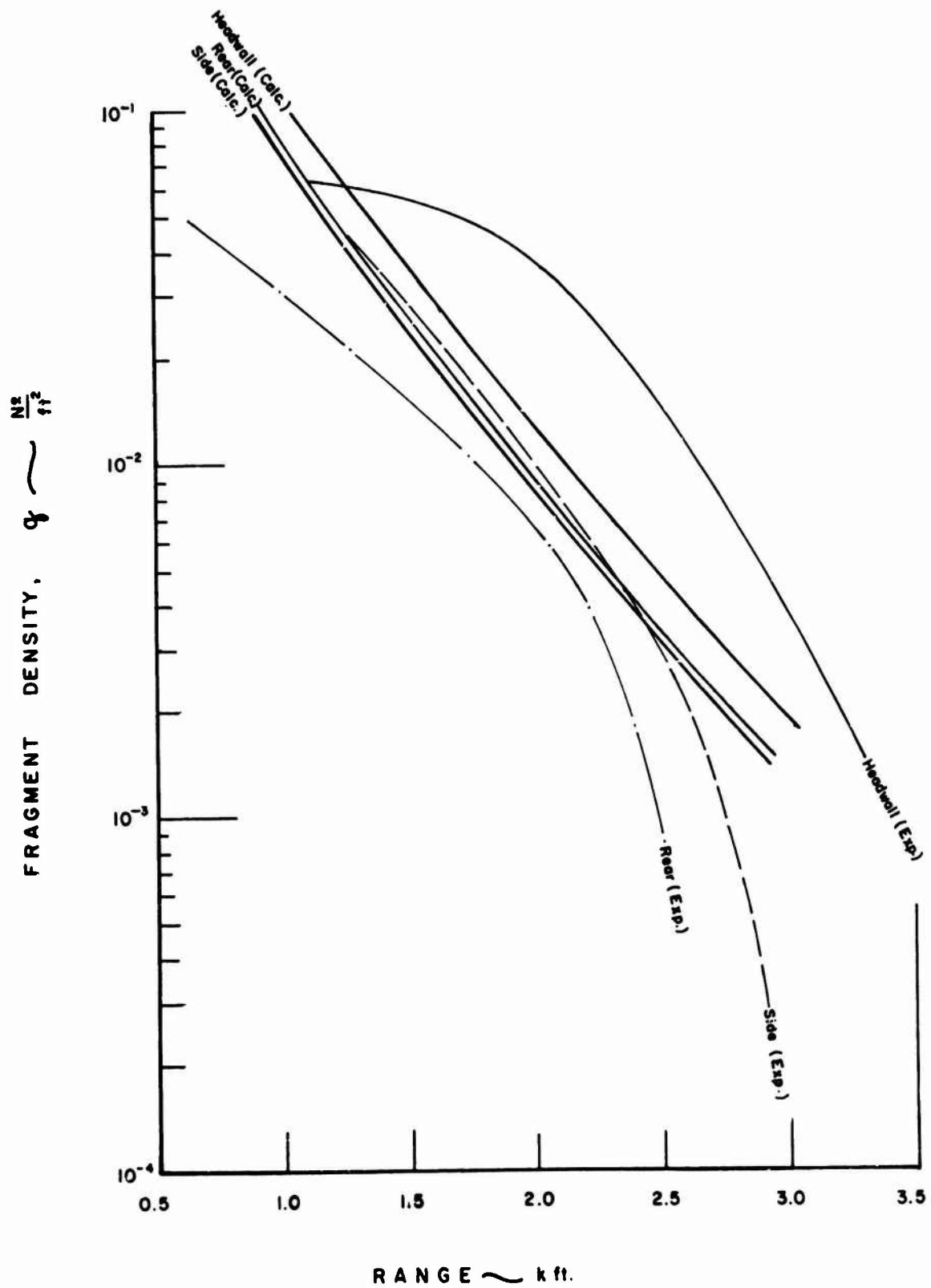
Figure 5-5. CALCULATED FRAGMENT DENSITY VERSUS RANGE,
ESKIMO I.

is considered. This effect of spin on the trajectory was not estimated, but it could be appreciable.

2. The ballistic equations allow the fragment density to be computed at large ranges from the specification of fragment number, mass, initial velocity and ballistic density at any specified azimuth and elevation on the unit hemisphere centered at ground zero. Given a set of arena data for a single munition, the far-field fragment densities may be readily computed.

3. The model for the stacks led to a definition of an effective number of single munitions. Only munitions in the top layer and the side layer nearest the observation point contribute significantly to the far-field fragment density. The bulk of the contribution comes from the side layer. Fragments from munitions in the interior of the stack are effectively stopped by the fragments, blast, and combustion products from the adjacent munitions.

4. The best model for describing the effect of an earth cover on the retardation of fragments is that the crown of the earth cover is blown apart by the blast and moves out as part of the fragment pattern and does not significantly interact with the munition fragments. At very low elevation angles the cover essentially remains in place and completely stops all fragments with very low elevation angles. The original purpose for the design of the earth cover is the prevention of intermagazine communication of the detonation by fragment impact and blast. As far as fragments are concerned, this objective is met. The cover affords little reduction in the far-field fragment numbers, though.

5. The distribution of fragment masses, total fragment numbers and fragment initial velocities from an accidental detonation in a stack, wherein one of the munitions detonates and the remainder are detonated

sympathetically, may differ significantly from the values obtained by detonating a single munition. In particular, larger fragments and higher initial velocities may be expected. The effect of larger fragments (together with its corollary property of fewer of them) do not significantly alter the densities that may be expected in the ranges 1000-3000 feet. Increases in initial velocity affect the fragment densities only slightly. The parametric studies indicate that the fragment densities in the far-field are extremely sensitive to effective ballistic density. A change in this variable by a factor of two leads to increases in the number of fragments observed in the far-field by better than an order of magnitude.

6. Use of arena data could not effect a match between theory and the measured data from the Big Papa and Eskimo I experiments. The detailed measurements of these experiments show that much smaller fragments are ejected to larger distances than could be expected using the initial velocities and the average shape factor from the arena. Modifications of either of these factors could account for the observed data. The velocity increments required are large, being a factor of 3-10 times the maximum arena velocity, while only small changes in the average effective shape factor are required.

7. An additional assumption for use in the theoretical calculations at this stage of development is that the initial hemisphere parameters should be chosen to be isotropic with the largest values of fragment number and velocity from the arena data chosen. The munitions in an accidental detonation will be tossed about prior to initiation of the sympathetic detonation and the actual orientation will be subject to some sort of statistical distribution. This project is interested in the determination of safe distances and to be conservative it should be

assumed that the maximum source is operative in any direction.

It is worth noting that either greatly enhanced initial velocity or an altered ballistic density is required to explain the measured far-field fragment density. We lean toward the latter as the fragment density is extremely sensitive to small changes in the shape factor, while extremely large initial velocity increments are required. If the latter case is descriptive, some thought must be given to the injury criteria. Fugelso (Fugelso, et al. 1960, 1961, 1966) has shown that perforation limit velocities for thin metallic plates are highly dependent on the mass to presented area ratio at impact. Sperrazza and Kokinakis (1968), and Kokinakis, (1970) have shown similar dependence for perforation limit velocities of skin. Their data yield

$$V_{limit} = a + b \frac{A}{M} \qquad a, b, \text{ constants}$$

The trauma data (Bowen et. al. 1968) for unilateral and bilateral lung hemorrhage by blunt missile impact is based on a set of data with two sizes of projectiles, M = .4 and .8 lb, with A constant for both. The skull fracture data (Feinstein, et al. 1968, and Feinstein 1971), is based on dropping skulls on a flat surface, not by impacting them with a projectile at all (Gurdjian 1949).

In view of the high possibility of the far-field fragments being highly elongated, it is suggested that the critical velocity requirements be reexamined quite thoroughly. For the present it is suggested that all fragments beyond 1000 feet be treated as potentially lethal.

Chapter VI

CONCLUSIONS AND CONJECTURES

6.1 Summary of the Model for Far-Field Fragment Density Calculations

On the basis of the theory and their limited comparisons with experimental data, the following model for the calculation of the far-field fragment density from the accidental detonation of stacks of munitions is tentatively proposed.

I. Each munition generates an isotropic fragment distribution with the total number of fragments from the arena data distributed uniformly over a unit sphere. These numbers have an upper bound given by the average densities in the arena data in the side direction. Since the calculations are to be conservative for safety purposes, we use these av. . es (Table 2). The average mass will be taken as that of the arena data. The initial fragment velocity will be the maximum velocity of the arena data, this is normally the maximum side-spray velocity. The ballistic density will be taken as twice that given in the arena data.

II. Let N_T denote the number of munitions in the top layer of the stack and N_S the number of munitions in nearest side. The total number of effective munitions is:

1) For an open stack

$$N_{eff} = 0.9 \, N_S + 0.1 \, N_T \qquad (6\text{-}1)$$

2) For a stack within a standard earth-covered igloo

$$N_{eff} = 0.7 \, N_S + 0.1 \, N_T \qquad (6\text{-}2)$$

In the headwall direction, treat it as in the open.

III. With these numbers as input, the far-field fragment density is calculated by the approximate formula

$$q_{stack} = N_{eff} \, q_{single}$$

and q_{single} is given by Equation (3-22).

IV. All fragments are considered hazardous. Figure 6-1 through 6-4 presents the fragment densities for the single munition for the four munition types considered.

6.2 Tentative Quantity-Distance Relationships

Tentative quantity-distance curves for the four munitions are presented. An assumption on typical stack shapes are required to illustrate the calculations. Let M equal the total number of munitions in the rectangular stack with dimensions $3n \times n \times n$ (Figure 6-5). For this example

$$N_T = 3n^2$$

and

$$N_S = 3n^2 \qquad \text{off the end}$$
$$= n^2 \qquad \text{off the side}$$

Thus

$$N_{eff} = 3n^2 \qquad \text{off the side} \left.\vphantom{\begin{array}{c}1\\1\end{array}}\right\} \text{open store}$$
$$= 1.2 \, n^2 \qquad \text{off the end}$$
$$= 2.4 \, n^2 \qquad \text{off the side} \left.\vphantom{\begin{array}{c}1\\1\end{array}}\right\} \begin{array}{l}\text{stored in earth-}\\\text{covered igloo}\end{array}$$
$$= n^2 \qquad \text{off the end}$$

and

$$M = 3n^3$$

The quantity of explosive, W, is

$$W = MW_1$$

where W_1 is the explosive weight in a single munition.
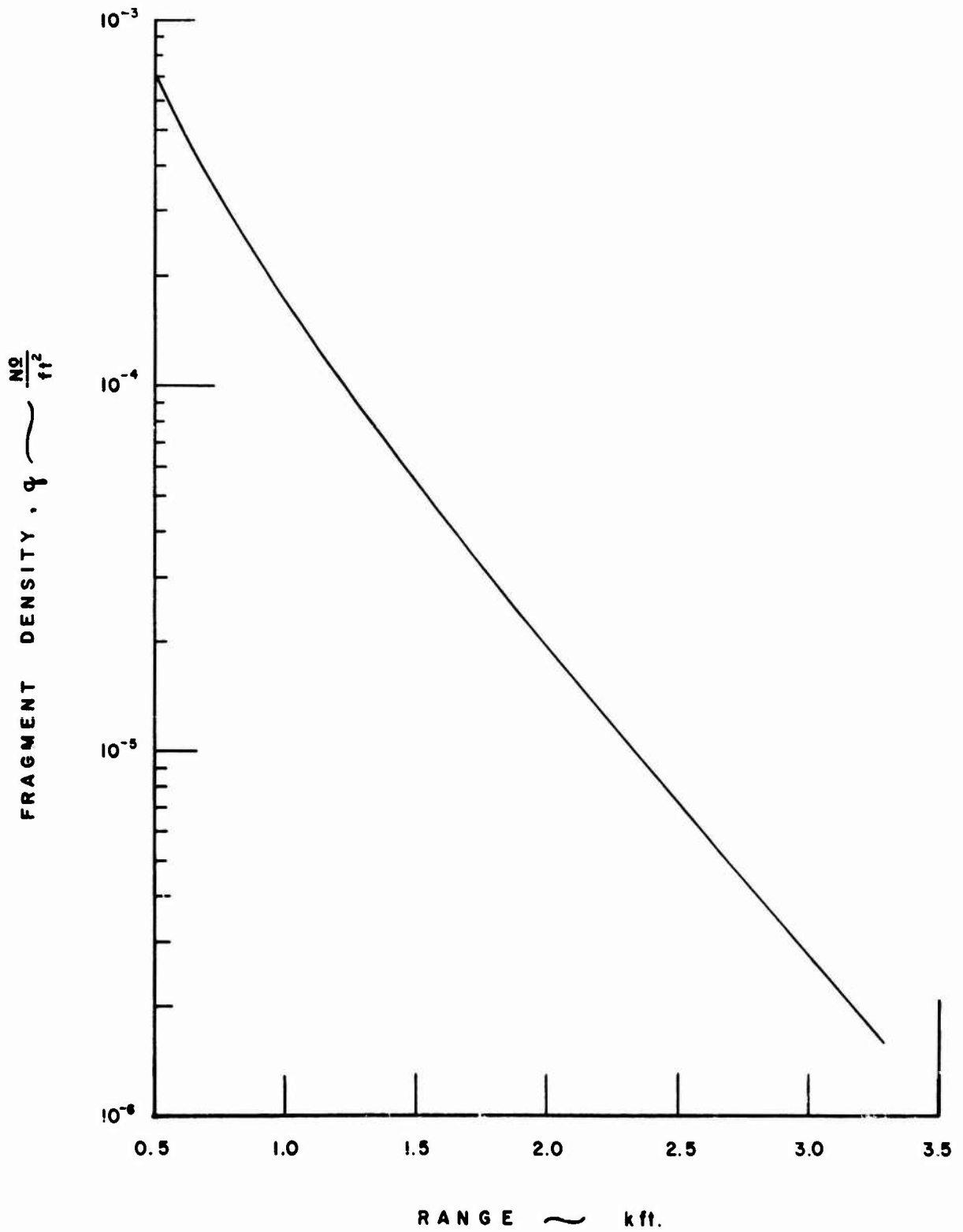
Figure 6-1.   FAR FIELD FRAGMENT DENSITY VERSUS RANGE
(M107   155mm PROJECTILE, $K = 1200$ gr. / in^3)
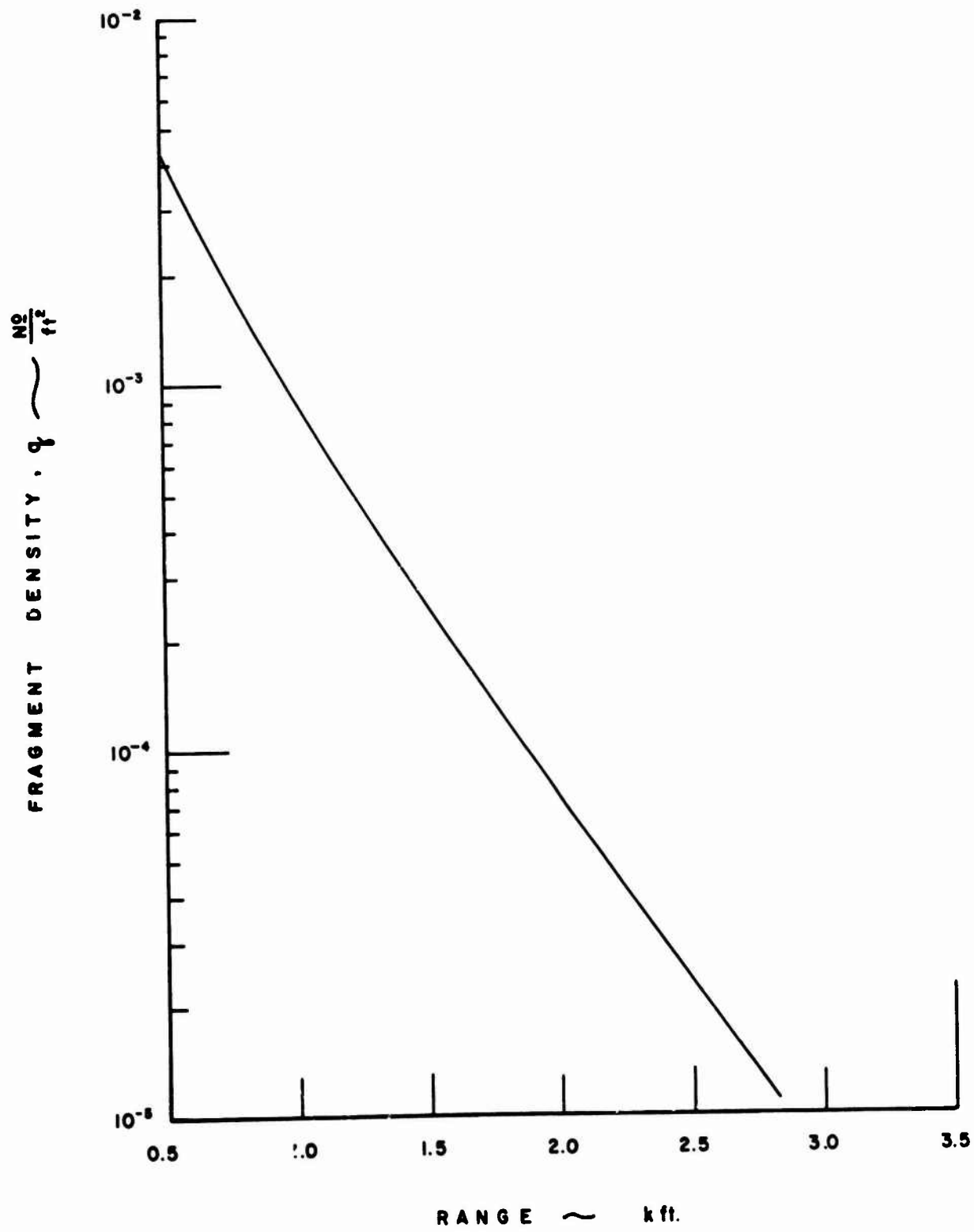
Figure 6-2. FAR FIELD FRAGMENT DENSITY VERSUS RANGE
(M437A2 175mm PROJECTILE, K = 1200 gr./in^3)
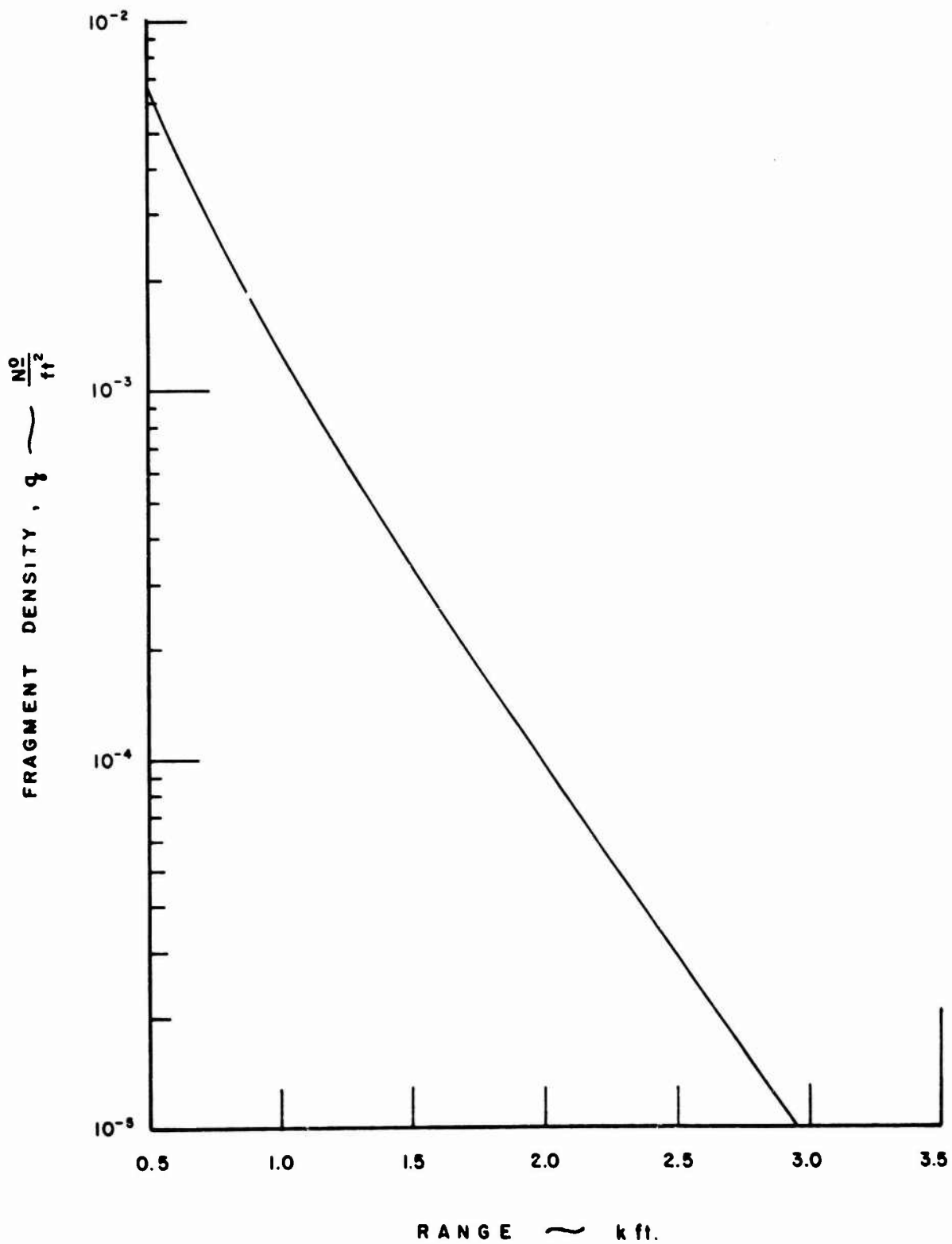
Figure 6-3,   FAR FIELD FRAGMENT DENSITY VERSUS RANGE
(MK82   500-lb BOMB, $K = 1200$ gr./in^3)

90
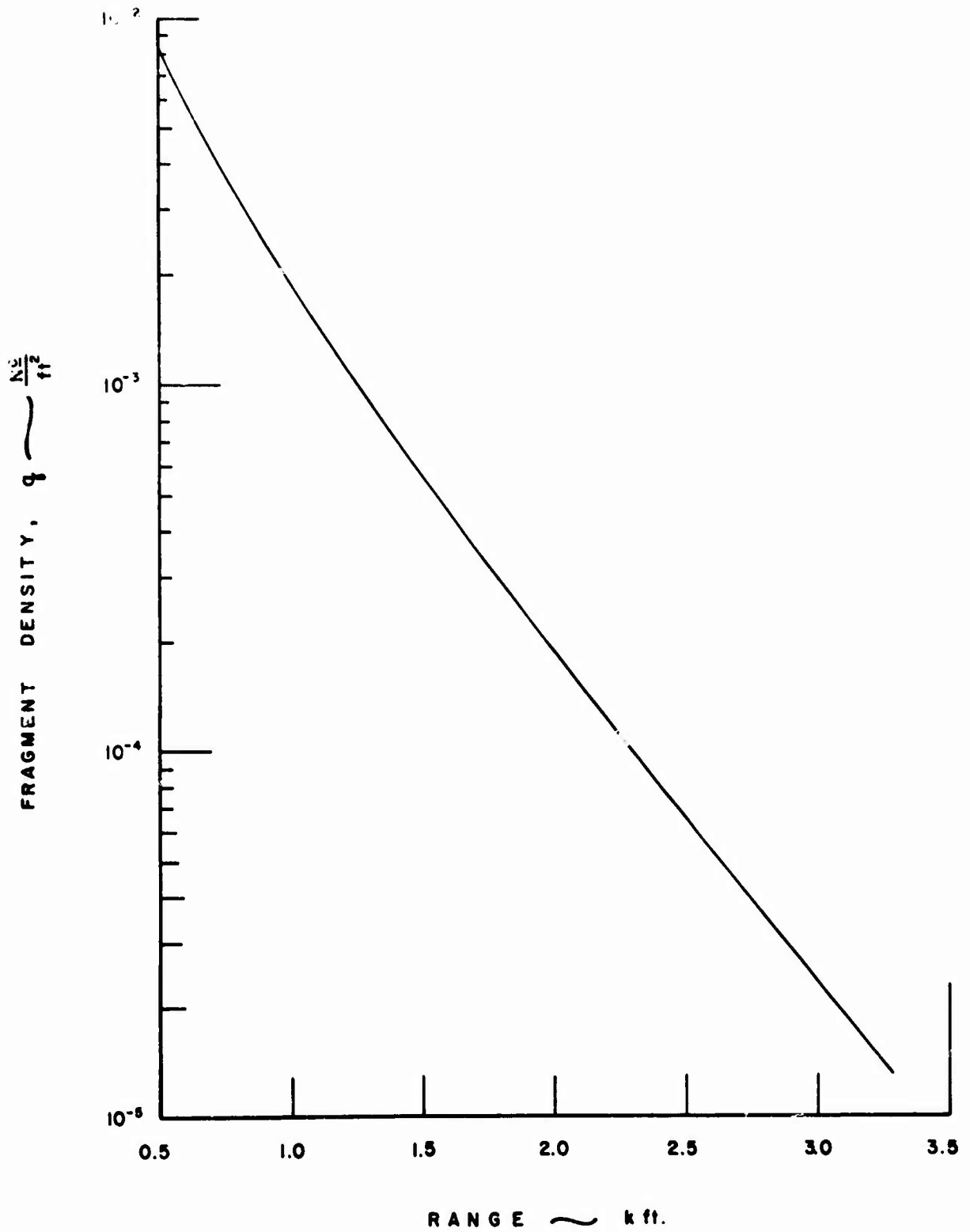
Figure 6-4, FAR FIELD FRAGMENT DENSITY VERSUS RANGE
(M 117 750-lb. BOMB, K = 1200 gr. / in^3)
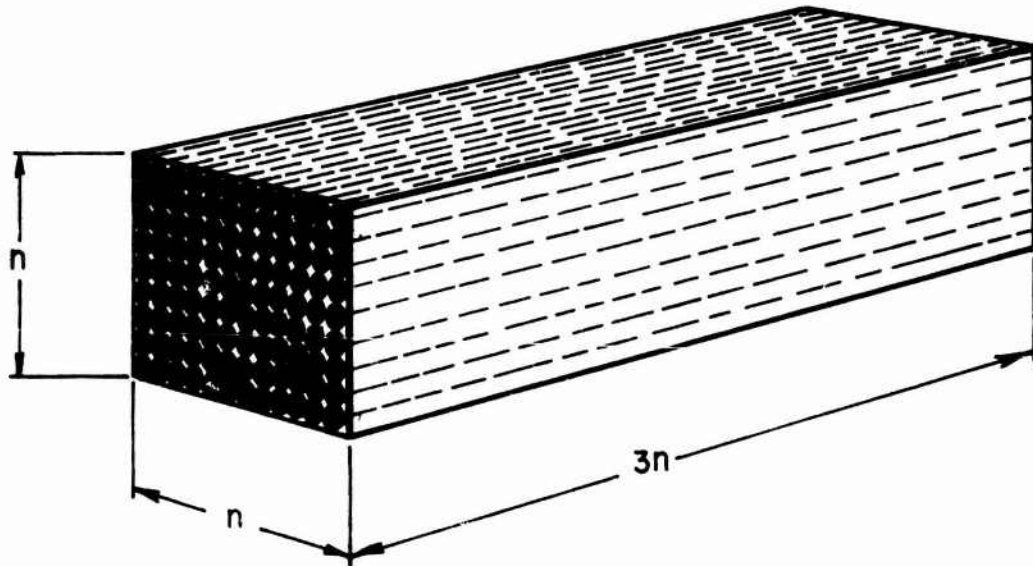
n = Number of munitions in a direction.

$3n^3$ = Total number of munitions in the stack.

Figure 6-5, SCHEMATIC DIAGRAM OF THE STACK CONFIGURATION FOR THE EXAMPLE QUANTITY – DISTANCE CALCULATIONS.

92

Figures 6-6 through 6-9 show the quantity-distance relations for these four cases for the four munitions. Values of the fragment density of 1/600 square feet and 1/6000 square feet are shown on each graph. Also plotted on each curve are the inhabited building distance for Class 7 explosives (DOD Manual 4145, 27M, 1971) and the British criteria $R = 515 \ W^{1/5}$ for a 10^{-5} probability of being struck by a fragment (Jarrett 1968). It should be noted that the tentative quantity-distances curves for the fragment hazard indicate that the fragment hazard might be the controlling safety feature for stacks with less than 100,000 to 200,000 lbs of explosive. The quantity-distance relation for these fragment hazards will increase the required safe distances for the smaller stacks.
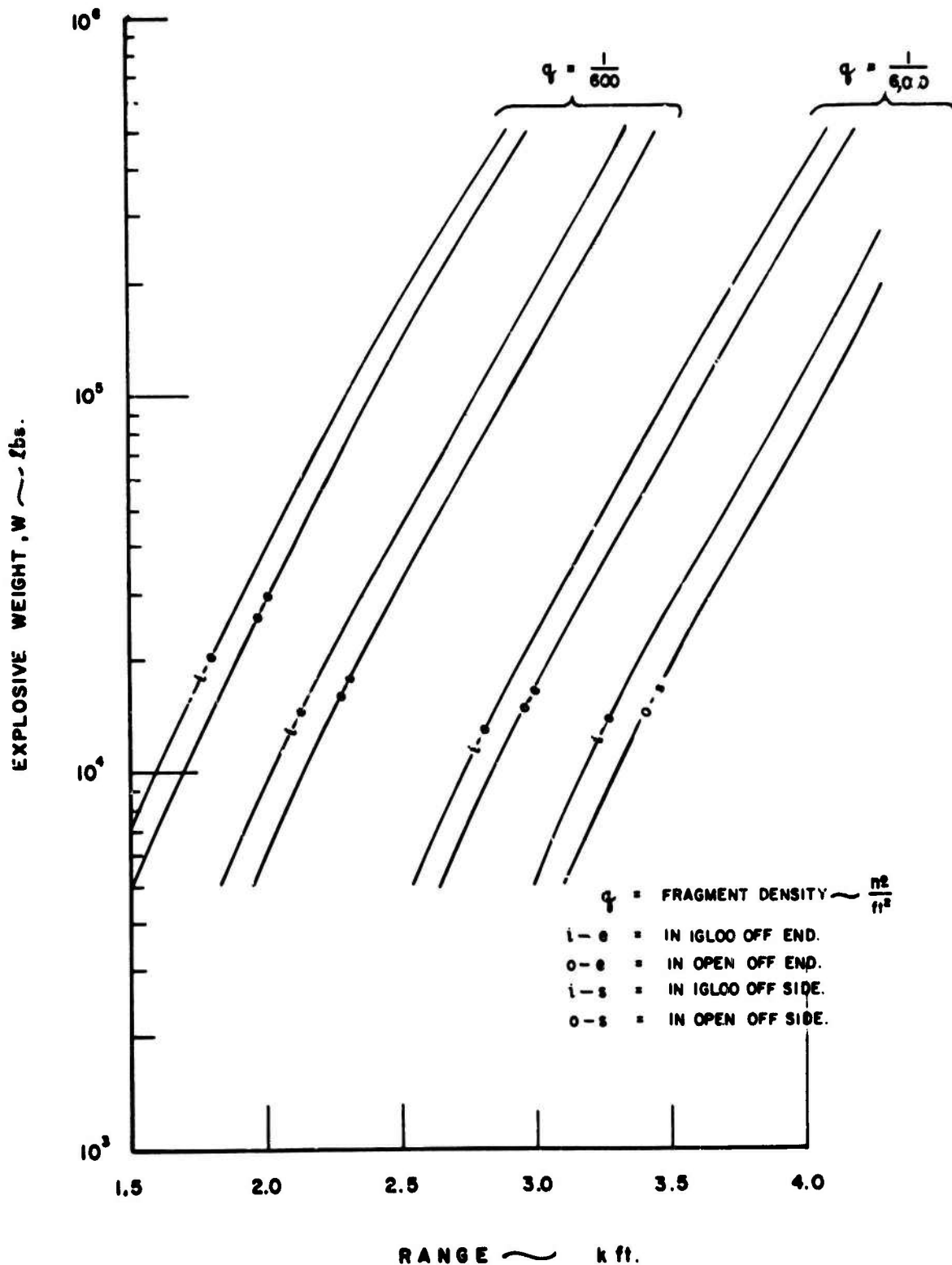
Figure 6-6. QUANTITY-DISTANCE FOR STACKS OF M107 155mm PROJECTILES

94
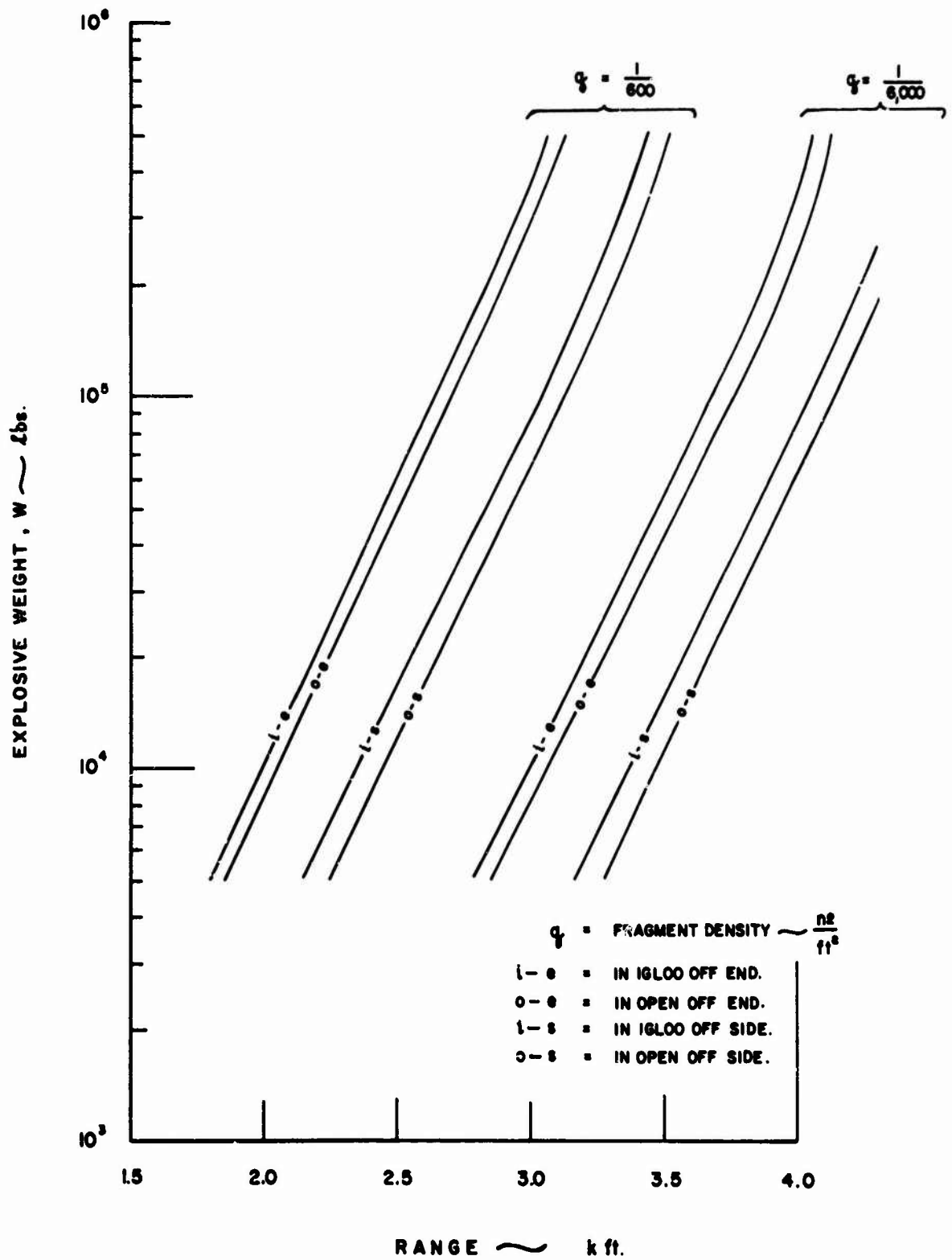
Figure 6-7. QUANTITY-DISTANCE FOR STACKS OF M437A2 175mm PROJECTILES
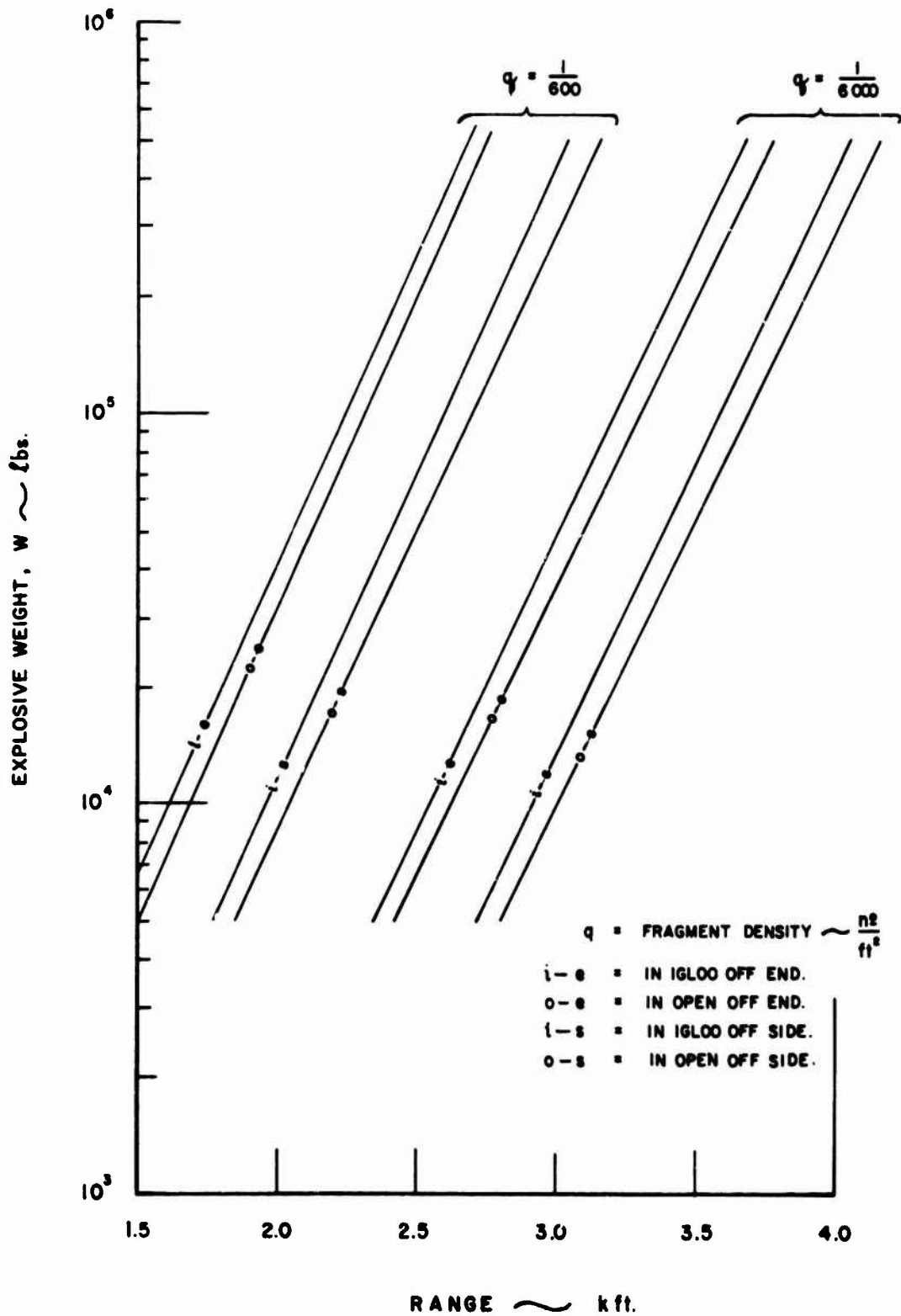
Figure 6-8, QUANTITY-DISTANCE FOR STACKS OF MK82 500-lb BOMBS.
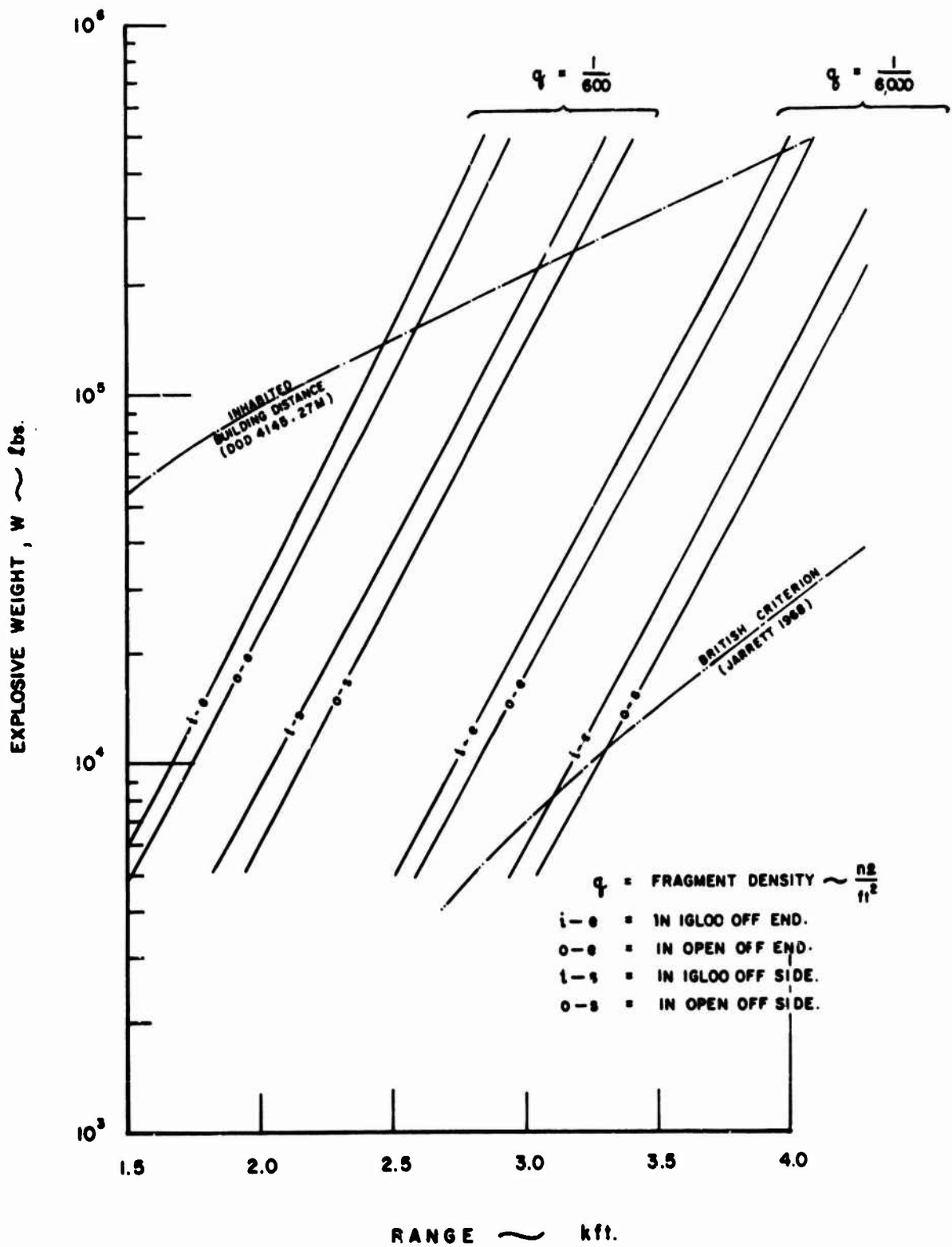
Figure 6-9. QUANTITY-DISTANCE FOR STACKS OF M117 750-lb. BOMBS.

Chapter VII

RECOMMENDATIONS

During the course of this work, the lack of a consistent set of experimental data on fragments from large size stacks, both contained and in the open, hampered conclusive evaluation of the theoretical work. This lack prohibits any generalizations or extrapolations to be made with any degree of confidence. The need for a well planned, consistent experimental program for fragment hazards from munition stacks is paramount if any form of quantitative predictions are ever to be made.

The original intent of this work was to define the quantity-distance relationship for fragment hazards in terms of the munitions, stack and cover parameters in such a manner that this information could be displayed on slide rule or nomograph in a manner similar to the quantity-distance relationships for blast effects from accidental detonation of munition stores (Fugelso et al.1972a,b). This current work has progressed to a point where the parameters have been identified and good theoretical agreement has been obtained with a very limited number of tests. While the agreement to date is encouraging, it is not conclusive enough to commit it to a general computation aid.

To start, a consistent experimental program for the fragment patterns from munitions in open stores should be made. The program consists of many detonations of a single type of munition, in a variety of configurations. First, the far-field fragment distribution from a single munition should be made, in both the horizontal and vertical orientations. This plan is necessary to determine the effect of initial fragment shape distribution. (Remember, the trajectory equations act as high ballistic

density and high initial velocity filters for long range propagation and the distances traversed by a fragment are extremely sensitive to small variations in these parameters. The arena data as presented, gives only average values for these parameters.) Sufficient duplication of the experiment must be made to give statistical significance to the far-field data.

From the tests of the individual munitions, we progress to stacks. A sufficient number of stack tests must be made to determine the surface, bulk and orientation dependence on long range propagation. Increased initial velocities, altered fragment distributions and the tendency to source isotropy must be evaluated. It is obvious that, in addition to far-field fragment measurements, measurements of the distribution of initial velocity and fragment distribution at the source must be made.

As a part of the stack tests, the effects of inter-munition spacing, munition orientation, and mode of initiation of the stack (e.g., all munitions primal, or the munition primed in the center or at the edge of the stack) must also be evaluated. Again, sufficient duplication of these experiments is essential.

Upon conclusion of these tests, the essential parameters of the sources as a function of stack parameters must be determined and the dependence of the far-field fragment densities as a function of these must be demonstrated.

Then, and only then, can the effect of the earth cover be tested, in the same manner. First, munition in revetments should be tested, followed by larger stacks in igloos. It is necessary in the igloo test that the destruction of the igloo be accomplished in the same manner as it would be in a larger scale accidental detonation.

Another area for possible study is the criterion for damaging fragments when the fragments are elongated. Studies of perforation of thin metal plates shows dependence of the ballistic limits on the impact velocity and the mass/presented-area ratio. Very slender projectiles penetrate and perforate plates more readily than blunt projectiles; maximum short duration stresses in the plate are dependent on the impact velocity only. If damage mechanisms react to these parameters $m^{1/3}V = am^{1/3} + C$ (or $V = $ constant)(See Chapter V, page 86) would be the form of the criterion. The necessity for study of damage by slender fragment is indicated by the conclusion of this study that these are the fragments that propagate to the larger ranges.

REFERENCES

Allen, W. P., Mayfield, E. B. and Morrison, H. L., 1957, "Dynamics of a Projectile Penetrating Sand", Jour. Appl. Phys. 28, 370-376.

Allen, W. P., Mayfield, E. B. and Morrison, H. L., 1957, "Dynamics of a Projectile Penetrating Sand, Part II", Jour. Appl. Phys. 28, 1331-1335.

Army Navy Explosives Safety Board, 1947, "Igloo Tests, Naval Proving Ground, Arco, Idaho, 1945", Tech. Paper No. 3.

Bowen, I. G., Fletcher, E. R., Richmond, D. R., Hirsch, F. G. and White, C. S., 1968, "Biophysical Mechanisms and Scaling Procedures Applicable in Assessing Responses of the Thorax Energized by Air-Blast Overpressures or by Nonpenetrating Missiles", Annals of the New York Academy of Sciences, 152, 118-171.

Department of Defense, 1969, DOD Ammunition and Explosives Safety Standards, DOD 4145.27M, (Revised 1971).

Draper, E. and Watson, R. R., 1970, "Collated Data on Fragments from Stacks of High Explosive Projectiles", Ministry of Defense, Directorate of Safety (Army Department) Tech Memo, February, 1970.

Feinstein, D. I., Hengel, W. F., Kardatzke, M. L., and Weinstock, N., 1968, "Personnel Casualty Study", IITRI Final Report J6067, Contract OCD-PS-64-201.

Feinstein, D. I., and Nagaoka, H. H., 1970, "Fragment Hazards From Munition Stacks", Minutes of the Twelfth Explosive Safety Seminar, 287-309.

Feinstein, D. I., 1971, "Fragment Hazard Criteria", Minutes of the Thirteenth Explosives Safety Seminar, 429-436.

Feinstein, D. I. and Nagaoka, H. H., 1971, "Fragmentation Hazard Study, Phase III; Fragment Hazards From Detonation of Multiple Munitions in Open Stores", IITRI Final Technical Report J6176, Contract DAHC-04-69-C-0056.

Feinstein, D. I. and Nagaoka, H. H., 1971, "Fragmentation Hazards to Unprotected Personnel", Minutes of the Thirteenth Explosives Safety Seminar, 53-75.

Feinstein, D. I., 1972a, "Fragmentation Hazards to Unprotected Personnel", IITRI Final Report J6176, Contract DAHC-04-69-C-0056.

Feinstein, D. I., 1972b, "Fragment Hazard Study Grading and Analysis of 155mm Yuma Test Fragments", IITRI Final Report J6272, Contract DAAB09-72-C-0051.

Fugelso, L. E., Arentz, A. A., and Poczatek, J. J., 1961, "Mechanics of Penetration I, Metallic Plates, Theory and Applications", GARD Final Technical Report 1127, Contract DP-19-129-QM-1542.

REFERENCES
(CONT'D)

Fugelso, L. E., 1962, "Mechanics of Penetration II, Single and Laminated Plates", GARD Final Technical Report 1127, Contract DA-19-129-9M-1542.

Fugelso, L. E. and Bloedow, F. H., 1966, "Studies in the Perforation of Thin Metallic Plates by Projectile Impact: I. Normal Impact of Circular Cylinders", GARD Final Technical Report 1250, Contract DA19-129-AMC-247(N).

Fugelso, L. E., Weiner, L. M., and Schiffman, T. H., 1972, "Explosion Effects Computation Aids", GARD Final Report 1540, Contract DAHC-04-72-C-0012.

Fugelso, L. E., Weiner, L. M., and Schiffman, T. H., 1972, "A Computation Aid for Estimating Blast Damage From Accidental Detonation of Stored Munitions", Minutes of the Fourteenth Explosives Safety Seminar, 1139-1166.

Gurdjian, E. S., Webster, J. E., and Lissner, H. R., 1949, "Studies on Skull Fracture with Particular Reference to Engineering Factors", Amer. Jour. Surgery, 78, 736-742.

Jarrett, D. E., 1968, "Derivation of the British Explosives Safety Distances", Annals of the New York Academy of Sciences, 152, 18-35.

Joint Munitions Effectiveness Manual, 1970, Air-Surface Weapons Characteristics, (C).

Kokinakis, W., 1971, "A Note on Fragment Injury Criteria", Minutes of the Thirteenth Explosives Safety Seminar, 421-428.

Peterson, F. H., Lemont, C. J., and Vergnolle, R. R.,1968, "High Explosives Storage Test: Big Papa", Final Technical Report, AFWL-TR-67-132.

Romesberg, L. E., 1971, "Analytical Model for High Explosive Munition Storage, Minutes of the Thirteenth Explosives Safety Seminar, 317-345.

Schreyer, H. L. and Romesberg, L. E. (1970), "Analytical Model for High Explosive Munitions Storage" Final Technical Report, AFWL-TR-70-20.

Sperrazza,J., and Kokinakis, W., 1968, "Ballistic Limits of Tissue and Clothing," Annals of the New York Academy of Science, 152, 163-167.

Thomas, L. H., 1944, "Computing the effect of Distance on Damage by Fragments", BRL Report 468.

Weals, F. H., 1973, "ESKIMO I Magazine Separation Test", NWC Final Technical Report, NWC TP 5430.

Zaker, T. A., Bauer, J., Feinstein, D. I., and Ahlers, E. B., 1970, "Fragmentation Hazard Study, Phases I and II: Single-Munition Fragment Hazards", IITRI Final Technical Report J6176, Contract DPHC-04-69-C-0052.

DISTRIBUTION LIST

	Number of Copies
Chairman Department of Defense Explosives Safety Board Rm GB-270, Forrestal Building Washington, D. C. 20314	5
Defense Documentation Center Cameron Station Alexandria, Virginia 22314	12
Director of Defense Research and Engineering Department of Defense Washington, D. C. 20301	1
Chief of Research and Development Department of the Army Washington, D. C. 20310	1
Commanding General Army Materiel Command Attn: W. G. Queen, AMCSF 5001 Eisenhower Avenue Alexandria, Virginia 22304	1
Deputy Chief of Staff for Personnel Department of the Army Attn: Director of Safety Washington, D. C. 20310	1
Chief of Engineers Department of the Army Attn: DAEN-MCZ-S Washington, D. C. 20314	1
Chief of Engineers Department of the Army Attn: Mr. G. F. Wigger, DAEN-MCE-D Washington, D. C. 20314	1
Commanding Officer Picatinny Arsenal Attn: SARPA-MTD Dover, New Jersey 07801	1
Commanding General U. S. Army Armaments Command Rock Island Arsenal Rock Island, Illinois 61201	1

Director   1
Ballistic Research Laboratories
Attn: Mr. D. J. Dunn
Aberdeen Proving Ground, Maryland 21005

Chief of Naval Materiel   1
Department of the Navy
Attn: MAT0441B
Washington, D. C. 20360

Commander   1
Naval Ordnance Systems Command
Office of the Inspector General
Attn: ORD-OON
       Capt. M. B. Lechleiter
Washington, D. C. 20360

Commander   1
Naval Ordnance Systems Command
Attn: Mr. H. M. Roylance, ORD-048
Washington, D. C. 20360

Chief of Naval Operations   1
Department of the Navy
Attn: Mr. J. W. Connelly, OP-41D
Washington, D. C. 20350

Commander   2
Naval Ordnance Laboratory, White Oak
Attn: Code 241
Silver Spring, Maryland 20910

Commanding Officer   1
Naval Ammunition Depot
Attn: NAPEC
Crane, Indiana 47522

Commander   1
Naval Weapons Laboratory
Attn: Mr. Frank Kasdorf, Code T
Dahlgren, Virginia 22448

Director   1
Defense Nuclear Agency
Attn: Mr. J. R. Kelso, SPTD
Washington, D. C. 20305

Director   1
Defense Nuclear Agency
Attn: Mr. E. L. Eagles,OALG
Washington, D. C. 20305

Director of Aerospace Safety   2
Headquarters, U.S. Air Force
Attn: IGD/SEOE (COL J. P. Huffman)
Norton AFB, California 92409

Headquarters, U. S. Air Force   1
Attn: IGI (LTC J. C. Allison)
The Pentagon
Washington, D. C. 20330

Air Force Systems Command   1
Attn: SCIZG (Mr. Howell)
Andrews Air Force Base
Washington, D. C. 20331

Director, Air Force Weapons Laboratory   1
Attn: WLDC (Mr. F. Peterson)
Kirtland Air Force Base, N. M. 87117

Commander   1
Air Force Armament Laboratory
Attn: ATBT
Eglin Air Force Base, Fla. 32542

U. S. Atomic Energy Commission   1
Division of Operational Safety
Attn: Mr. J. P. H. Kelley
Washington, D. C. 20545

Albuquerque Operations Office   1
Atomic Energy Commission
Attn: ODI
P. O. Box 5400
Albuquerque, N. M. 87115

Mason & Hanger-Silas Mason Co., Inc.   1
Pantex Plant - AEC
Attn: Director of Development
P. O. Box 647
Amarillo, Texas 79105

Dr. Robert W. Van Dolah   1
Research Director, Explosives Research Center
Bureau of Mines, Department of Interior
4800 Forbes Avenue
Pittsburgh, Pennsylvania 15213

Institute of Makers of Explosives   1
Attn: Mr. Harry Hampton
Graybar Building, Rm 2449
420 Lexington Avenue
New York, N. Y. 10017

Assistant Secretary of Defense (I&L)   1
Attn: ID (Mr. H. Metcalf)
Washington, D. C. 20301

Directorate of Safety (Army Dept)   1
Ministry of Defence
Attn: Mr. R. R. Watson
Lansdowne House, Berkeley Square
London W1, England

IIT Research Institute   1
Engineering Mechanics Division
Attn: Mr. E. P. Bergmann
10 West 35 Street
Chicago, Illinois 60616

DOCUMENT CONTROL DATA - R & D

(Security classification of title, body of abstract and indexing annotation must be entered when the overall report is classified)

1. ORIGINATING ACTIVITY (Corporate author)	2a. REPORT SECURITY CLASSIFICATION
General American Transportation Corporation General American Research Division 7449 No. Natchez Ave., Niles, Illinois 60648	Unclassified
	2b. GROUP

3. REPORT TITLE

EFFECT OF EARTH COVER ON FAR-FIELD FRAGMENT DISTRIBUTION

4. DESCRIPTIVE NOTES *(Type of report and inclusive dates)*

Final Report

5. AUTHOR(S) *(First name, middle initial, last name)*

Leif E. Fugelso, Carl E. Rathmann

6. REPORT DATE	7a. TOTAL NO. OF PAGES	7b. NO. OF REFS
December 1973	102	29

8a. CONTRACT OR GRANT NO.	9a. ORIGINATOR'S REPORT NUMBER(S)
DAAB09-73-C-0010	
b. PROJECT NO.	
RDT&E	
c. 4A76502M857	9b. OTHER REPORT NO(S) *(Any other numbers that may be assigned this report)*
d.	

10. DISTRIBUTION STATEMENT

Distribution limited to US Government Agencies only because of test and evaluation (Dec. 73). Other requests for this document must be referred to Chairman, Department of Defense Explosives Safety Board, Washington, D.C., 20314.

11. SUPPLEMENTARY NOTES	12. SPONSORING MILITARY ACTIVITY
	Department of Defense Explosives Safety Board

13. ABSTRACT

The effect of earth cover on the far-field fragment density expected from the accidental detonation of stored munitions was estimated by preparing three models of fragment-cover interaction. Comparisons of the theoretical calculations with limited experimental data show that the model wherein the crown of the earth cover does not retard any fragments gives the best agreement. Models for fragment-fragment interaction which effectively account for stack configuration lead to a simplified model for the effective number of munitions contributing to the far-field fragment density. An approximation technique for the rapid calculation of the far-field fragment density was prepared to assist in the ready evaluation of any model. Tentative quantity-distance relationships for four munitions were prepared. Parametric studies of the effect of altered mass distributions and fragment shape were conducted to assess possible differences between accidental detonation source parameters and arena data source parameters.

DD FORM **1473**
I NOV 65

14 KEY WORDS	LINK A		LINK B		LINK C	
	ROLE	WT	ROLE	WT	ROLE	WT
Fragments						
Accidental Explosions						
Fragment Hazards						